THE DISTRIBUTION AND TRANSPORT OF HEAVY METALS IN BED SEDIMENTS OF THE OTTAWA RIVER

by

Dennis G. Waslenchuk

- submitted in partial fulfillment of the requirements of the degree of Master of Science, Geology, at University of Ottawa
- submitted August 5, 1974

ABSTRACT

The sandy sediments of a three mile study section on the Ottawa River are supplied largely by the Gatineau River (a nearby tributary of the Ottawa) as indicated by provenance studies made on the heavy mineral assemblage. Unlike the metamorphic mineral grains of the Gatineau, sedimentary rock fragments introduced by another tributary, the Rideau River, do not survive in the Ottawa.

Geochemical studies indicate that components of the bed material with high surface area to volume ratios, namely fine grains and wood debris, control in part the concentration of iron hydroxide coatings on the bed material. The Fe coatings in turn provide sites for adsorption and coprecipitation of Hg and Mn and thus control their concentrations. Current speed also affects the precipitation of Fe hydroxide, such that higher concentrations of Fe, and thus of Hg and Mn, are found in areas of quiescent flow conditions.

Hg concentration levels in the study section bed sediments are declining, with a half-life on the order of 12 months. Chemical desorption and transportation of contaminated grains out of the study area are indicated as the mechanisms responsible for the decrease.

Sand dunes ranging from .5 to 3 meters in height

and 10 to 70 meters in length vary in size according to water depth. A ripple bed prevails in areas where depth is less than about 5 meters, and a plane bed prevails in areas of cohesive sediments.

Two methods were used to determine the bed load discharge, a dune-tracking method utilizing sonic depth-sounding, and a bed load sampling method employing a diver operated bed load sampler designed for the project. Results from the two methods are in good agreement, with discharge on the order of 4×10^5 kg. bed sediment per day.

The weight of adsorbed Hg discharged with the bottom sediments is on the order of 10 grams/day.

ACKNOWLEDGEMENTS

I thank my supervisor, Dr. Brian Rust, and my advisors Dr. Doug Scott and Dr. Jan Viezer of the Geology Department, University of Ottawa for providing assistance in many forms. I am grateful to Dr. Morley Brownstein of the National Research Council for reading the manuscript and offering his advice, and for conducting one phase of the chemical analyses presented herein.

I received assistance both in the field and in the laboratory from several summer assistants: Margo Burgess, Marcel Gauthier, Ron Hartree, Marc Higgins, Maryse Lapointe, Jean Lemieux, and Ed Lisle, whom I also thank.

I give special thanks to my wife, Lorraine, for helping in the field, for typing the manuscript, and for supplying constant encouragement.

TABLE OF CONTENTS

LIST OF FIGURES

LIST OF TABLES

LIST OF PLATES

PROLOGUE

The object of this report is to study various physical and chemical aspects of the Ottawa River bed sediments as they pertain to the occurrence, distribution and transport of persistant chemicals in the ecosystem. In particular the mineralogy, facies and source of the sediments comprising the bed material of a three mile study section are studied, along with some geochemical factors which control heavy metal concentrations (especially Hg concentrations) in the bed sediments. Finally, the transport characteristics of the sediments were investigated.

The three mile study section is the object of a multidisciplinary environmental investigation, being conducted jointly by scientists of the National Research Council of Canada and the University of Ottawa, under the general theme of "The Transport and Distribution of Persistant Chemical Pollutants in a Flowing Water Ecosystem". The author has undertaken to elucidate the nature of, and the processes operating on, the bed material compartment of the ecosystem.

PART I - INTRODUCTION

PART I- INTRODUCTION

A. THE GEOLOGY OF THE AREA AROUND THE OTTAWA RIVER AT OTTAWA

Rocks of three major time divisions occur in the Ottawa area, and are of Precambrian, Lower Palaeozoic, and Pleistocene-Recent ages.

The oldest rocks in the area are those of the Canadian Shield; Precambrian igneous and metamorphic rocks outcrop mainly north of the Ottawa River. The Shield terrain averages 800 feet elevation above sea level. Lower Palaeozoic sedimentary rocks fringe the Shield to the south, lying with generally low dips on the Precambrian rocks at an elevation between 150 feet and 250 feet above sea level. The area was glaciated in Pleistocene times, and Pleistocene glacial deposits and recent sediments derived therefrom are widespread in the area.

a. Precambrian

Figure 1 shows the extent of Precambrian and Palaeozoic rocks which outcrop in the area. Near Ottawa, the Precambrian rocks are confined mainly to the north of the Ottawa River, with the exception of a Precambrian outcrop between Arnprior and South March. The southern margin of the Shield is separated from the low-lying Palaeozoic sedimentary rocks by irregular scarps and clearly defined changes in elevation.

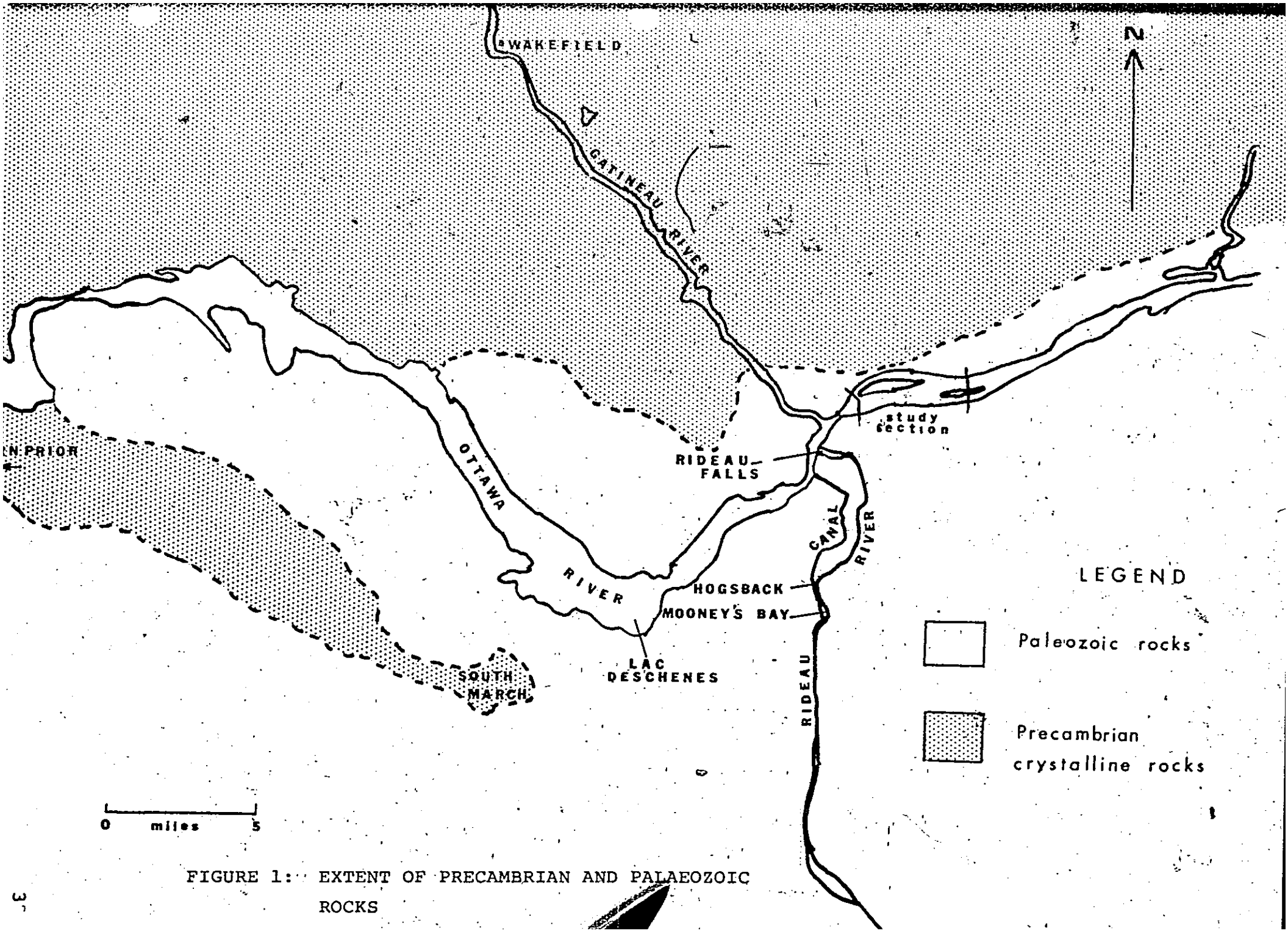

FIGURE 1: EXTENT OF PRECAMBRIAN AND PALAEOZOIC ROCKS

The metamorphic Shield rocks are part of the Grenville Province. Metasedimentary rocks and the meta-igneous Wakefield batholith comprise the large part of the Shield terrain. Diabase dikes (dated at approximately 450 m.y.) commonly intrude the Shield rocks (Baird, 1972).

Calcite and dolomite marble, biotite gneiss, diopside gneiss, and feldspathic quartzite are characteristic rock types. Mineral assemblages such as anti-perthite - garnet - sillimanite - biotite and plagioclase - quartz - hypersthene - garnet - biotite are frequent, and are in accord with the hornblende granulite subfacies (Baird, 1972, p.5).

b. Palaeozoic

Lower Palaeozoic rocks outcrop largely to the south and east of Ottawa. Cambro-Ordovician quartz sandstone, and Ordovician shale and limestone lap onto, or are in fault contact with the Precambrian rocks. The contact generally dips to the south. The sedimentary rocks are present in flat lying sheets and faulted blocks along the southern margin of the Shield.

A basal quartzose sandstone is succeeded by sandy dolostones, limestones, shales, and shaly limestones which extend upward into the Upper-Ordovician. The sequence is thick (approximately 3000 feet) in the Ottawa area, thins quickly to the west, and thickens gradually to the east (Baird, 1972, p.16; Wilson, 1946, p11).

c. Pleistocene

The Wisconsin ice sheet deposited till over much of the area and caused down warping, so that the area was covered first by a fresh water lake, and then by invading marine waters (the Champlain Sea), when the ice sheet retreated. In the Champlain Sea were deposited extensive clay and silt sheets, and deltas of outwash gravels and sands. Some glacial deposits were reworked to produce spits and wave-cut platforms.

As the land rebounded subsequent to glaciation, a complex series of terraces and other deposits were formed by downcutting streams, and the present day drainage pattern was established (Baird, 1972; Johnston, 1917, pp.6-10).

B. THE GEOLOGY AND CHEMISTRY OF THE OTTAWA RIVER: PREVIOUS WORK

The initial field work, directed by Dr. Brian Rust, consisted of a bed sediment sampling survey in the summer of 1972, and in the early part of the summer of 1973, before the author joined the project. The samples were analyzed with respect to various textural parameters, namely mean grain size, sorting (standard deviation), skewness, and kurtosis. The sampling surveys were very complete, with over 400 samples taken from within the study section. Figures 2, 3, and 4 show the bottom sampling arrays of 1972 and 1973. Figure 5, compiled by the author using information gathered by the sampling programs, and from a few of his own observations, is a lithofacies map of the bed sediments of the study sedtion and adjacent areas. The occurrence and distribution of the sediment types will be discussed in Part II: Mineralogy and Provenance.

A bathymetric map of the study reach has been produced (Miller, 1974, p2.33). The main features of the bathymetry correspond closely to the main elements of the surface velocity map (Figure 22, this report; modified after Warnock, 1974, p3.49, in Miller, 1974) as one would expect. The sediment grain size distribution should be ultimately controlled by flow speed, but the

sediment size distribution in the study reach (Fig. 23, this report) does not correspond exactly to the surface velocity and bathymetry patterns mentioned above. Divers have determined that sand occupies only that part of the main channel north of the thalweg; the bottom south of the thalweg is composed of outcropping Pleistocene clay. In addition, a coarse grained anomaly south of Upper Duck Island occurs, and is probably the result of a dredging operation of the 1960's. Hence, if the southern portion of the channel and the anomalous area south of Upper Duck Island are ignored, mean sediment grain size, flow speed, and bathymetry are closely related. Rust (1974, p4.14, in Miller, 1974) shows graphically that depth and grain size are directly proportional for sediments outside the anomalous areas.

The Ontario and Quebec Provincial Governments surveyed the water quality of the Ottawa River, and indicated the sources of industrial and municipal loading in their report of 1971 (Ontario Water Resources Commission and Quebec Water Board, 1971). Several sources contribute effluent to the study reach or to the immediate upstream area, namely the municipal discharges of the cities Ottawa and Hull just west of the study area, the E.B. Eddy Pulp and Paper Mill on the Ottawa, 4 miles upstream from the study area, and the C.I.P. (Gatineau) Paper Mill on the

north shore of the channel north of Kettle Island, in the study reach. Each of these sources discharged large amounts of suspended solids, and caused high related sludge deposition in the downstream areas. According to the report (p.5), mercurial compounds were formerly used by the Eddy and C.I.P. operations, and discharges of these compounds has resulted in significant contamination of fish in the lower river.

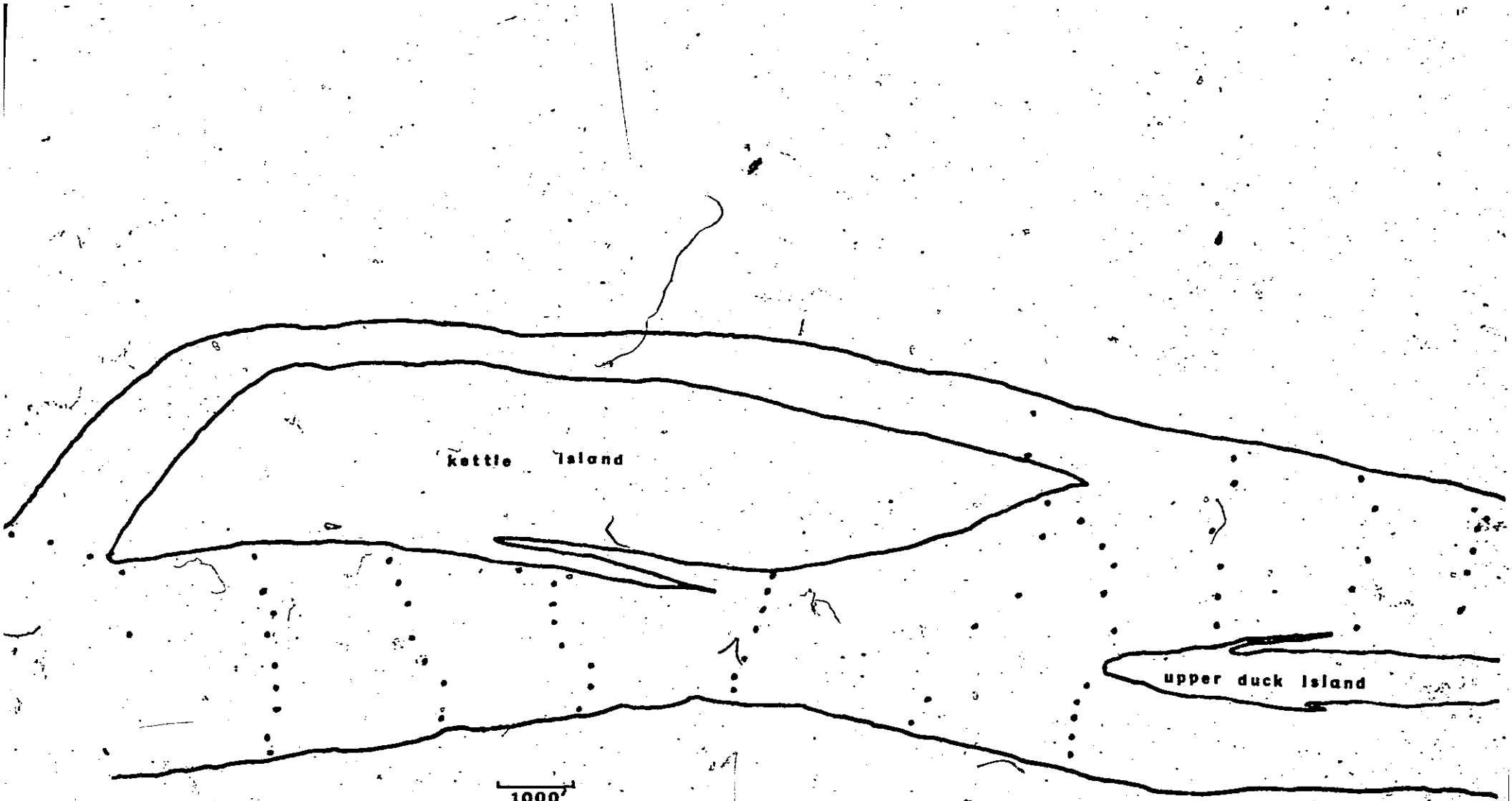

FIG. 2 : 1972 SAMPLE LOCATIONS.

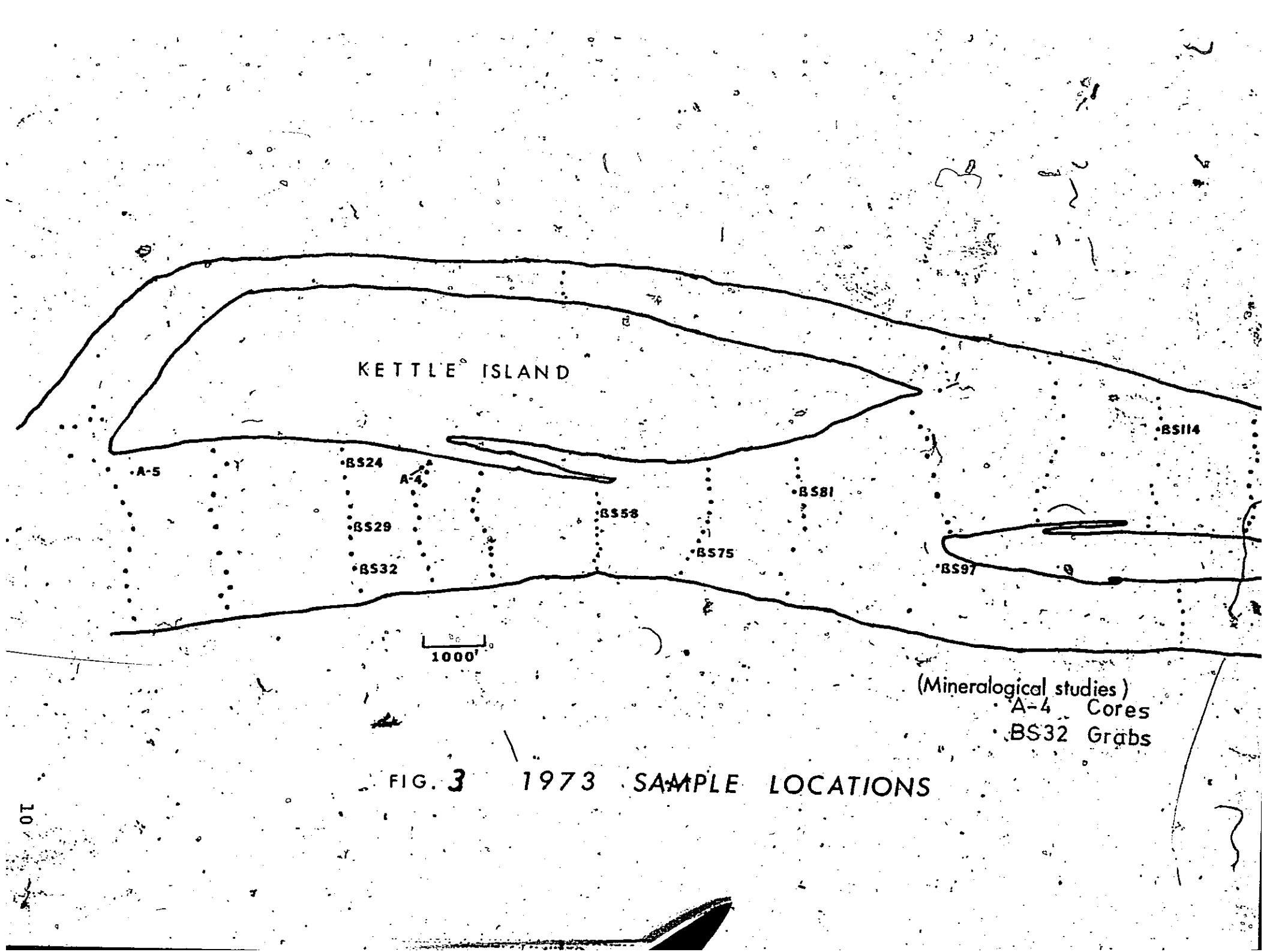

FIG. 3 1973 SAMPLE LOCATIONS

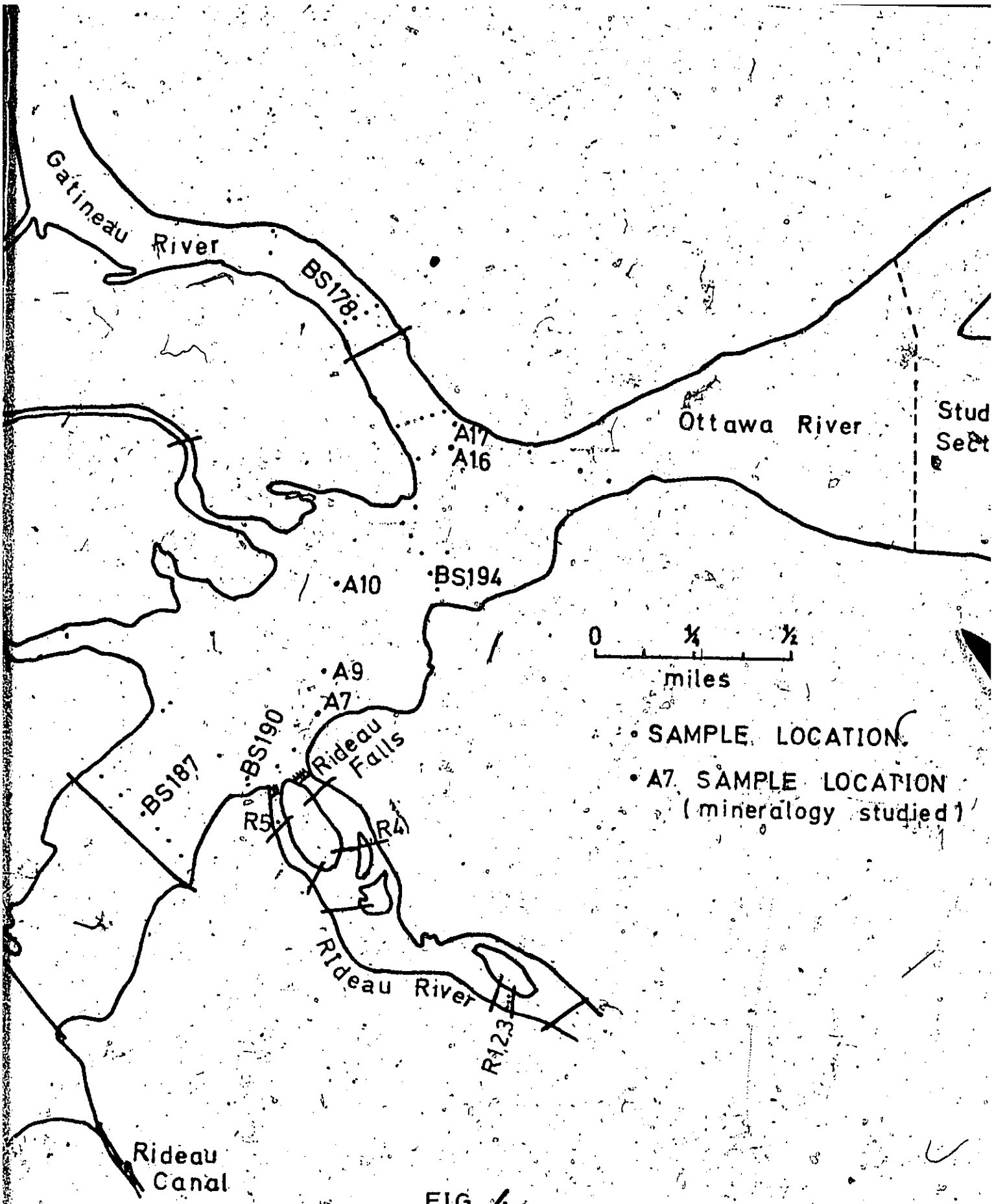

FIG. 4

SAMPLE LOCATIONS - ADJACENT AREAS.

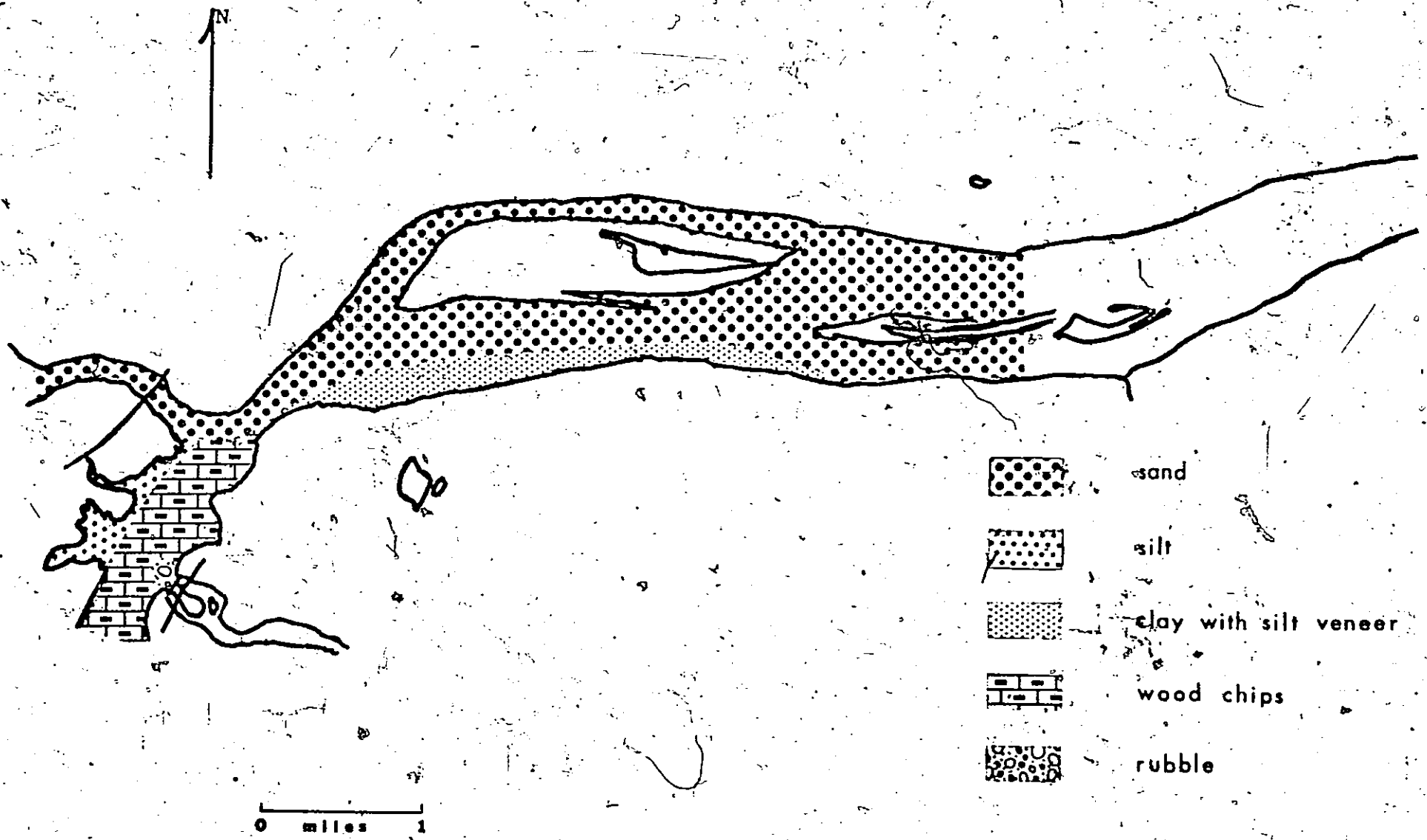

FIG. 5 : LITHOFACIES MAP OF STUDY SECTION AND ADJACENT AREAS

PART II - MINERALOGY AND PROVENANCE OF OTTAWA RIVER BED SEDIMENTS

PART II - MINERALOGY AND PROVENANCE OF OTTAWA RIVER BED SEDIMENTS

A. METHODS OF EXAMINATION AND CONFIDENCE LIMITS

a. Heavy Mineral Separations

To facilitate microscopic study of heavy minerals, the heavy minerals were separated from the light fraction by standard heavy mineral separation techniques. Bromoform with specific gravity of 2.85 was used to float off the light fractions. Care was taken to ensure that the separations were complete.

b. Index of Refraction Oils

Sediment grains were mounted on slides in index of refraction oils (immersion oils) to facilitate study with the polarizing microscope. Fresh Cargille oils which had not been used previously were used for this work. The true index of refraction of all oils was checked with the Abbe Refractometer at the outset, and at the conclusion of the study. In every case the error in refractive index was less than .005, and hence the determinations of mineral refractive index were made with sufficient accuracy.

c. Index of Refraction Oil Grain Mounts

Grinding of thin sections to achieve parallel, flat surfaces on the sediment grains was considered unnecessary, as all of the anisotropic minerals encountered were lath-

shaped, and thus presented natural flat, parallel surfaces. An exception to this condition was the mineral zircon, but despite its often highly rounded character, all optical properties were easily measured.

The rounded nature of the isotropic grains was of no concern, since refractive index is independent of crystal shape, and no other optical properties apply.

d. Representative Samples in Microscope Study

In an attempt to avoid sampling error and bias, the heavy mineral fraction of all sieve groups of several samples was studied. It was found that the greatest variety of heavy minerals occurred in a sieve fraction two or three groups smaller than the modal sieve group, as expected. Furthermore, that sieve group with the highest concentration and variety of heavy minerals was visibly recognizable. Therefore, succeeding groups were chosen for study on the basis of the highest visible content of heavy (dark coloured) minerals in the sieve groups of a particular sample.

Cone and quartering techniques were employed to obtain representative samples for the slide mounts. In those cases where the complete mineral assemblage expected was not encountered on a specific mount, successive mounts were made until the author was satisfied that the particular species were either absent or present in very low concentrations at the sample site.

In a much broader sense, the significance of the mineralogic study as a whole was questioned. Do the bottom samples studied actually represent the whole sedimentary compartment, or do they merely represent a temporary situation that prevailed during the sampling period? The mineralogy of grab samples (shallow sediment penetration) was compared to the mineralogy of core samples (depth of penetration up to 3 feet). It became obvious that areas of sandy sediment are homogenous at least to core depths, and hence the grab samples are representative of that mass of sediment which is under study.

e. Methods in Mineral Identification

A systematic examination of each mineral species encountered was conducted. The observations were tabulated (see Appendix I), and were compared with those of Milner (1962) and Moorhouse (1959) for identification. The systematic examination used is as follows (modified after Milner, 1962):

i) With transmitted plane-polarized white light,
   a) transparency, translucency or opacity
   b) colour
   c) habit: presence or absence of crystal faces
   d) shape: angular, subangular, rounded
   e) fracture: uneven, conchoidal, etc.
   f) parting: linear or irregular
   g) cleavage: principal directions

h) abrasion (degree), pitting or other surface features

i) refractive index

j) inclusions (if any)

k) pleochroism: presence or absence, weak or strong, colour change.

ii) With transmitted light, crossed nicols

a) isotropism or anisotropism

b) birefringence

c) extinction: straight or oblique (in latter case determine angle)

d) relative retardation and vibration directions

iii) With convergent light, crossed nicols, Bertrand lens

a) detection of interference figure: uniaxial or biaxial

b) determination of optic sign

c) optic axial angle

d) dispersion of optic axes

B. HEAVY MINERAL ASSEMBLAGE OF STUDY SECTION BED SEDIMENTS

The following minerals were identified. The list is complete in that no other species were encountered in the study section bed sediments. The minerals are listed in decreasing frequency of occurrence, with observed characteristics noted for each.

1) Magnetite/Ilmenite - separated magnetically, not studied further

2) Diopside - transparent pale green and colourless grains, lath-shaped, angular to rounded, uneven fracture. Refractive Index variable, approx. 1.676, strong birefringence, abundant varied inclusions. Pleochroism, in coloured grains, colourless to pale green. Biaxial positive, with oblique extinction (Z^c), approx. 20^{o}. Intermediate 2V, approx. 50^{o}.

3) Hypersthene - transparent green grains, prismatic, angular, irregular to sub-conchoidal fracture, pyroxene cleavage, striation parallel to elongation. Refractive Index 1.676 to 1.700, brown prismatic inclusions, some oriented perpendicular to elongation. Pleochroism strong, pale grey-green to pink, maximum absorption perpendicular to elongation. Biaxial negative, low 2V, approx. 20^{o}, straight extinction, strong dispersion. Alteration evident as haloes, giving anomalous birefringence, and perhaps accounting for low 2V. (see plate 1)

4) Phlogopite - transparent to translucent amber grains, occurring as irregular plates of subangular shape, with uneven fracture, good basal cleavage. Refractive Index slightly less than 1.600. Pleochroism strong, dark brown to brownish yellow. Biaxial negative, very small 2V, approx. 5^{o}.

5) Almandite - transparent red grains, highly spherical euhedra to faceted grains, subangular to rounded, sub-conchoidal fracture well developed. Refractive Index approx. 1.765, abundant inclusions. Isotropic, with some exceptions of weakly birefringent grains.

6) Biotite - transparent to translucent, yellow, brown and green flakes, some exhibiting tabular habit, irregular fracture. Good basal cleavage, with perhaps a subordinate parting. Refractive Index 1.645 to 1.700, variable. Abundant inclusions. Pleochroism evident, yellow to dark green, maximum absorption, parallel elongation. Moderate to high birefringence, biaxial negative, with 2V approx. 10°. Evidence of alteration on some grains, perhaps chloritic matter, producing bleached grains. The variety lepidomelane may be present, as some grains are so strongly coloured as to be almost opaque, and the Refractive Index range is too high for biotite.

7) Hornblende - transparent green grains, prismatic angular, uneven fracture, prismatic cleavage. Striations occur parallel to prism elongation. Refractive Index less than 1.700, opaque inclusions. Pleochroism weak, pale green to dark green. Moderate birefringence, oblique extinction at approx. 25°, biaxial negative, 2V approx. 60°.

8) Epidote - transparent, yellowish-green grains of variable habit, angular, uneven fracture, one moderate cleavage. Refractive Index greater than 1.700, aligned prismatic inclusions. Pleocroism weak, green to greenish-yellow. Moderate to strong birefringence, extinction parallel to crystal edges, biaxial negative, large 2V, greater than 60^{o}. Poor interference figures.

9) Grossularite - transparent, colourless grains, some showing poor hexagonal outline, subangular to rounded, conchoidal fracture well developed. Refractive Index slightly greater than 1.735, opaque and purplish, prismatic inclusions present. Isotropic. (see plate 2)

10) Spinel - transparent, colourless to blue, subangular, conchoidal fracture, one poor cleavage. Refractive Index approx. 1.735. Aligned purplish, prismatic inclusions. Isotropic.

11) Sphene - transparent, amber grains, diamond shaped faces, subangular to rounded with uneven fracture, one poor cleavage. Refractive Index greater than 1.710. Opaque inclusions present. Pleochroism strong, yellow to dark red. Incomplete extinction of most grains, biaxial, positive, 2V approx. 30^{o}, strong dispersion. (see plate 3)

PLATE 1 : HYPERSTHENE, PLEOCHROIC COLOURLESS TO GREEN

PLATE 2 : GROSSULARITE, UNDER NON-PERPENDICULAR CROSSED NICOLS, SHOWING ABUNDANT (FLUID?) INCLUSIONS

PLATE 3 : SPHENE, SHOWING CHARACTERISTIC SHAPE AND HIGH RELIEF

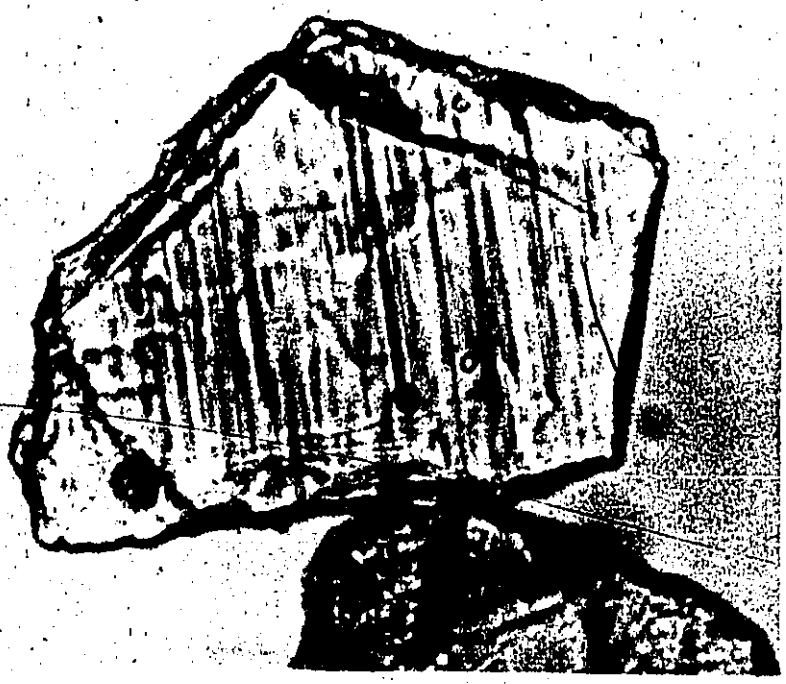

PLATE 4 : SILLIMANITE, WITH OBVIOUS PARALLEL STRIATIONS

PLATE 5 : CORDIERITE, LATH SHAPED, HIGH RELIEF

12) Zircon - transparent, colourless to brownish well-rounded grains, crystal faces absent. >1.700 Refractive Index, slight pleochroism, brown to reddish brown. High birefringence, uniaxial, positive.

13) Tremolite - transparent, colourless, prismatic grains, angular, irregular to uneven fracture, one good cleavage parallel to prism edge. Refractive Index less than 1.700. Opaque inclusions present. Strong birefringence, oblique extinction, approx. 25^{o}, biaxial, negative, 2V greater than 60^{o}. Note: incipient alteration to scaly mineral (talc?) observed on surface of most grains.

14) Sillimanite - transparent, colourless, prismatic grains, angular to subangular, uneven fracture, one good cleavage parallel to prism edge. Notable parallel parting striations, regular, and parallel to prism edge. Refractive Index slightly greater than 1.660. Pleochroism weak, colourless to pink. Moderately birefringent, straight extinction, centered biaxial figure, positive, 2V approx. 30^{0}. (see plate 4)

15) Tourmaline - transparent, colourless, green or brownish prismatic grains, angular conchoidal fracture, one poor cleavage. Refractive Index approx. 1.690, inclusions varied and abundant, high birefringence, straight extinction, uniaxial, negative, some grains show anomalous biaxial nature, 2V approx. 5^{o}.

16) Cordierite - transparent, colourless, prismatic grains, angular, conchoidal fracture, Refractive Index low, less than 1.596. Slight pleochroism, yellow to brownish orange. Moderately birefringent, incomplete straight extinction, biaxial, negative, large 2V. (see plate 5)

17) Monazite - transparent, yellow grains, absence of crystal faces, rounded, uneven fracture, one poor cleavage. Refractive Index greater than 1.700. Pleochroism evident, light yellow to dark yellow. Moderate to high birefringence, biaxial, positive, small 2V, approx 10°.

C. LIGHT FRACTION MINERALOGY

The minerals comprising the light fraction of several samples were briefly examined. The light fraction is composed entirely of quartz and feldspar grains, without any remarkable features. Quartz and feldspar are present in approximately equal proportions. The presence of carbonate minerals was tested gasometrically on about 50 samples from the study reach, but in all cases the amount of carbonate was below the .2% limit of detection.

D. SEDIMENT CORRELATIONS

a. Within the Study Section

i) Lateral and Longitudinal Persistence

Table I records the relative frequency of occurrence

	BS24	BS29	BS32	BS58	BS75	BS81	BS97	BS114	BS148	CORES A4	CORES A5
DIOPSIDE	A	A	A	A	A	A	A	A	A	A	A
HYPERSTHENE	A	A	A	A	A	A	A	A	A	A	A
PHLOGOPITE	A	A	A	A	A	A	A	A	A	A	A
ALMANDITE	A	A	A	A	A	A	A	A	A	A	A
BIOTITE	C	A	A	A	C	A	A	A	A	C	A
HORNBLENDE	C	A	A	C	C	A	A	A	A	A	A
EPIDOTE	A	C	C	C	C	C	C	C	C	C	C
GROSSULARITE	C	C	C	S	C	C	S	C	C	S	C
SPINEL	C	C	C	C	C	S	S	C	S	C	C
SPHENE	C	C	C	S	C	S	S	C	C	C	C
ZIRCON	C	S	C	C	C	S	C	C	S	C	S
TREMOLITE	S	S	C	S	NP	C	NP	C	NP	S	S
SILLIMANITE	C	C	C	C	S	S	NP	S	NP	S	NP
TOURMALINE	S	S	S	NP	NP	S	S	S	S	S	S
CORDIERITE	S	S	S	S	NP	S	NP	S	S	S	NP
MONAZITE	S	NP	NP	NP	NP	NP	NP	NP	NP	NP	S

A ABUNDANT

C COMMON

S SCARCE

NP NOT PRESENT

TABLE I. LATERAL AND VERTICAL PERSISTENCE OF HEAVY MINERAL ASSEMBLAGE - STUDY SECTION -

of each of the heavy minerals encountered in the samples studied. Magnetite/Ilmenite are ubiquitous, and are not recorded.

A basic assemblage consisting of diopside, hypersthene, phlogopite, almandite, biotite, hornblende, epidote, grossularite, spinel, sphene, and zircon is present in all samples, without any trend of decreasing concentration of any mineral either laterally or longitudinally (the mineralogy of the areas of silt-sized sediments were not studied, however). The minerals tremolite, sillimanite, tourmaline, cordierite, and monazite show variability in their presence or absence, again without any noticeable trends.

On the whole, the mineral assemblage, including all the minerals in Table I, shows good lateral and longitudinal persistence within the study section.

ii) Vertical Persistence

The minerals occurring in shallow-penetrating grab samples might be expected to persist to some depth within the sediment due to the effect of sand dunes observed in the study section (see part IV, Bedforms). The downstream migration of sand dunes repeatedly buries and re-exposes individual grains, thus homogeneity of the sediments to the effective depth of the sand dunes should be achieved. Two cores, A-4 and A-5 (Table I), were obtained at

localities where sand dunes occur and show that the heavy mineral assemblage persists to at least 3 feet deep in the bed sediments.

The sand sized sediment of the study area may therefore be considered as an homogenous unit, on the basis of the vertical and horizontal persistence of the heavy mineral assemblage.

b. Adjacent Areas

Possible source areas for the sediments comprising the sedimentological unit described above were investigated. A geographical study was conducted to determine possible areas of interaction with the study section. The confluence of the Gatineau and Ottawa Rivers is located one mile upstream from the study section's western boundary. The Gatineau River is medium-sized, with mean annual discharge on the order of 20,000 cfs. It flows south across the Canadian Shield, which outcrops to the north of the confluence.

The Rideau River flows north across the Palaeozoic sediment and drift covered Ottawa Valley and joins the Ottawa River two miles upstream from the western boundary of the study section. The Rideau Falls (which expose the Cobourg unit of the Ottawa Formation) form the actual junction, lowering the waters of the Rideau River some 50 feet to the level of the Ottawa River. The Rideau

River is shallow, and at some cross-sections maximum depth is only one foot. A discharge figure was not obtained, but is estimated to be less than 10,000 cfs, mean annual discharge.

Five miles south of the Rideau Falls (at Hogsback Road), the Rideau River is dammed, and sediment ponding would be expected to occur in Mooney's Bay directly upstream. Mooney's Bay is the head of that part of the Rideau Canal which roughly parallels the Rideau River, as it passes through the city of Ottawa. The canal enters the Ottawa River one mile upstream from Rideau Falls. The canal lowers a portion of the Rideau River, by a series of locks, to the level of the Ottawa River. Since the canal is a navigation route, with very low current velocities it would not be expected to contribute significantly to the sediments under study. Any contribution to the sediments of the Ottawa River is therfore probably derived in the reach downstream from Hogsback Road, along the main river channel.

There are therefore three potential sources for the study section sediments, the Gatineau River, the Rideau River, and the Ottawa River itself.

Two miles above the confluence of the Rideau River, the Chaudière Falls (formed by a resistant outcrop of the Rockcliffe Formation) interrupt the flow of the Ottawa

River. Upstream from the Chaudière Falls, three sets of shallow rapids occur where Ordovician (Ottawa Formation) bedrock outcrops below the river waters.

The third set of rapids in this series, the Deschênes Rapids, forms a shallow (approx. 10') sill at the mouth of Lac Deschênes. Lac Deschênes, a widening of the Ottawa River, has an average depth of 50 feet and depths up to 180 feet occur. Therefore, sediment ponding would probably occur in Lac Deschênes, with only suspended material being transported downstream to the study section.

The Gatineau River is dammed at Wakefield, some ten miles upstream from the Ottawa River. Here again, the probability of sediment ponding exists, and any contribution of sediments from the Gatineau River to the study section would most probably be derived downstream from Wakefield. The river in this section flows over Precambrian Canadian Shield rocks, south of Wakefield for six miles, then across drift and alluvium for the last four miles to the Ottawa River.

(i) Mineralogy of Gatineau River Sediments

Sand samples taken from the Gatineau River were examined in the same manner as the Ottawa River samples. Table II lists the mineral assemblage compiled from three representative grab samples, BS178, A17, and A16. The assemblage is very similar to that compiled for the study section as a whole, with the notable addition of apatite

	UPSTREAM OTTAWA R.										
	GATINEAU R.					BELOW RIDEAU R.				RIDEAU R.	
	BS178	A17	A16	BS187	BS190	A7	A9	A10	BS194	R1	P3
DIOPSIDE	A	A	A	A	A	A	A	A	A	A	A
HYPERSTHENE	A	A	A	C	C	A	A	A	A	A	A
PHLOGOPITE	A	A	A	C	C	A	A	A	A	A	A
ALMANDITE	A	A	A	C	C	A	A	A	A	A	A
BIOTITE	A	A	A	NP	NP	C	C	C	C	A	A
HORNBLENDE	A	A	A	S	NP	A	A	A	A	C	C
EPIDOTE	C	C	C	S	S	C	C	C	C	C	C
GROSSULARITE	C	C	S	NP	NP	S	C	S	C	C	C
SPINEL	A	C	S	S	S	C	C	C	C	C	C
SPHENE	A	C	S	S	NP	C	C	C	C	A	A
ZIRCON	C	S	S	C	C	C	C	C	C	S	S
TREMOLITE	S	S	S	NP	NP	NP	NP	NP	NP	NP	NP
SILLIMANITE	C	C	S	NP	NP	NP	NP	NP	NP	S	S
TOURMALINE	C	S	S	S	S	C	S	S	S	S	S
CORDIERITE	S	S	S	NP	NP	S	S	S	S	S	S
MONAZITE	S	NP	S	NP	S	NP	NP	NP	NP	NP	NP
APATITE	C	C	S	NP	NP	C	C	C	C	C	C
GOETHITE	NP	NP	NP	C	C	NP	NP	NP	NP	S	S

A ABSENT
C COMMON
S SCARCE
NP NOT PRESENT

TABLE II : PERSISTENCE OF THE HEAVY MINERAL ASSEMBLAGE IN ADJACENT AREAS

as a common constituent. As encountered in the Gatineau sediments, the characteristics of apatite are:

1) Apatite - transparent, colourless grains; rounded, egg-shaped; Refractive Index approximately 1.650, notably weak birefringence, yields a good centered BXa interference figure, uniaxial, negative, straight extinction. Shows arrays of minute opaque inclusions.

(ii) Mineralogy of Upstream Ottawa River Sediments

"Upstream Ottawa River" is meant to be that part of the river above the Rideau Falls. Only two grab samples (BS187 and BS190) yielded sand-sized grains, the remainder consisted of masses of wood chips(1). Samples BS187 and BS190 were also largely composed of wood chips, but a small amount of sand was attached to and mixed with the chips. The abundant wood chips are probably effluent from a large paper products industry located on the river near the Chaudière Falls. The wood chips seem to be distributed somewhat randomly among the sediments of the study section. Analysis of the sand resulted in the heavy mineral assemblages listed in Table II. The list shows notable absence of of some species, which were basic to the Gatineau and study section sediments. Biotite, hornblende (BS190 only), grossularite, and sphene (BS190 only) are absent,

(1) The wood particles range in size from 1mm fibres to 2cm chips.

as well as some of the "secondary" minerals, namely tremolite, sillimanite, cordierite, and apatite. The relative frequency of occurrence of most species is dissimilar to the frequency of the corresponding species in the Gatineau and study section sediments. One additional species was encountered in the 'upstream' samples, however; the mineral goethite, which occurs as a scarce constituent, with the following properties:

1) Goethite - translucent, fibrous, yellowish particles; amorphous; Refractive Index high, >2.000.

(iii) Mineralogy of Ottawa River Sediments between Rideau Falls and the Confluence of Gatineau River

Sand-sized sediment was taken at grab sample sites A7 and A9, sand and wood chips were taken at A10 and BS194. Analysis of the sand fraction of these samples gave the results listed in Table II. The assemblages are similar to Gatineau River and study section assemblages, with the exceptions of the species tremolite and sillimanite, which are absent from A7, A9, A10, and BS194, and of the species apatite, which is not present in the study section sediments.

(iv) Mineralogy of Rideau River Sediments

Five grab samples, denoted R1 to R5, were taken in the lower Rideau River, with an Eckman-type hand operated grab sampler. The Eckman grab penetrates

bottom sediments to about five centimeters in depth. The Rideau River sediment is markedly different from the other sediments examined with respect to the light fraction. The light fraction is wholly composed of lithic fragments and minor quartz grains. The lithic fragments are shales and argillaceous limestones, which are in accord with the Ottawa limestone beds over which the Rideau flows. The quartz grains are well rounded, and are evidently derived from an older sedimentary deposit. Maloney (1969) has recognized rounded quartz grains in thin beds of sandstone within the Ordovician Pamelia Formation, which he considers to be derived from an earlier sedimentary cycle, the Nepean sandstone. The Pamelia formation outcrops at the Hogs Back, on Rideau River. The light fractions of sediments from other areas, in contrast to Rideau sediments, are made up entirely of quartz and feldspars, with no notable characteristics.

Heavy minerals were separated from the Rideau samples and studied in the same manner as samples from other areas. Table II shows the assemblages as compiled for two representative Rideau samples, R1 and R3. The absolute amount of heavy species in the Rideau samples is small compared to Gatineau or Ottawa samples, but the assemblages are remarkably alike. Of the 18 heavy min-

erals recognized in all samples combined, only two species, monazite and tremolite, do not occur in Rideau sediments. The Rideau River heavy minerals must be derived from Pleistocene drift deposits which are present along the course of the Rideau. The ultimate origin of the Pleistocene material, is however, the Precambrian Shield area to the north.

E. PROVENANCE OF THE STUDY SECTION BED SEDIMENTS

On the basis of the heavy mineralogy of bed sediments from the study section and other areas, it is evident that the provenance of the study section sediments is the local Precambrian Shield Terrain. Mineral assemblages described by Baird (1972) and Hogarth (1962) for the metamorphic rocks of the Precambrian Shield are in accord with the heavy mineral assemblage observed in the study section, both assemblages being indicative of the hornblende-granulite subfacies (Winkler, 1965, p.115; Fyfe et al, 1962, p.232).

The Gatineau River contributes the largest part of the study section sediments directly from the shield terrain to the north. The Upper Ottawa River and the Rideau River may contribute minor amounts of sediment to the study area; the sediments so contributed are probably derived from Pleistocene deposits, which originated ultimately from the Precambrian Shield rocks to the north.

The fact that the notable Rideau River light assemblage was not recognized in the study section may indicate that the amount of material contributed by the Rideau is overwhelmingly diluted by Gatineau River contributions. However, another explanation for the non-occurrence of the lithic Rideau River light fraction may be that these fragments simply do not survive under the new and different energy conditions of the Ottawa River. The significance of the contribution of sediments from upstream Ottawa River is difficult to establish, but the extensive cover of wood chips may indicate that sand is not being actively transported in this reach, therefore little of the study section bed material comes from the Ottawa.

F. SUMMARY OF THE MINERALOGY AND PROVENANCE OF OTTAWA RIVER STUDY SECTION BED SEDIMENTS

Petrographic studies show that the sand sized bed material in the study section is a homogenous unit, laterally, longitudinally and to a depth of at least three feet.

No maturing trends are noted of the sediments within the study section. However, the absence of apatite, goethite, and lithic shale and limestone fragments in the study section suggests that sediments bearing these species undergo maturation upon entering the Ottawa

River, where they become subject to different energy and transport conditions.

The Gatineau River is the source of the large part of the study section sediments, and the Rideau and upstream Ottawa Rivers may contribute minor amounts of sand sized bed material. The upper Ottawa River probably contributes all the wood chips found in the Kettle Island South reach of the study section.

All mineral species encountered in the study section sediments have been observed in the local Precambrian rocks and are in accord with the horneblende-granulite subfacies (Winkler, 1965, p.115; Fyfe et al, 1962, p.232). The study section alluvial deposit is therefore a good representative of the metamorphic source area. On the other hand, the deposit is not indicative of the Ordovician sedimentary rock area which comprises a large portion of the Ottawa River drainage basin. This is probably due to the contrast in the detrital stability of the constituents of the two rock types. Hypothetically, if the study section alluvial deposit was encountered in the geologic record, the examiner might well be led to the erroneous conclusion that the entire drainage basin upstream of the deposit was composed of metamorphic rock types. Paleogeographical analyses, therefore, must be conducted with great care.

PART III - HEAVY METALS IN THE OTTAWA RIVER BED SEDIMENTS

PART III - HEAVY METALS IN THE OTTAWA RIVER BED SEDIMENTS

A. INTRODUCTION

a. Statement of the Problem

Mercury (Hg) is a potentially dangerous element which due to metabolic build-up in plants and animals, can reach toxic concentrations; it is therefore deemed that the study of Hg in the ecosystem should be an important area for investigation.

The distribution of mercury throughout the bed sediments of the study section is of obvious interest, and is presented here. Equally important, perhaps, is the elucidation of the various mechanisms which control or affect the concentration of Hg in the bed sediments, and which may indeed also control or affect the concentrations of a host of other trace metals. One process that results in the concentration of heavy metals in sediments, (and one that has recently received much attention) is the adsorption of heavy metals by hydrous oxides of iron (Fe) and manganese (Mn). The object of this paper, then, is to test the hypothesis that Fe and Mn coatings on sediment grains provide sites for the adsorption of other heavy metals, especially Hg.

A review of the literature is presented in order to establish the significance of heavy metals occurring

in hydrous oxide coatings on bed sediments, with respect to the other possible modes of occurrence in the aquatic environment.

B. LITERATURE REVIEW

a. Stable Forms of Fe, Mn, and Hg in Natural Systems

Hydrous oxides of Mn and Fe are ubiquitous in sediments (Jenne, 1968, p.342). Iron is readily available to river waters as a result of life processes (Hem, 1972, p.443) or by the oxidation of iron bearing minerals such as pyrite (Hem, 1960, p.58). Manganese is a common constituent of igneous rock forming minerals, and "wad" mixtures of Mn minerals are common in near surface environments. Weathering of these two hosts provides a ready supply of Mn to solution. Mercury is a rather rare constituent of silver and telluride minerals and of some igneous rocks (Fairbridge, 1973, p.704). Important localized sources have been effluent discharges of the pulp and paper industry (Oliver and Kinrade, 1972).

The concentration of dissolved Hg in river waters is low (parts per trillion levels) probably because Hg compounds are easily adsorbed by particulate matter (Brownstein, pers. comm., 1974). Dissolved iron concentrations are low mainly because iron compounds have low solubilities (Weast, 1974, p.B232). Depletion of oxygen from originally oxygenated water will increase iron solubility significantly,

however, as will complex formation with organic matter (Hem, 1972, p.449).

Eh - pH diagrams (Hem, 1972, p.444) indicate that ferric hydroxide (solid) is the stable compound of iron in aerated waters, ferrous hydroxide (solid) and perhaps some sulfide are the stable forms in reducing environments (Hem, 1960, p.58). Uncomplexed ferrous iron, upon entering aerobic natural waters is quickly oxidized (in a few hours or less) and is precipitated from solutions (Hem and Cropper, 1959, p.23; Hem, 1960, p.87). Precipitating iron takes the form of x-ray amorphous ferric hydroxide, $Fe(OH)_{3(s)}$ (Jenne, 1968, p.342; Langmuir & Whittemore, 1971, p.210), and may undergo changes to poorly crystalline goethite and poorly crystalline lepidocrocite with time (Langmuir & Whittemore, 1971, p.211).

The stable form of Mn should be $MnO_{2(s)}$ at normal pH of 5 to 7, and oxidizing conditions normal to rivers (Gibbs, 1973; Tanaka, 1964, p.118). The solubility of manganese is slightly greater than that of Fe, and oxidation of MnII to MnIV is extremely slow, unless biochemical processes are active (Hem, 1964, p.B40). The oxidation of MnII to MnIV requires a higher pH than the oxidation of FeII to FeIII, in the Eh - pH range of natural waters.

b. Mechanisms of Heavy Metal Transport in the Aquatic Environment

Gibbs (1973) outlined five possible mechanisms of transport of trace metals in the aquatic environment. The mechanisms that he considers are (i) in ionic solution or in solution as organic complexes, (ii) adsorbed on suspended solids (colloids and fine particulate matter), (iii) precipitation and coprecipitation on solids (as coatings), (iv) incorporation in solid biological materials, and (v) incorporation in crystalline structures. Each of these mechanisms are discussed below, in the light of other authors' works in the field.

i) In Solution

The solubilities of the oxides of the ferrous and ferric ions in natural waters are so low that the quantities of these species transported in solution are insignificant (Hem, 1960, p.84; Hem, 1972, p.443). The solubility product for ferrous hydroxide is 1.64×10^{-14} at 18°C, for ferric hydroxide 1.1×10^{-36} at 18°C, for MnII hydroxide 4×10^{-4} at 18°C (Weast, 1974, p.B232); the solubility of $Mn(IV)O_2$ is not published. The solubility of manganese is greater than that of iron at all pH - Eh levels (Hem, 1972) so metal concentration in solution may be greater for Mn than for Fe. However, Fe readily forms complexes with natural water organic substances

(Lee, 1973; and many others) and this feature permits much more Fe to exist in solution than would otherwise be possible. Complexing of Fe with tannic acid (a common constituent in organic debris of soils and forests, and thus common in rivers) retards oxidation of ferrous iron, and hence retains the Fe in solution. Transport times on the order of one month are possible before oxidation finally occurs. Uncomplexed ferrous iron, on the other hand, is oxidized and precipitated from solution in a few hours or less at pH greater than 5 (Hem, 1960, p.84). Other Fe complexes form with organic ligands (negatively charged organic units), chelation (a chelate compound is a ring structure with a central bonded metal atom) readily occurs, and all complexes have the property of maintaining iron in solution. In the light of organic complexing, then, Gibbs' first mechanism of trace metal transport may be significant for Fe. In contrast, Mn-organic complexes may exist, and may be responsible for maintaining Mn in solution (Hem 1963, p.A51), but Morgan and Stumm (1964, p.105) point out that organic ligands cannot compete with hydroxyl for coordination to MnIV in the pH range of natural waters, thus organo-chemical interaction with MnIV should not be prevalent in natural waters.

ii) Adsorbed on Suspended Solids

The second mechanism proposed by Gibbs, transport of trace metals adsorbed on suspended solids, is

responsible for only a small fraction of total Fe and Mn transport in the aquatic environment (Gibbs, 1973). The suspended particles, or colloids, comprise a solid-liquid system. A sol (solid-liquid colloid) consists of a central particle of finely divided material (such as silica, clay mineral, organics or metal hydroxide) which is larger than molecular (greater than 10Å) and smaller than detrital (less than 10,000Å) size. The particle has some pH dependent surface charge (silica and manganese oxide particles are negatively charged, ferric hydroxide particles are either positive or negative) resulting from unsatisfied bonds along surfaces or from atomic substitutions such as Al^{+3} for Si^{+4} in silicate lattices. The solid particle thus attracts a closely held liquid layer of ions of opposite charge, and this layer adsorbs yet another layer of counter-ions, in a more loosely bound manner. The "electric double-layer" which results is the same for all sols in any one system, and thus two such colloids will repel each other, so that flocculation of the particles is not permitted. Heavy metal ions so adsorbed, then, may be transported until flocculation occurs. Flocculation will occur when the effective radius of the sols is reduced, as upon entering a strongly electrolytic environment (such as sea-water) where multivalent ions,

H^+ and OH^- ions are held very closely to the particle. Colloidal particles have large surface area to weight ratios, and hence their adsorption capacity is very high. If the surface charge of the solid particle is negative, then significant amounts of heavy metals could be adsorbed in the manner described, and could therefore be transported to the oceans.

Adsorption as a process grades into the phenomenon known as ion exchange. A colloid, an intra-lattice position, or any surface whatever with one kind of ion adsorbed, when added to an electrolytic solution containing different ions, will liberate some of the original ions and adsorb some of the new species in their place, by the process known as 'ion exchange'. In nature, cations are most commonly exchanged, and the process is then called 'cation exchange'. The ion exchange reaction is simply $AX+B^+ \rightleftharpoons BX+A^+$ where A^+ and B^+ are exchangeable cations and X^- is the negatively charged framework. The framework is usually an aluminosilicate or silicate network held together by predominantly covalent bonds with excess negative charges at well defined sites, occupied by cations held by electrostatic attraction. Exchangeability depends on how the cations are attached to the host, the thermodynamic activity of each cation species, the cation-exchange

capacity, and the adsorbability of the species. (Colloid chem., ion exchange refs: Adamson, 1960, p.179-196 & p.457-520; Bear, 1964, Chapts. 3 and 4; Garrels, 1965, p.267-280; Krauskopf, 1967, p.150; Truesdell, 1972, p.591).

iii) Precipitation and Coprecipitation

Gibbs' third mechanism of trace metal transport is closely related to the preceeding discussion, but applies to precipitation and coprecipitation of heavy metals at the sediment-water interface. The occurrence of metal oxide or hydroxide coatings on sediment grains accounts for the great part of the total Fe and Mn in an aquatic system (de Groot, 1973; Gibbs, 1973). Since hydrous oxides of Fe and Mn are ubiquitous in sediments (Jenne, 1968, p.342), the importance of this mode of heavy metal occurrence is profound.

The amount of heavy metal hydroxide found coating sediments is related to the surface area of the sediment rather than to the cation exchange capacity, which implies that the method of attachment is physical adsorption, rather than ionic bonding, (de Groot, 1973; Jenne, 1968, p.343). Jenne (1968, p.341) proposed that where concentrations of a heavy metal in an aquatic system are high (macro-concentrations), precipitation will occur as the metal's hydroxide (ie. $Cu(OH)_2$,

$Fe(OH)_3$, $Zn(OH)_2$, etc.) but where the heavy metal has only a small concentration (micro-concentration) sorption reactions may predominate. He does not, however, put limits to the micro and macro ranges. Elements such as Co, Hg, Zn, Cr, Cd, Ni, Pb and Cu occur in "micro-concentrations" (approx 1/100 of Fe concentration in natural waters), and hence these species will be found adsorbed to fine surfaces or coprecipitated with other metals' hydroxides (Gibbs, 1973; Goldberg, 1954, p.249; Hem and Skougstad, 1960, p.108; Posselt et al, 1968, p.1087; Shimomura et al, 1969). Lee (1973) points out that these minor elements would necessarily be bound by adsorption rather than by cation exchange, since exchange sites would be preferentially filled by the bulk metals such as calcium and magnesium.

The surface charge or zeta potential (Adamson, 1960, p.190), is of prime importance in determining whether or not a surface will adsorb cations. As mentioned before in the discussion of adsorption of heavy metal ions on colloids, some surfaces have positive and others have negative charges. The sign of the charge on the surface of a given material is often pH-Eh dependent, and there is a specific pH that is the null point, or boundary condition for the sign of the charge. This pH value has been variously termed "isoelectric point", and "zero point of charge (ZPC)" (Krauskopf, 1967, p.156).

The charge on a surface exists for the same reasons as described in the discussion of colloids. In natural waters (ie. pH range from slightly acidic to slightly alkaline) the observed zeta potential of ferric hydroxide can be either positive or negative, but is negative in non-acidic aerated waters (Hem and Skougstad, 1960, p.98), the ZPC being between pH 6 and 7. Ferric hydroxide in a river system can therefore be expected to adsorb cations. Hydrated manganese dioxide ($MnO_2 \cdot xH_2O$) also has a net negative zeta potential within the pH range (5 to 11) of natural waters (Posselt, et al, 1968, p.1088). However, Parks (1967, p.122) finds that its ZPC is near pH 7. In fresh waters, where natural pH may be more acid than 7, the cation adsorption capacity of precipitated MnO_2 will be small, reducing the importance of $MnO_2 \cdot xH_2O$ in determining the concentration of trace metals in fresh waters (Parks, 1967, p.122).

The sorption capacity of a material or a surface is a measure of the amount of dissolved ionic species that can be associated with that material or surface through adsorption. Sorption capacity is dependent upon the zeta potential of the solid material, the surface area of the solid material, and the adsorbability of the ions in solution. Jenne(1968, p.344) notes that the amount of iron adsorbed on clay material

is directly proportional to the surface area[a] of that material. De Groot (1973) observed that the amount of heavy metal adsorbed is directly related to fineness (and hence surface area) of clay sized material. The high cation sorption capacities observed for hydrous manganese dioxide are in accord with the high specific surface areas exhibited by hydrous MnO_2 preparations (Morgan and Stumm, 1964, p.357). The measured surface area of colloidal (hydrous) manganese dioxide varies by author, but is on the order of 300 m^2/gram (Posselt, 1968, p.1088). It is evident then, that the hydroxides of Fe and Mn are high surface area states, allowing them to exert chemical activity far out of proportion to their concentrations (Jenne, 1968, p.343). Quantitatively, the sorption capacity of $Fe(OH)_3$ and MnO_2 for Mn ions

---

(a) Determination of specific surface area can be done in a variety of ways, but the most popular methods involve gas adsorption. Basically the methods consist of exposing a weighed quantity of material to a gas (nitrogen, krypton, or others) which coats the exposed surfaces with a mono-layer of molecules. The amount of gas adsorbed is determined by heat or pressure change, or some other parameter, and knowing the area occupied by each gas molecule, the total surface area may be calculated (Adamson, 1960; Brunauer et al, 1938; Medema, 1969; Taylor, 1951).

is high, .3 mole/mole for $Fe(OH)_3$ and 1 mole/mole for MnO_2 (ie. .3 and 1 mole of Mn is adsorbed per mole of solid $Fe(OH)_3$ and MnO_2, respectively). The sorption capacity of these two materials for Ni, Zn, and Co is slightly less (Jenne, 1968, p.344). The relative adsorption on $MnO_2 \cdot xH_2O$ is Mg(II) and Ca(II) < Zn(II) < Mn(II) (Morgan and Stumm, 1964, p.112).

The adsorbability of the ions in solution necessarily affects the sorption capacity of any surface exposed to the solution. Krauskopf (1967, p.162) proposes three general rules to explain the adsorbability of ions: (i) the smaller of two ions will be more firmly held to a surface, (ii) multivalent ions will be more firmly held than univalent ions, and (iii) covalent character predominates over ionic character. These rules have several common exceptions, which indicate that some unknown factors are involved, but still they are useful in understanding the behaviour of many ions.

Sorption capacity, adsorbability, and specific surface area combine to help explain observed precipitation/co-precipitation units. Several authors have demonstrated the importance of the hydrous metal oxides in the fixation of heavy metals. Often, Fe and Mn hydroxides are found to be the main control on the concentrations of other heavy metals. Gibbs (1973) has observed Co, Ni, and Mn to coprecipitate with ferric hydroxide as

adsorbed species, and Hem (and Skougstad, 1960; & 1963) has studied the coprecipitation of Cu and Mn with ferric hydroxide. Interestingly, Mn and Cu will adsorb to and coprecipitate with ferric hydroxide even at pH levels where Mn and Cu are stable in solution (for Mn, at pH = 6.7, for Cu, at pH = 5.5). According to Krauskopf, the reason that Cu is adsorbed at a lower pH than Mn is that it is the smaller of the two ions, and hence is more adsorbable. The explanation for the coprecipitation of Mn and Cu at such low pH levels is given by Jenne (1968, p.355): one observed property of $Fe(OH)_3$ is to catalyze oxidation reactions such as Mn(II) to Mn(IV) at the solid/water interface, thus rendering the cations insoluble.

Krauskopf (1956, p.24) determined that Fe and Mn hydroxides were a major controlling factor in the concentration of Zn, Cu, Pb, Bi, Cd, Ni, Co, Hg, Ag, Cr, Mo, W, and V in sea water. Shimomura et al (1969) demonstrated that Hg will adsorb to and coprecipitate with ferric hydroxide at some optimum conditions of alkalinity and low halide ion concentrations. Finally, the tendency for Mn oxides to adsorb cations is demonstrated by the high trace metal concentrations in manganese nodules of the Pacific ocean (Goldberg, 1954 & 1963). The high Na/K ratio in sea water may be explained by the greater ease of adsorption of K^+ ions than Na^+ ions on hydrous

precipitates (Garrels & Christ, 1965). Gibbs' third mechanism of heavy metal occurrence in the aquatic environment, the precipitation and coprecipitation of trace metals on solids as coatings, is well supported by the literature, and would appear to be of major importance.

iv) Incorporation in Solid Biological Materials

Gibbs' fourth proposal is the transport of trace metals by incorporation in solid biological materials. Certainly in the course of metabolism the biota in the aquatic system will take up varying amounts of heavy metals. These metals may become concentrated in the cells of living matter by complexing with organic substances, and if so, will be effectively removed from the inorganic compartments of the system until the death and decomposition of the organism. The significance of this mode therefore depends upon the metal uptake of organisms and the concentration of the metals in solution. However, Reimers (1973) has noted a correlation between organic content of sediments and Hg concentration, and Gibbs (1973) has shown that up to 10% of the total Fe, Mn, Co, and Cu in a river system occur in organic solids.

Organisms have a secondary effect on the chemistry of heavy metals that may also be significant. Hem (1963, p.A57; & 1964, p.16) has found that oxidation of MnII to the relatively insoluble MnIV state is rapid only in the presence of organisms. Lee (1964, p.124) states

that photosynthetic organisms cause local MnO_2 precipitation because their life processes increase the pH of the surrounding water and encourage oxidation of dissolved MnII, such that insoluble MnIV precipitates. Hence in biologically active waters, organisms can cause the oxidation and subsequent precipitation of Mn.

v) Incorporation in Crystalline Structures

Gibbs attaches much importance to his fifth mode of trace metal transport. He records that up to 75% of total Cu and Cr, up to 50% of total Co, Fe, and Ni, and up to 35% of total Mn in rivers is transported incorporated in crystalline structures. This may be the case, but this method cannot be considered as one likely to fix pollutants, since the process of solid state diffusion is very slow, and the amount of trace metals incorporated by lattice penetration is small compared to the total amount sorbed (Jenne, 1968, p.339). Weathering of minerals containing trace metals will introduce natural concentrations of metals to the ecosystem, however.

c. Summary of Literature Review

The literature reviewed above indicates that precipitation and co-precipitation as grain coatings is an important fixation mechanism for heavy metals in the aquatic environment. More specifically, hydrous

oxide coatings of Fe and Mn possibly control the concentrations of several other heavy metals, including Hg, by providing adsorption sites for those species. Sediment fineness (or more correctly, sediment surface area) is an important factor in the concentrations of heavy metal grain coatings.

A study of the relationships between grain size and the concentrations of Fe, Mn, and Hg in coatings, and between the metal concentrations themselves is therefore important to the understanding of the mechanisms of trace metal transport in the Ottawa River bed sediments.

C. EXPERIMENTAL WORK

a. Laboratory Methods, Results and Levels of Confidence

i) Sampling and Subsampling

Bottom sediments were taken at various locations in the study area (Fig. 6) with a Shipek grab. The shipek grab penetrates unconsolidated sediments down to depths of about 15 cm., and so the samples can be considered to be representative of the large scale sedimentation in progress. Each sample that was to be chemically examined was subsampled as follows: (i) approximately 50 grams for Hg determination, and (ii) approximately 50 grams for Fe and Mn determinations. Care was taken to avoid subsampling error and bias, and new containers were used everywhere to avoid contamination.

ii) Hg Determination

The subsamples for Hg determination were sent to the laboratories of NRC for professional analysis. Flameless atomic adsorption methods were usod to measure the amount of Hg in the samples. The samples were partially dried at low temperature to avoid vaporisation of Hg. Duplicate samples were fully dried then ashed at 450°C to determine moisture content and organic matter concentration. Surface Hg in nannograms/gram, (ppb) dry weight was measured at least twice for each sample to test reproducibility, and the mean and range

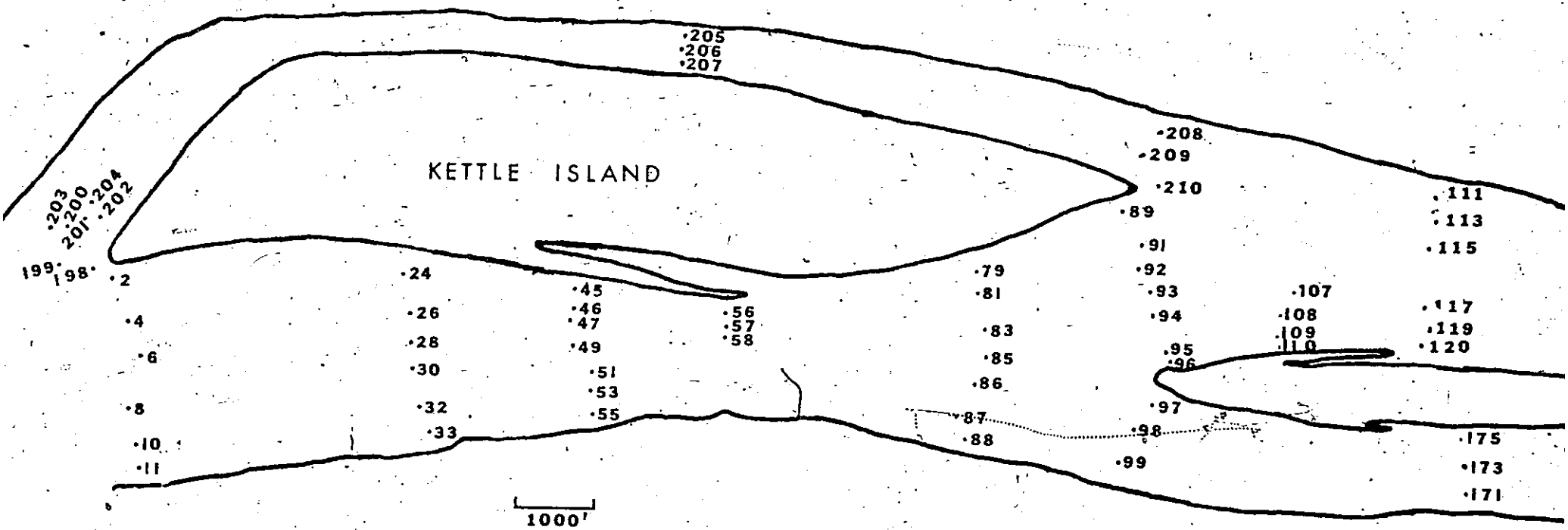

.55 Sample Location

FIG 6 : SAMPLE LOCATIONS

of the values obtained were reported.

iii) Fe and Mn Determinations

Since only the Fe and Mn present as coatings on the sediment grains were to be measured, various leaching experiments were conducted to determine the best method of dissolving the metallic coatings only. Once brought into solution, the concentrations of Fe and Mn were measured by conventional atomic absorption spectrophotometry methods, with a Techtron instrument. The absorbance of the unknown concentrations of Fe and Mn in solution were compared with working curves prepared after running the standard solutions of the metals both before and after the unknowns were tested. Appendix II contains two representative working curves, one for Fe, the other for Mn, both in 12% HCl. The analyses of Fe and Mn by A.A.S. techniques are not subject to interference effects, according to the Techtron instruction manual.(a)

The first leaching method tested used 10% acetic acid. Five equivalent 5g subsamples were each exposed to 150 ml of acid. The leachate of one sample was filtered off after 1 hour, and others after 2 hours, 4 hours, 6 hours, and 10 hours. The concentrations of iron and

---

(a) Interim Instruction Manual for Techtron Model AA-4, Atomic Absorption Spectrophotometer; Techtron Pty. Ltd., Melbourne, Victoria, Australia; p.27.

manganese in the leachate were then determined. There was no detectable manganese in any of the solutions, and iron was barely detectable in only the 10 hour sample.

The same samples (BS8, BS56, and BS85) were then exposed to 150 ml of 12% HCl for the same exposurestimes as before, and the concentrations of Fe and Mn were tested again. The results of leaching the three samples with 12% HCl are given in graphical form (Figs. 7 and 8) with leached iron and manganese concentrations plotted against leaching time.

Each of the six plots consists of two basic parts. A linear section, which begins at or before one hour and continues on past 10 hours, follows a steeper portion of the curve which begins at the origin. The steep slope of the first portion of the curves represents the relatively fast dissolution of highly susceptible forms of iron and manganese, probably the dissulution of hydrous oxide coatings of those two elements. For iron, the less steep slope of the linear portion of the curve that follows must represent the slower dissolution of more firmly bonded iron, such as that which is incorporated in the crystalline structure of iron bearing minerals such as magnetite. The parallelism of the linear portions of the BS8 and BS85 curves for iron implies that the previous statement is valid; one would expect

FIG. 7 : LEACHED Fe CONC. vs. LEACHING TIME
(12% HCl)

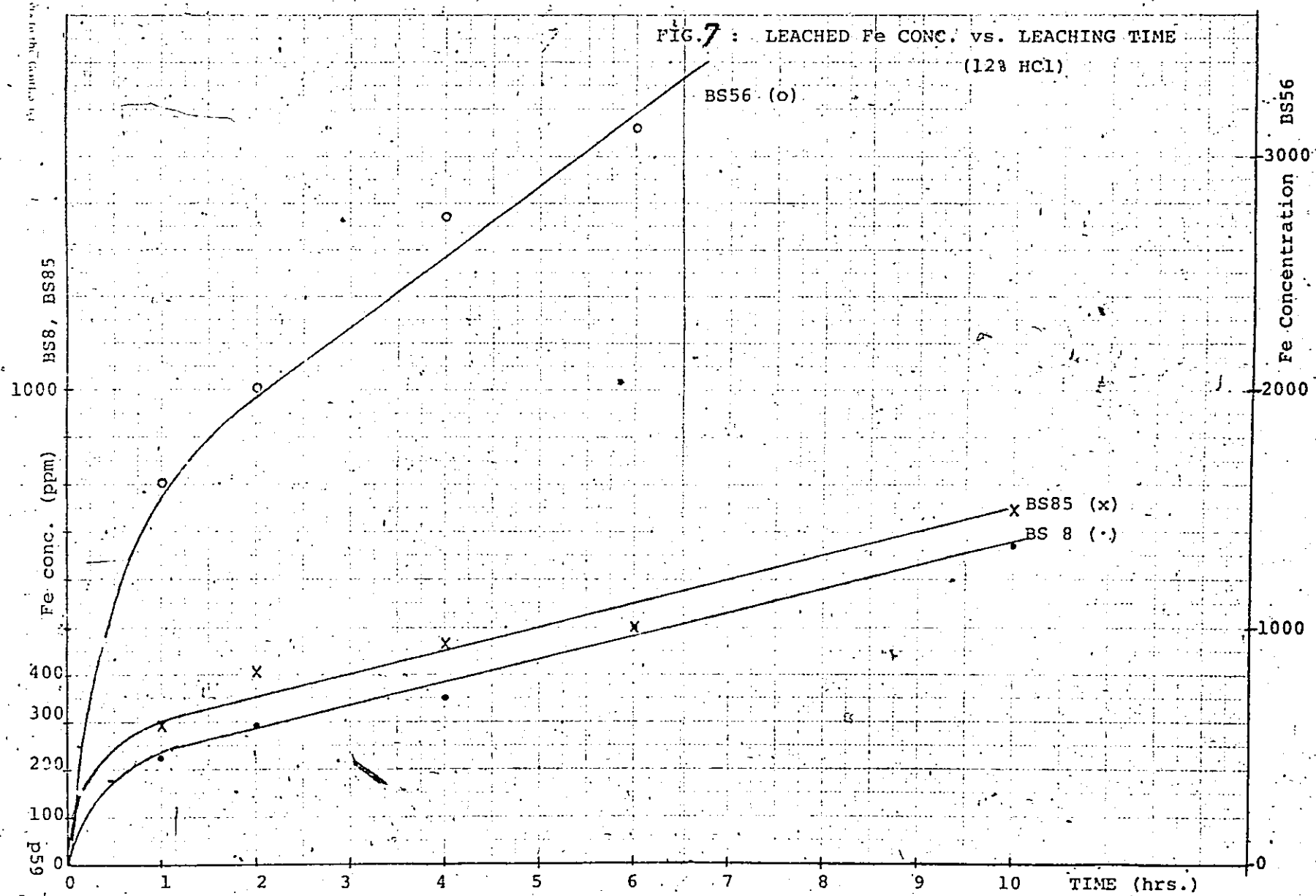

FIG. 8 : LEACHED Mn CONC. vs. LEACHING TIME
(12% HCl)

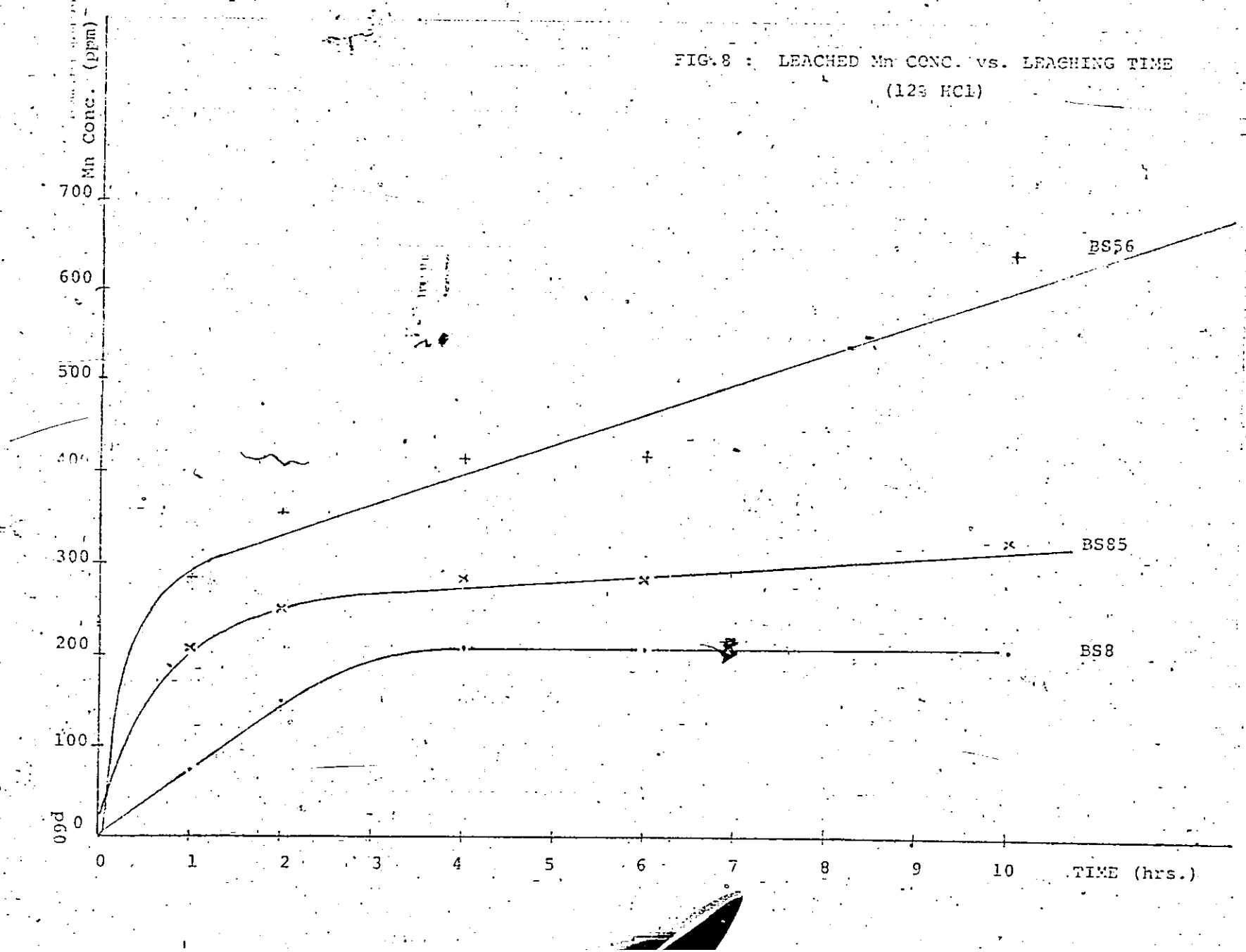

the amount of metal coating to vary from one sample to another, but since mineralogical work shows that the mineralogy of samples BS8 and BS85 are the same (see PART II, MINERALOGY), the slopes of the linear portions of the two curves should be parallel, which they are. The separation of the linear portions of the two curves is explained simply by the fact that the two samples had different concentrations of iron in the coatings.

In order to determine the effect of magnetite on the leached Fe concentrations, 3 subsamples were made from BS26, one "bulk" subsample was left as it was, the second subsample had all (magnetic) magnetite grains removed, and the third consisted of magnetite grains only. Magnetite grains comprised only about 5% of the bulk sample, therefore considerable concentration was necessary to obtain enough magnetite for analysis. The subsamples were subjected to the acid leach, and leached Fe concentrations were measured after 1½, 2½, and 3 hours. The results of this test are displayed graphically in Fig. 9.

It is apparent that the dissolution of magnetite alone does not account for the slope of the linear portion of the leaching curves. The "magnetite-excluded" curve has only a slightly lower slope than the "bulk" curve. It is likely, then, that other phases of iron

FIGURE 9: LEACHED Fe CONCENTRATION vs LEACHING TIME
(MAGNETITE SEPERATED FROM SAMPLE BS26)

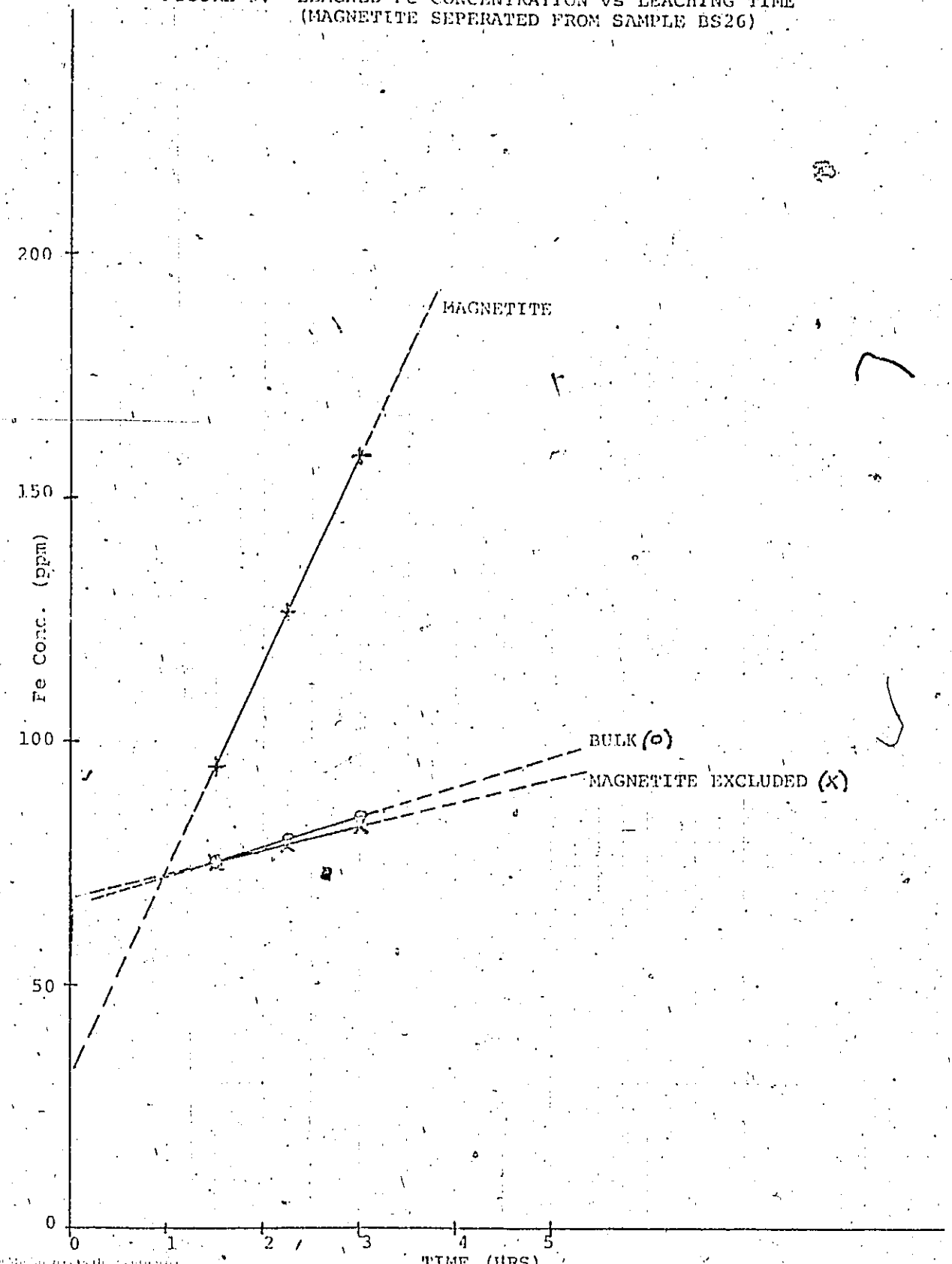

are also being dissolved, probably from a constituent more common than the 15% concentration of magnetite. Mineralogic work (see Part II) showed that quartz and feldspars were the only constituents with higher concentrations than magnetite, so it is likely that Fe associated with those minerals contribute the large part of the Fe after one hour.

Magnetite itself was dissolved quickly by the leach, but not as quickly as the highly susceptible Fe coatings, as was postulated above. For manganese, the two basic portions of the curves represent the same sort of dissolution sequence. However, for manganese samples BS8 and BS85, the horizontality of the linear portions of the curves indicates that perhaps only one (highly susceptible) phase of Mn is being attached, that within the first hour.

The finer grained sample BS56 is different from the coarser grained samples BS8 and BS85 in that the amount of Fe and Mn occurring as coatings is significantly higher. Also, Fe and Mn from other more stable phases are attacked more vigorously in the fine grained sample than in the coarse grained samples. This is indicated by the steeper slope of the second (linear) portion of the Fe and Mn leaching curves. The higher Fe and Mn concentrations present in the finer grained sample are

in accord with several authors' findings that the concentration of heavy metals is directly proportional to sediment fineness (de Groot, Jenne, etc.). That the Fe and Mn from other more stable sources are more readily dissolved in a fine grained sample than in a coarse grained sample is perhaps explained by the high surface areas of fine grained sediments and which are therefore more susceptible to acid attack than the particles of a coarse grained sample.

The leaching experiment was repeated once more, using the same three samples (BS8, BS56, and BS85) with 5% HCl as the solvent. The results of this test are illustrated by figures 10 and 11. These graphs are very similar to those plotted for 12% HCl, the only differences being that for 5% HCl the breaks-in-slope are less will defined and occur later (ie. shifted to the right), and that the dissolution rates of Fe and Mn from lattice positions are slower than for 12% HCl.

The amount of Fe and Mn in solution after one hour of exposure of the sediment sample to 12% HCl is considered to be the most correct value of the absolute concentration of Fe and Mn occurring in coatings, on the basis of the experiments described above. The fact that the break-in-slope, which represents the total amount of leachable Fe and Mn, is better defined on the plots of the 12% HCl test, and the fact that in general, the

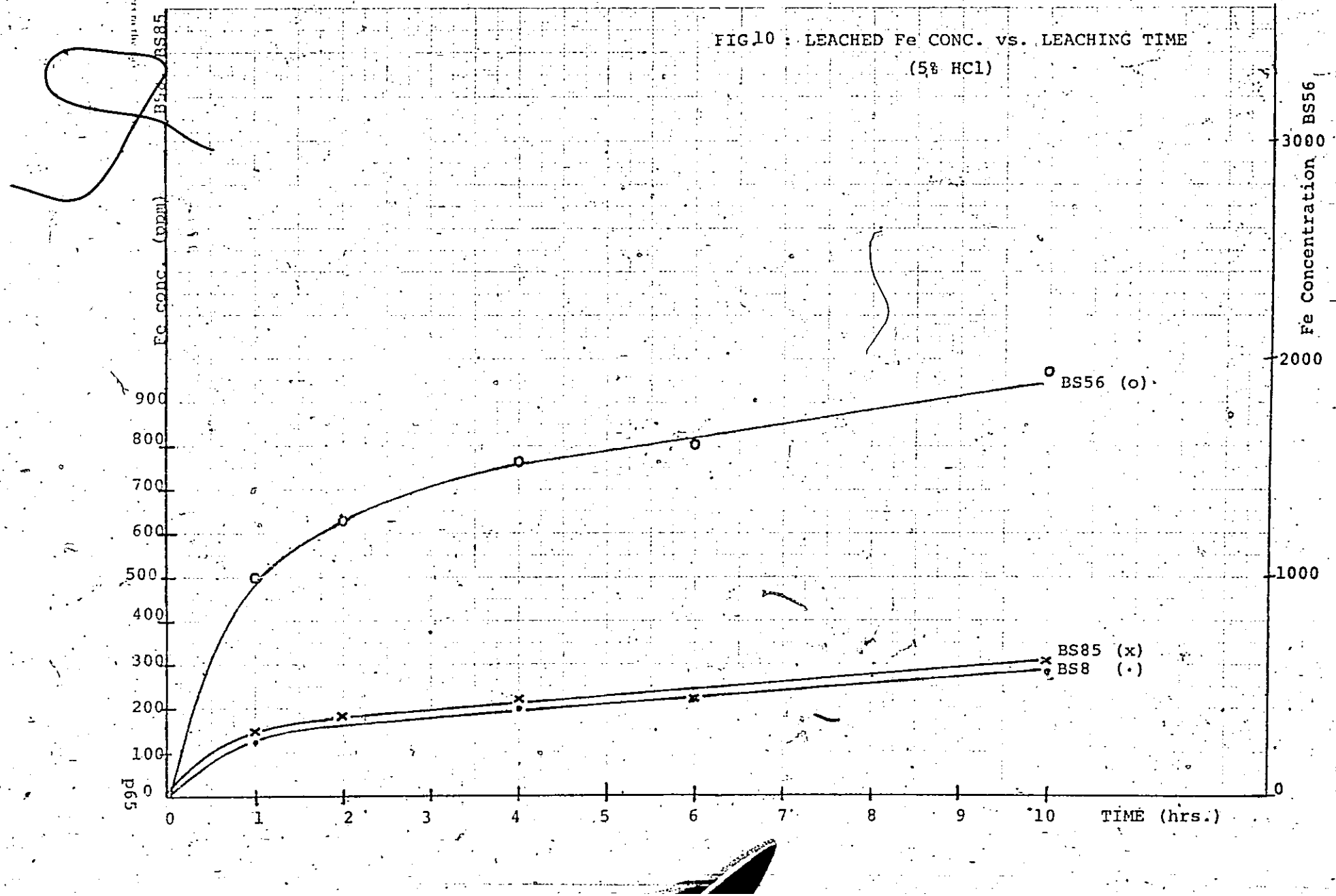
FIG.10 : LEACHED Fe CONC. vs. LEACHING TIME
(5% HCl)
Fe conc. (ppm)
Fe Concentration BS56
BS56 (o)
BS85 (x)
BS8 (·)
TIME (hrs.)
0
100
200
300
400
500
600
700
800
900
1000
2000
3000
0
1
2
3
4
5
6
7
8
9
10

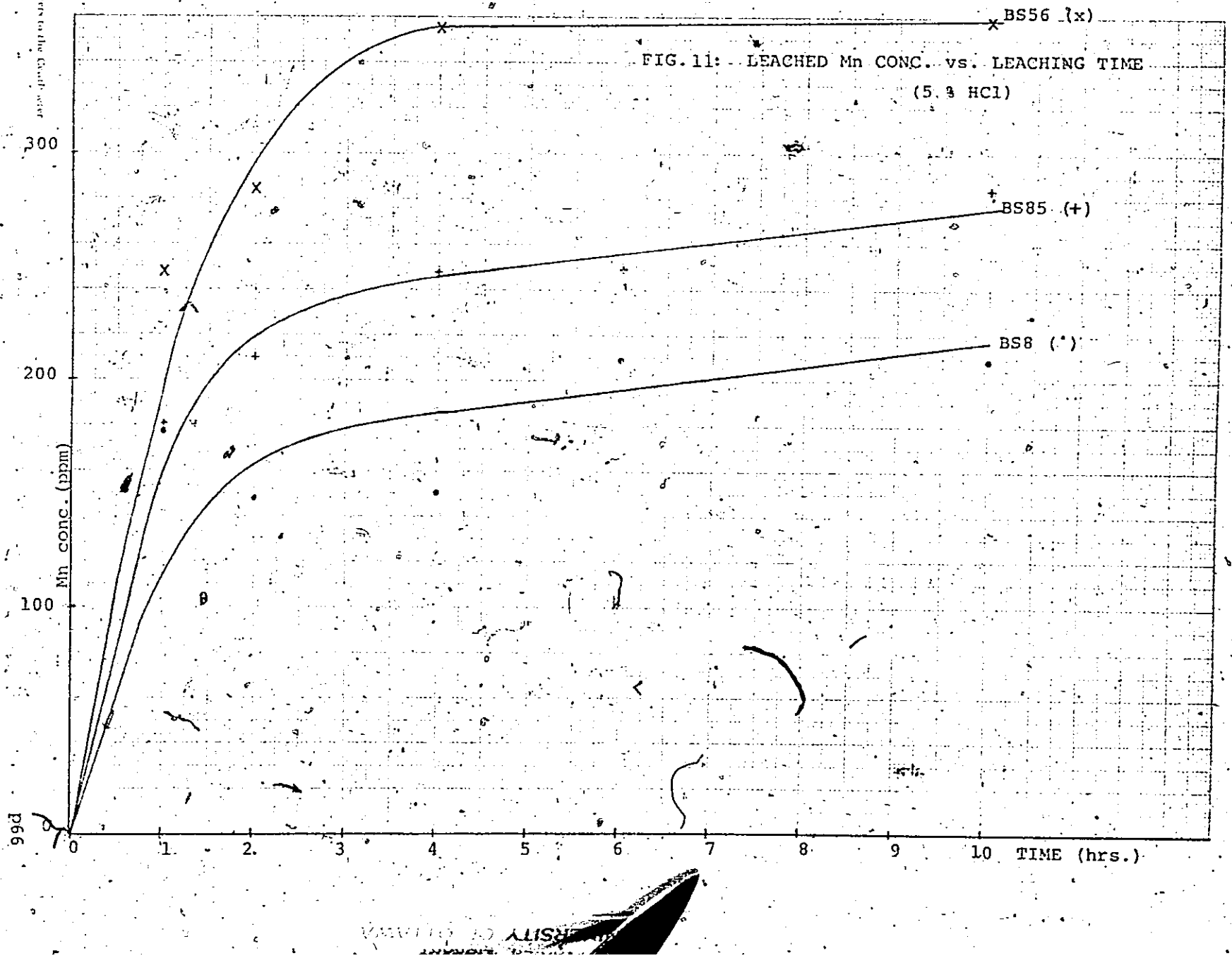

FIG. 11: LEACHED Mn CONC. vs. LEACHING TIME
(5 % HCl)

break-in-slope occurs at or before one hour for five of the six curves in figures 7 and 8 indicate that the one hour/12% HCl value is valid. The obvious error in using this value is that the exact time within the first hour at which the break-in-slope occurs is not known. If one assumes that the coatings went into solution within the first few minutes, then by extrapolating the linear portions of the curves in figures 7 and 8 back towards the ordimate, one obtains new values for Fe and Mn concentrations. These values are in the neighborhood of 10% less than the one hour values for Fe in samples BS8, BS56 and BS85, and approximately 5-10% less for Mn in the same samples. Maximum errors of these magnitudes should not have an adverse affect on the results obtained, since trends and general relationships are of greater importance than absolute values in the study of natural systems.

The 41 other samples analysed for Fe and Mn were treated with 12% HCl for one hour, and the concentrations of Fe and Mn calculated are reported in Table IV, along with Hg concentrations for each sample. Most samples were analysed in duplicate, and mean values are reported. The results of the duplicate analyses were usually within 10%. Where two results were more than 10% apart, subsequent analyses were conducted to establish reproducibility. In addition, samples BS2, BS8, BS85, BS110,

TABLE III: SEPARATION OF SAMPLES INTO COARSE AND FINE FRACTIONS

Sample	Ø Grain Size Boundary	Facies
BS2a	≥ 2.5	Medium & coarse sand
2b	< 2.5	medium & fine sand
8a	≥1.5	coarse sand & wood chips
8b	<1.5	medium & fine sand & fibres
85a	≥2.0	medium & coarse sand
85b	< 2.0	medium & fine sand
110a	≥3.0	sand & wood chips
110b	< 3.0	fine sand & silt & fibres
207a	≥3.0	wood chips & minor sand
207b	< 3.0	fine sand & silt
209a	≥ 3.0	sand & wood chips
209b	< 3.0	fine sand & silt
210a	≥ 2.5	wood chips
210b	≥ 3.5 < 2.5	sand & wood fibres
210c	< 3.5	silt & wood fibres

TABLE IV: HEAVY METAL CONCENTRATIONS

SAMPLE	MEAN SIZE (Ø)	Hg	Fe	Mn
BS 2	2.057	15ppb	175ppm	14ppm
4	1.664	56	568	32
6	1.043	9	116	10
8	0.749	33	254	17
10	1.378	76	525	41
24	1.923	14	178	13
26	1.731	5	179	23
28	1.605	19	218	9
30	1.325	10	183	17
32	0.764	12	193	22
45	1.955	3	196	13
46	1.832	10	203	6
47	1.808	12	147	12
56	3.613	43	1421	17
57	2.068	68	222	10
58	1.981	15	240	15
79	2.173	102	425	26
81	1.648	10	138	6
85	0.580	24	207	16
87	0.644	12	229	31
89	3.968	47	1296	27
91	1.798	66	437	8
92	1.835	19	204	10
93	1.288	9	255	21
94	1.293	6	241	8
95	0.531	1	199	5
98	3.000	262	1390	57
107	1.450	28	228	14
108	1.403	33	259	8
109	1.434	56	372	26
110	2.544	174	1550	71
199	2.000	36	499	23
200	2.056	18	309	41
201	2.083	6	309	17
202	2.012	37	393	24
203	2.017	24	425	52
204	2.157	22	350	59
205	1.533	478	1428	588
206	2.088	16	245	25
207	8.656	121	2040	104
208	1.700	600	1199	280
209	1.337	62	779	56
210	8.631	821	1906	54

BS207, BS209, and BS210 were divided into the coarse and fine fractions listed in Table III. These and all other size separations were conducted by standard sieve and pipette procedures. Each size fraction of each sample was exposed to 12% HCl for 1, 2, and 6 hour periods, and the concentration of iron and manganese was determined. As with the leaching experiments conducted previously, the plot of metal concentration vs. leaching time consists of a curve with two basic parts. A steep initial portion of the curve is followed by a linear portion. The results of this experiment are plotted in figures 12 to 18. A discussion of the results obtained in all experiments is presented in the following section.

b. Discussion and Conclusions

i) on the separation of samples into coarse and fine grain size fractions

The leachable Fe and Mn concentrations of the sample groups tabulated in Table III are plotted against leaching time in figures 12 to 18. Three characteristics can be seen in the behavior of leachable Fe and Mn with respect to the size fractions in which they occur.

Samples BS2 and BS85 are well sorted, non-organic sands with minor silt. The fine fractions (BS2b and BS85b on figures 12 and 14 respectively) clearly have higher concentrations of leachable iron and manganese

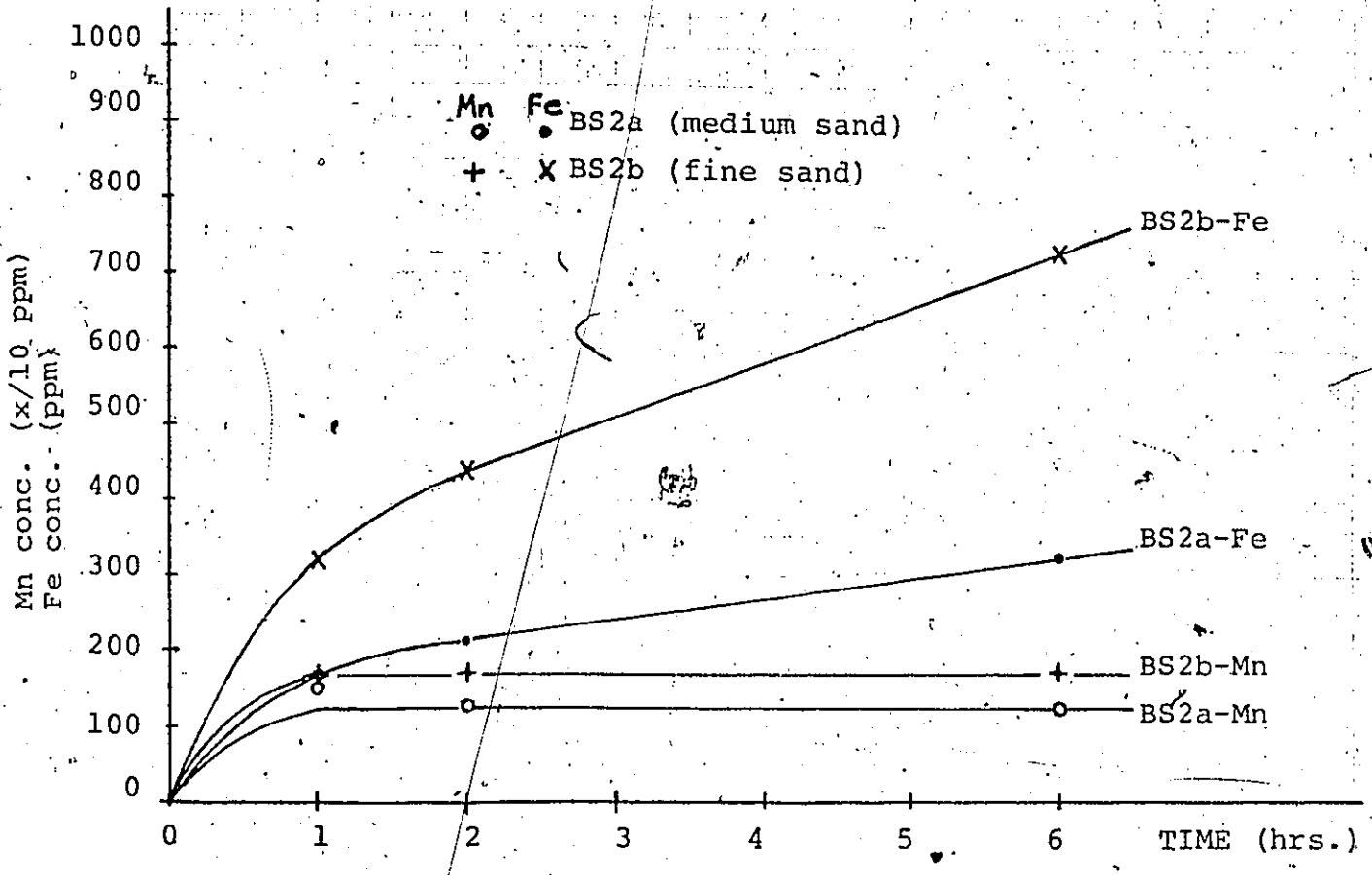

FIG. 12: LEACHED Fe & Mn CONC. vs. LEACHING TIME (12% HCl)

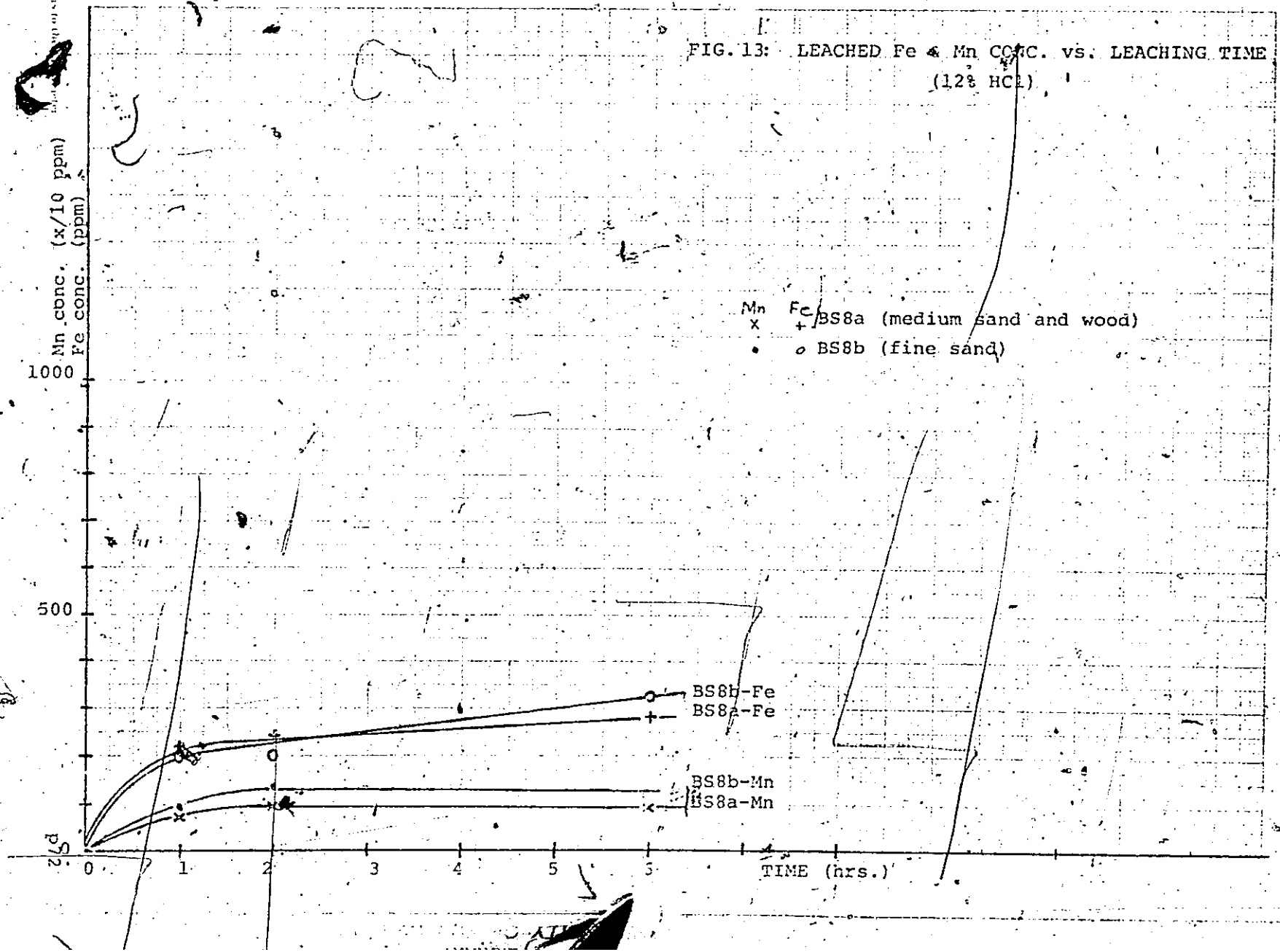

FIG. 13: LEACHED Fe & Mn CONC. vs. LEACHING TIME (12% HCl)

FIG. 14: LEACHED Fe & Mn CONC. vs. LEACHING TIME
(12% HCl)

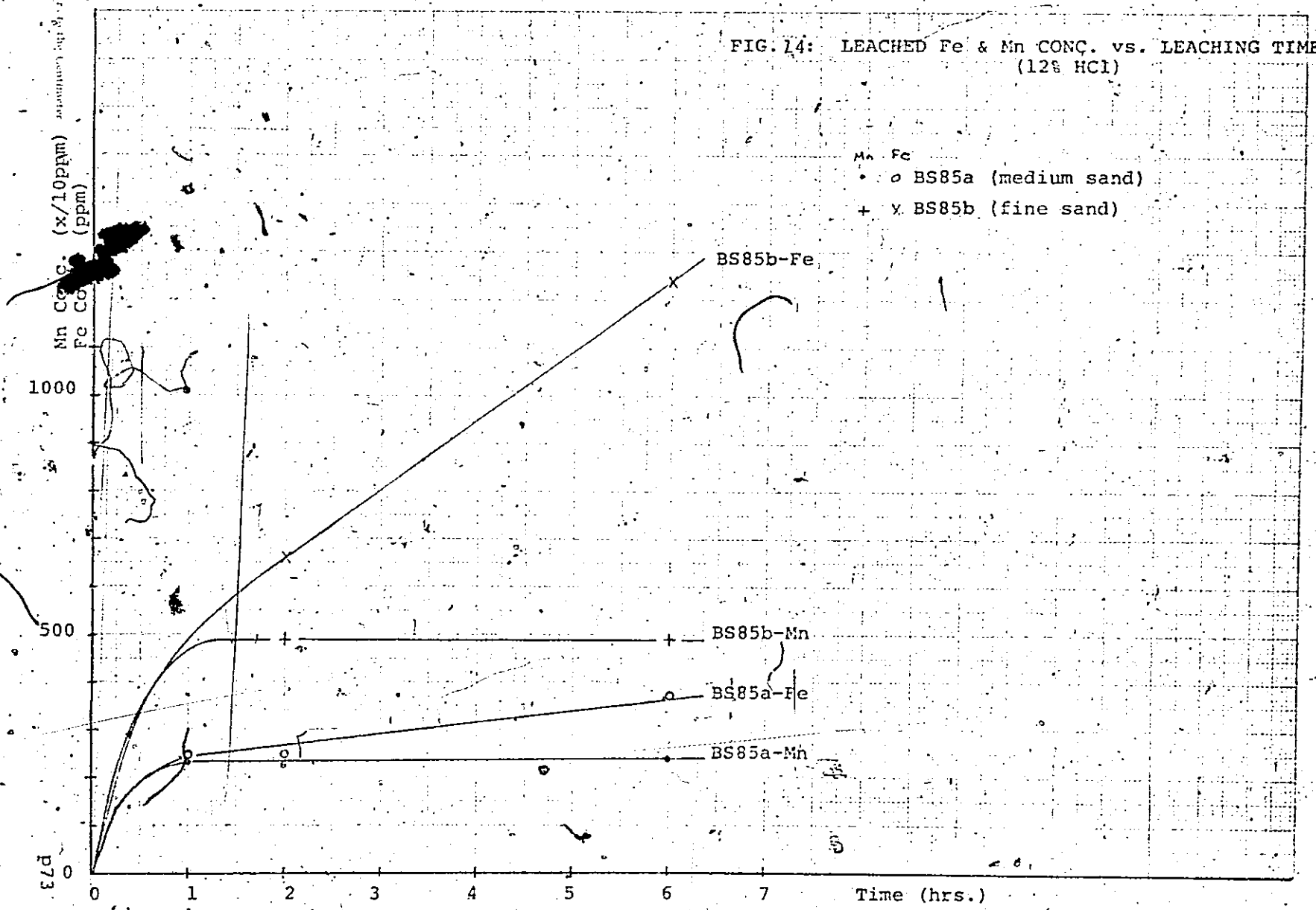

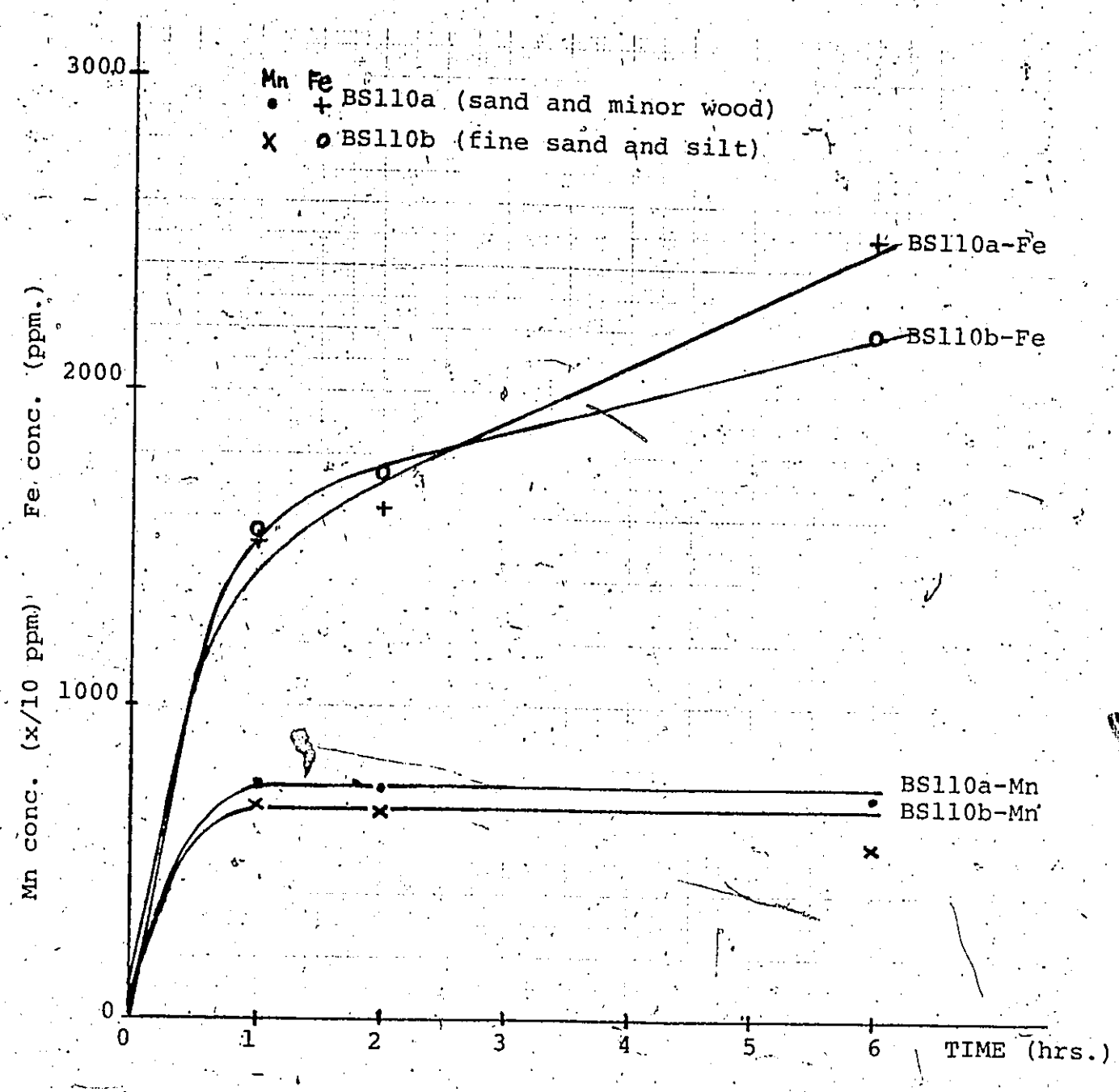

FIG. 15:- LEACHED Fe & Mn CONC. vs LEACHING TIME
(12% HCl)

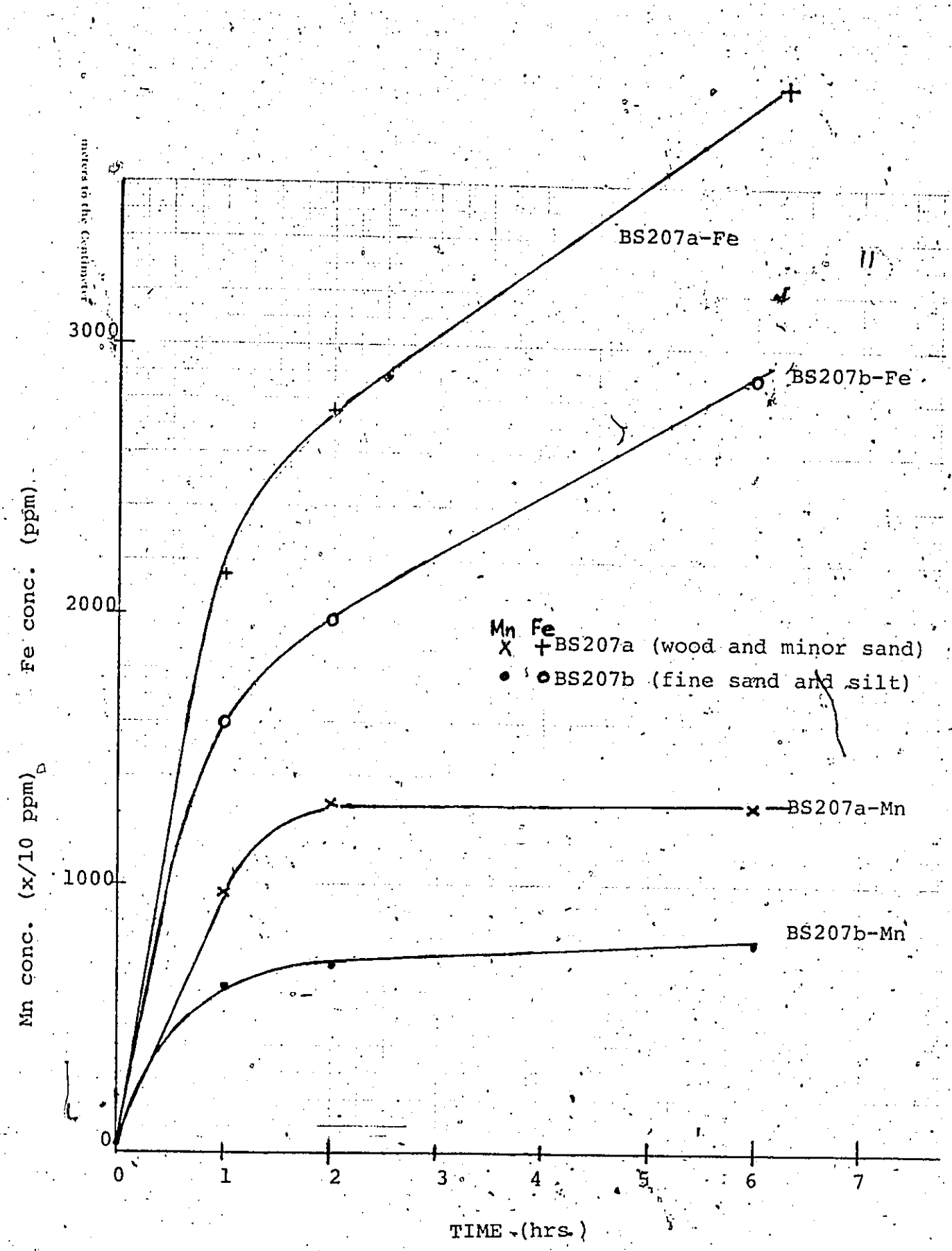

FIG. 16: LEACHED Fe & Mn CONC. vs. LEACHING TIME (12% HCl)

FIG.17: LEACHED Fe & Mn CONC. vs. LEACHING TIME (12% HCl)

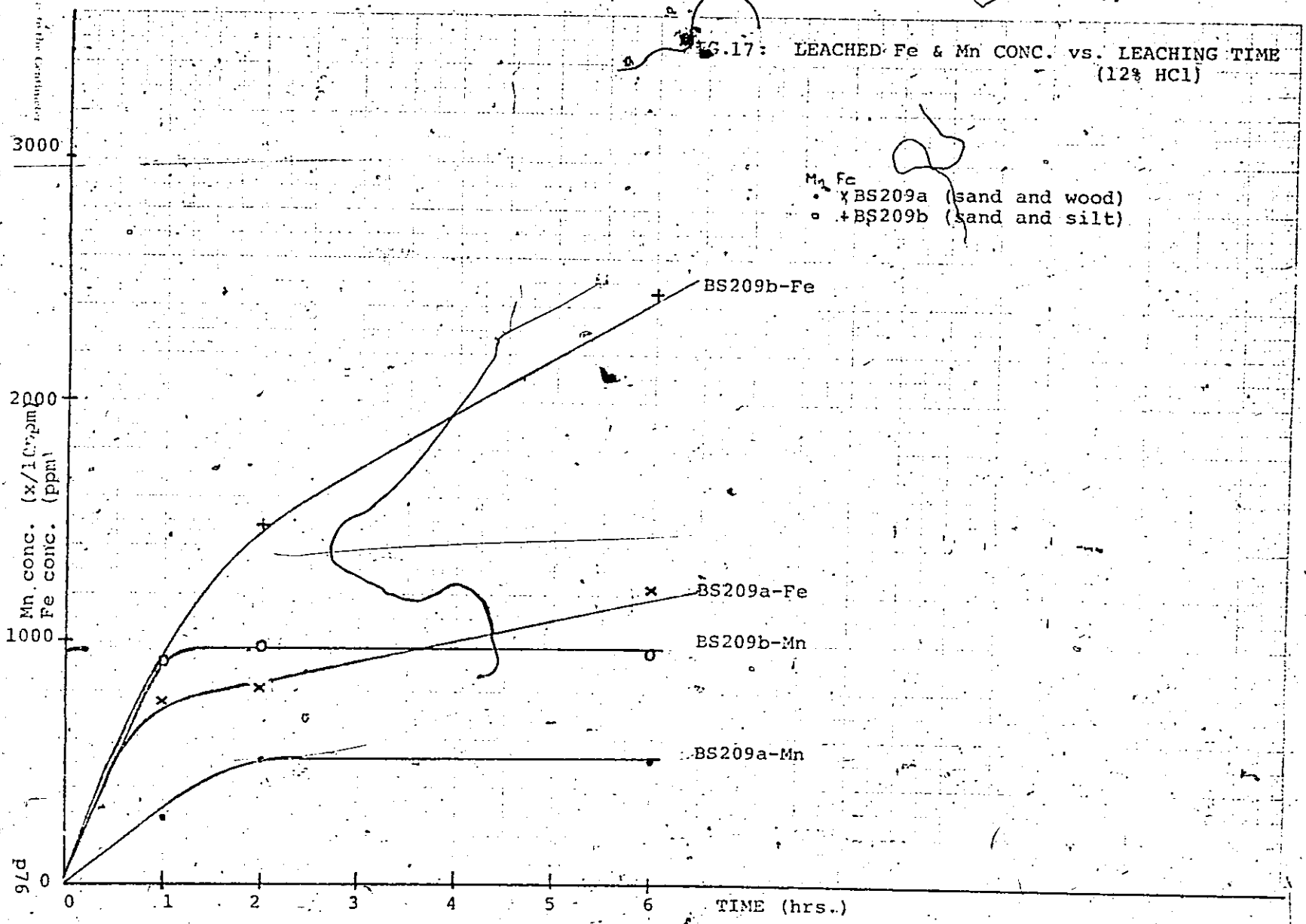

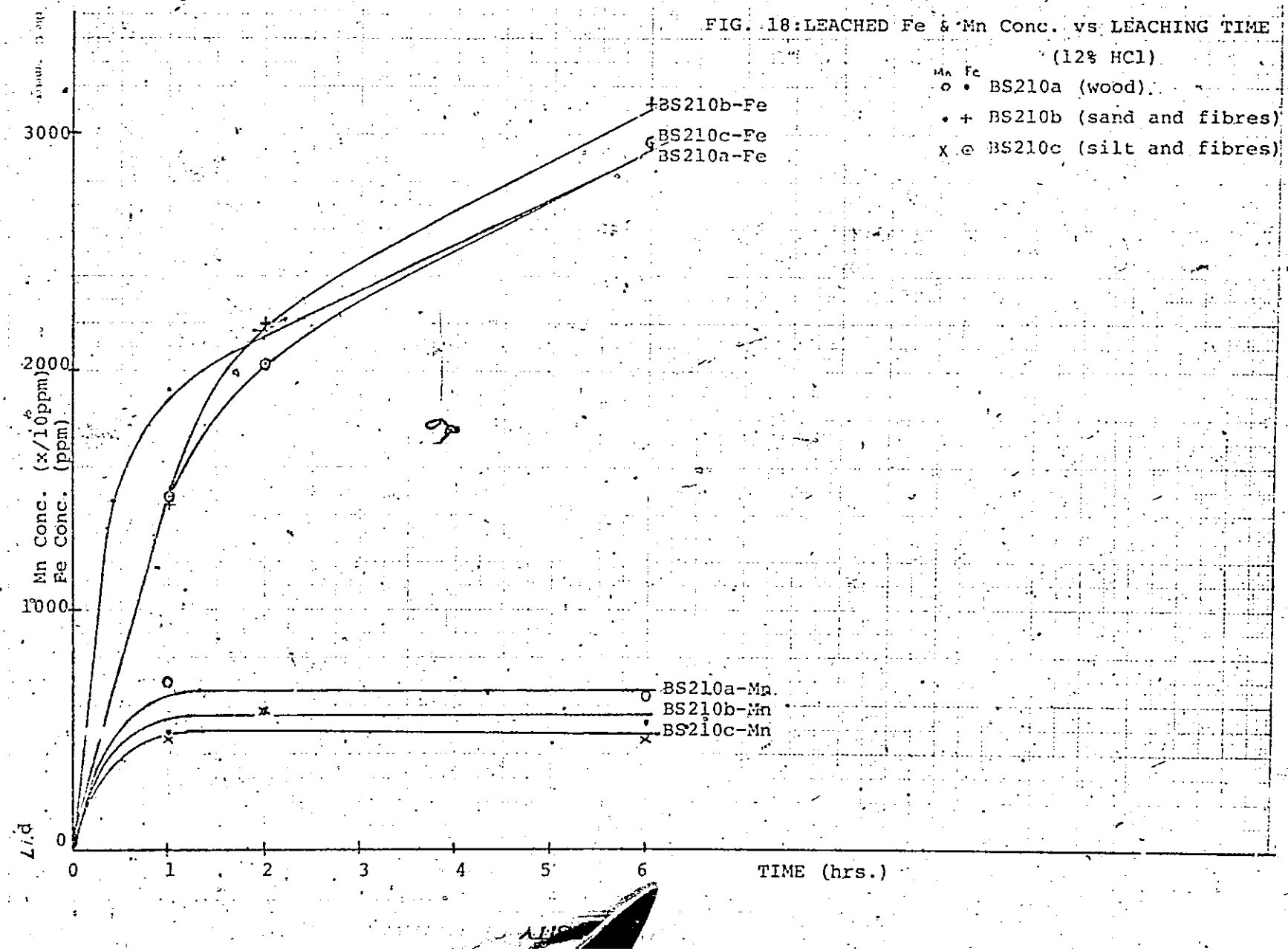
FIG. 18:LEACHED Fe & Mn Conc. vs LEACHING TIME
(12% HCl)
Mn Fe
o • BS210a (wood)
• + BS210b (sand and fibres)
X ⊙ BS210c (silt and fibres)
BS210b-Fe
BS210c-Fe
BS210a-Fe
BS210a-Mn
BS210b-Mn
BS210c-Mn
Mn Conc. (x/10ppm)
Fe Conc. (ppm)
3000
2000
1000
0
0
1
2
3
4
5
6
TIME (hrs.)

than do the coarse fractions (BS2a and BS85a). The leachable iron content of the coarse fractions is only 40 to 50% of the iron content of the fine fractions. The leachable Mn content of the coarse fractions is 50 to 70% of the Mn concentrations in the fine fractions.

Samples BS8, BS110, and BS210 are similar in that the various size fractions of each sample contain practically equal concentrations of leachable Fe and Mn (Figs. 13, 15, & 18). The presence of wood debris in the coarser fractions appears to be the key to the high Fe and Mn concentrations found there. The effect of wood debris is clearly seen in the plot of sample BS210a (Fig. 18). This sample group is the coarsest fraction of BS210, but it consists entirely of wood chips. The Fe and Mn concentrations in this are as high as in the two finer fractions of BS210. Sample BS209 (figure 17) also has some wood debris in the coarse fraction, although not as much as in samples BS8, BS110, and BS210, and so the concentrations of Fe and Mn are distributed more like the non-organic samples (BS2 and BS85) discussed previously.

Sample BS207 shows the third characteristic of Fe and Mn concentration with respect to the grain size fractions examined. Figure 16 shows a high Fe and Mn concentration in the coarse group (BS207a) and a much lower Fe and Mn concentration in the fine group (BS207b). This reversal of behavior as compared to the non-organic

samples (BS2 and BS85) is due to the fact that the coarse fraction is almost wholly composed of wood chips, whereas the finer group has no organic debris whatever. This is also in contrast with samples BS8, BS110, and BS210 which have wood debris present in all size fractions.

The conclusion to be drawn from this experiment is that wood debris in the Ottawa River bed sediments is an important factor in the concentration of Fe and Mn in the sediments. That wood chips and wood fibres should be such good sorbers of heavy metals such as Fe and Mn seems logical, considering the high surface areas that they must present to the aqueous environment. Evidently this wood material is not actively decomposing (oxidizing) in the river system, as the oxidation of organic material would cause a reducing condition in the surrounding water, which would encourage solution of Fe and Mn rather than adsorption of Fe and Mn to the wood. In fact, on inspection the wood chips do appear fresh and unaffected by their environment.

The expected trend of higher heavy metal concentration in fine, rather than coarse sediments is borne out by this experiment. This trend occurs, in the absence of wood debris, as a result of the high surface areas of fine grained sediment as compared to coarse grained sediment.

ii) On the distribution of Fe, Mn, and Hg in the bottom sediments of the study area

The results of the analyses of leachable Fe, Mn and Hg are presented in Tables IV and V. The concentrations of Fe vary widely from 116ppm to 2040ppm, Mn concentrations vary from 5ppm to 588ppm, and Hg concentrations vary from 1ppb to 821ppb. Figures 19, 20, and 21 show the areal distribution of the three heavy metals in the study area. The three contour maps show several striking similarities. In the channel south of Kettle Island there is a general increase in heavy metal concentration towards the shores from a minimum which follows a line somewhat south of center-channel. In the western half of this channel, the highest heavy metal concentrations occur against the southern shore, and in a node which parallels the southern shore of Kettle Island about one-third of the channel south of Kettle Island. This node continues into the eastern half of the channel, but swings north to lie against the southern shore of Kettle Island.

In the eastern half of the channel south of Kettle Island the distribution patterns become more complex. The highest values of heavy metal concentration occur along the southern shore of Kettle Island and along the south shore of the channel. However, the band of high concen-

TABLE V: SAMPLES FOR WHICH Hg ANALYSES ALONE WERE CONDUCTED (in ppb)

Sample	Hg	Sample	Hg
BS 11	145	BS 99	5
33	17	111	402
49	27	113	40
51	9	115	5
53	7	119	5
55	23	117	10
86	8	120	2
88	26	171	4
97	14	173	9
98	12	175	20
		198	9

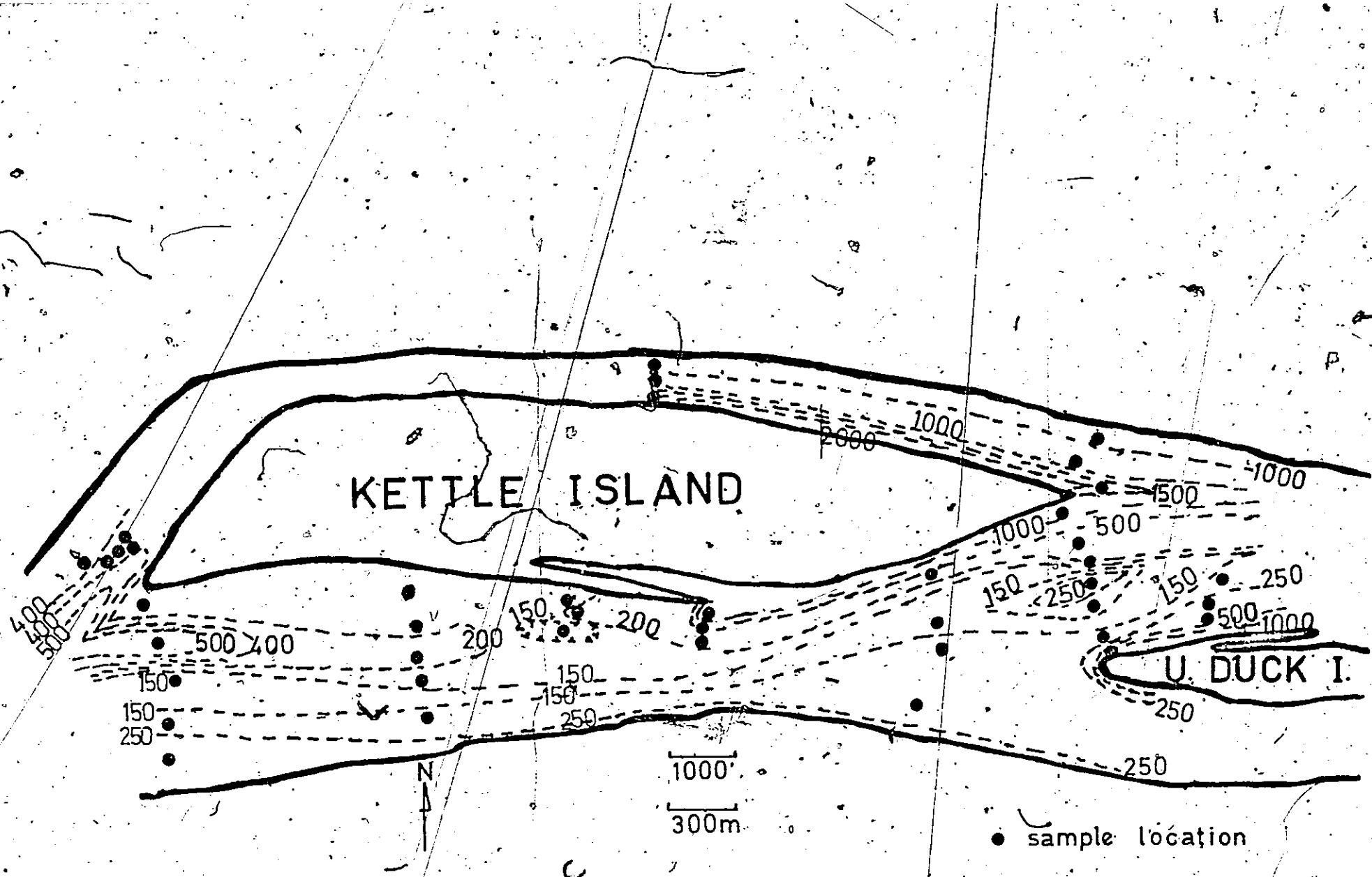

FIG. 19: Fe DISTRIBUTION IN BOTTOM SEDIMENTS (ppm)

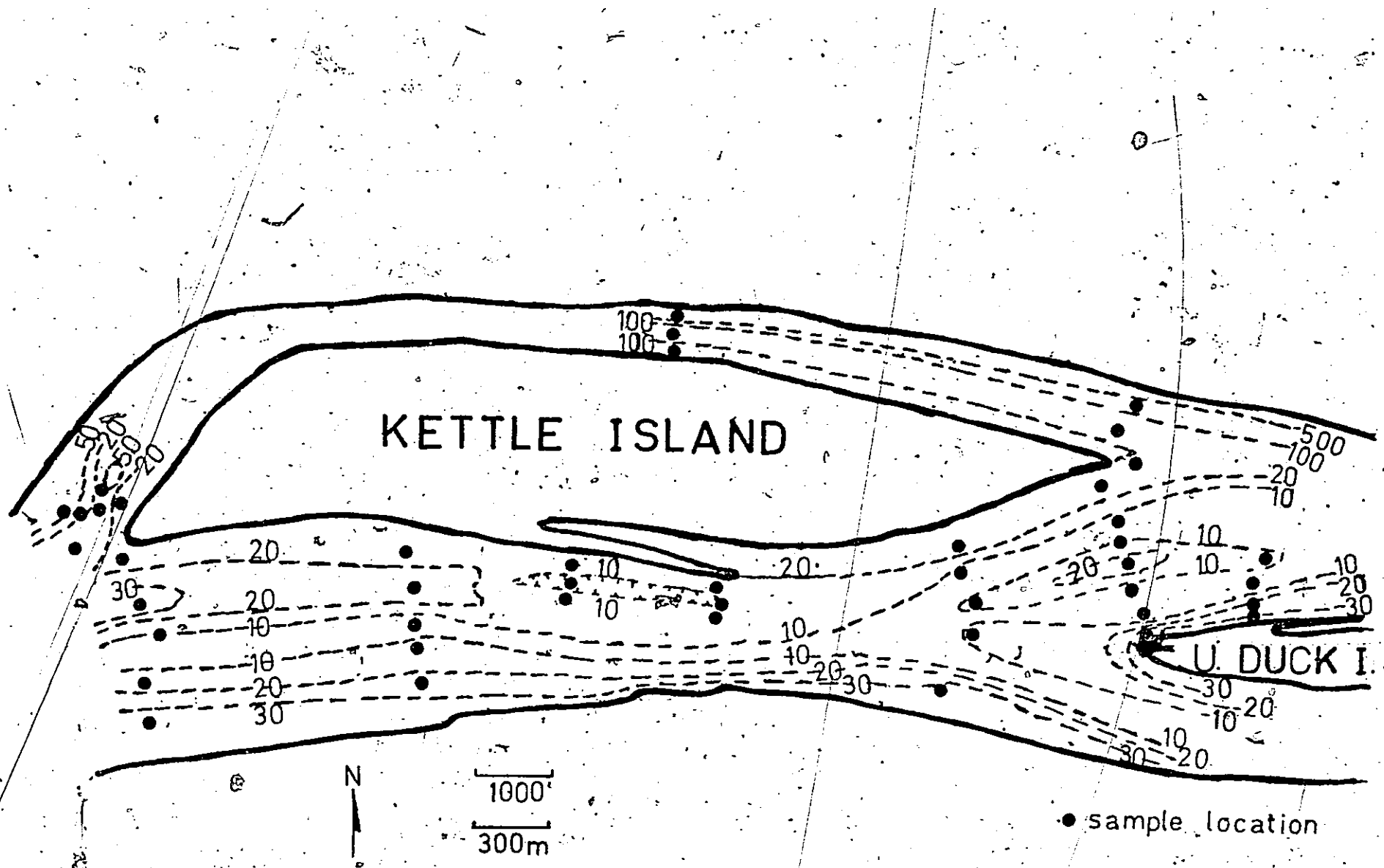

FIG. 20: Mn DISTRIBUTION IN BOTTOM SEDIMENTS (ppm.)

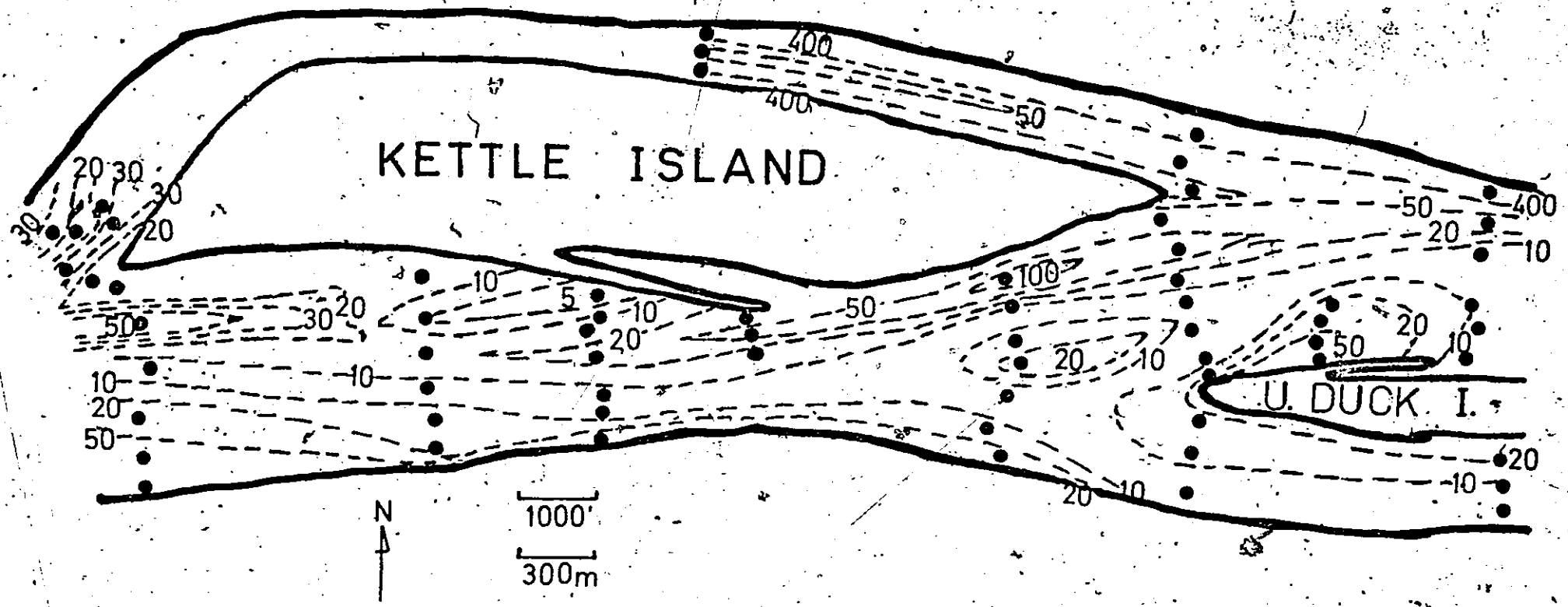

FIG. 21: Hg DISTRIBUTION IN BOTTOM SEDIMENTS (ppb)

trations seems to terminate against the south shore, just south of the upstream tip of Upper Duck Island. High concentrations are found around the shoreline of Upper Duck Island, and although the record is incomplete in the channel to the south, the concentrations appear to decrease towards the southern shore (especially Hg concentration).

In the channel between Kettle Island and Upper Duck Island there is again a tendency for heavy metal concentrations to increase from mid-channel towards both shores, but here there is an anomalous area of high concentrations between the two islands, within the central band of minimum heavy metal concentrations.

The channels north of Kettle Island was sparsely sampled due to the presence of large booming grounds, so it is not possible to present a complete distribution pattern. However, the upstream part of this channel shows that the western point of Kettle Island splits an area of high heavy metal concentrations, which must begin upstream of the study area, into two areas, one directed into the north and one into the south channel. The general trend, apart from the anomalous area (perhaps 'band' is a better description in the case of Mn and Hg) of high concentrations, is of increasing values from center channel towards either shore.

The eastern half of the channel which lies north of Kettle Island has rather simple distribution patterns in regard to the Fe, Mn and Hg concentrations. A center channel minimum is flanked on both sides by quickly increasing values. Although there is a lack of samples in the western part of the channel, it is evident that Fe, Mn, and Hg concentrations are lower at the head of the channel than at the mouth. In the area where the north channel again joins the main channel, sediments with high heavy metal concentrations are evidently diluted by sediments with lower metal concentrations from the main channel.

Each of the distribution patterns of heavy metal concentrations in the bed sediments show notable similarities to the others. The factors in control of the occurrence and distribution of heavy metals in the study area, then, are likely to be the same for all three metals, Fe, Mn, and Hg.

Figure 22, a map of the relative flow velocities encountered in part of the study area, shows a very strong correlation with the maps of heavy metal distributions. The line of maximum flow velocity from base line A to base line D on figure 22 follows very closely the central band of minimum heavy metal concentrations seen on figures 19, 20, and 21. The velocity profile constructed on

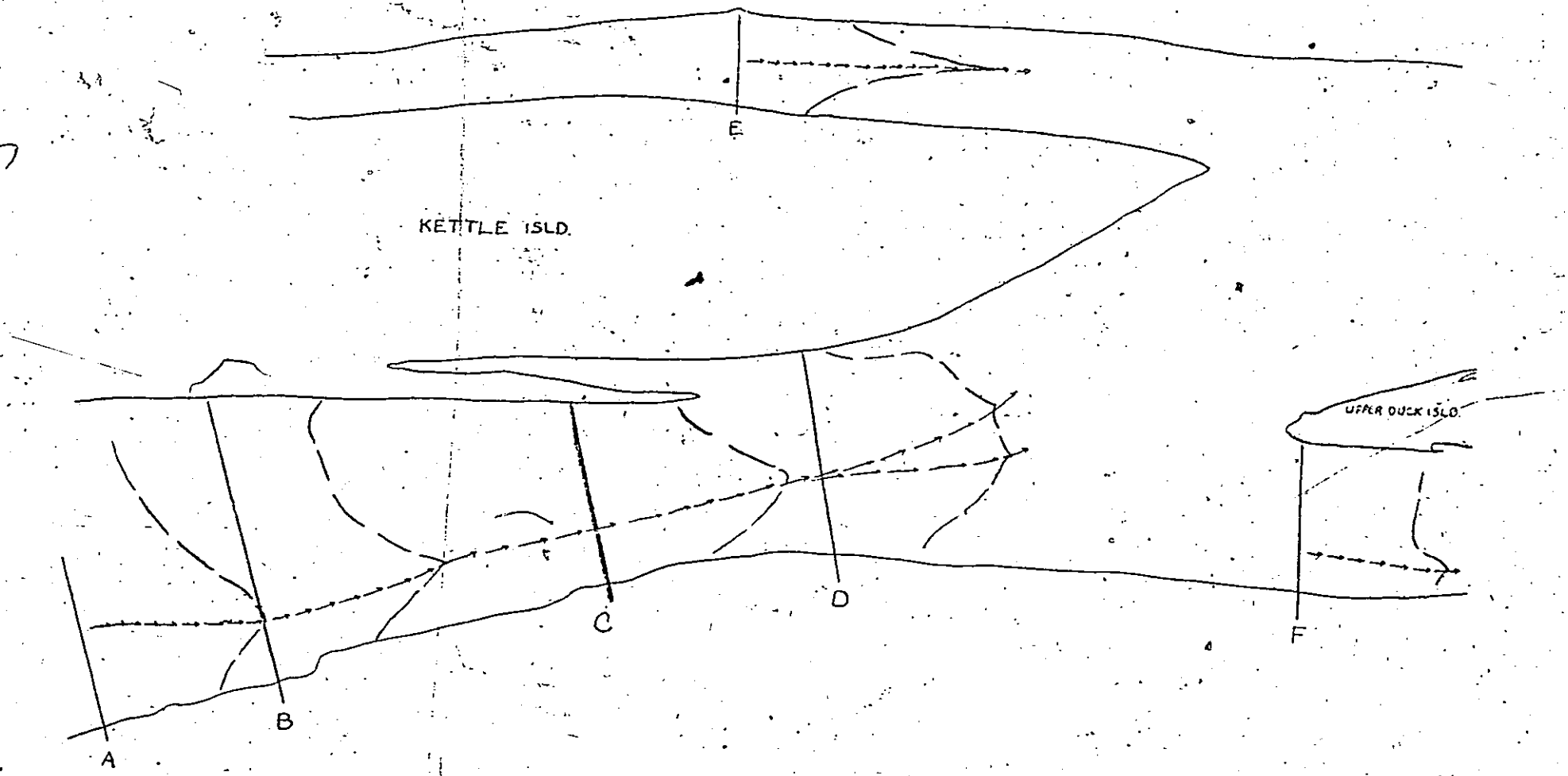

FIG. 22 : FLOW VELOCITY DIAGRAM

MAX. FLOW LINE

A–D, E & F BASE LINES

VELOCITY PROFILE

N.B. DISTANCE BETWEEN BASE LINE AND VELOCITY PROFILE EQUALS SPEED

SCALE: 0 2

base line D shows a divergence of flow, just upstream of Upper Duck Island. The divergence is probably due to the presence of Upper Duck Island. The velocity profile in the channel north of Kettle Island also shows an inverse relationship with respect to the heavy metal distribution in that channel, as does the velocity profile representing flow in the channel south of Upper Duck Island.

The obvious conclusion to be drawn at this point is that flow velocity and the occurrence and distribution of Fe, Mn, and Hg concentrations in the study area are somehow related. The relationship is an inverse one as far as the magnitudes of flow velocity and heavy metal concentrations are concerned. (ie. heavy metal concentration $\propto$ 1/flow speed). The direction of the flow velocity coincides with the orientation of the distribution pattern of heavy metal concentrations.

The relationship between flow velocity and heavy metal concentration may be only secondary, since a previously discussed experiment (p.70) showed that sediment grain size is a major factor controlling heavy metal concentration. Flow velocity of course primarily determines the size distribution of the sediments. Figure 23 shows the pattern of distribution of mean grain size for the study area sediments, as determined from textural

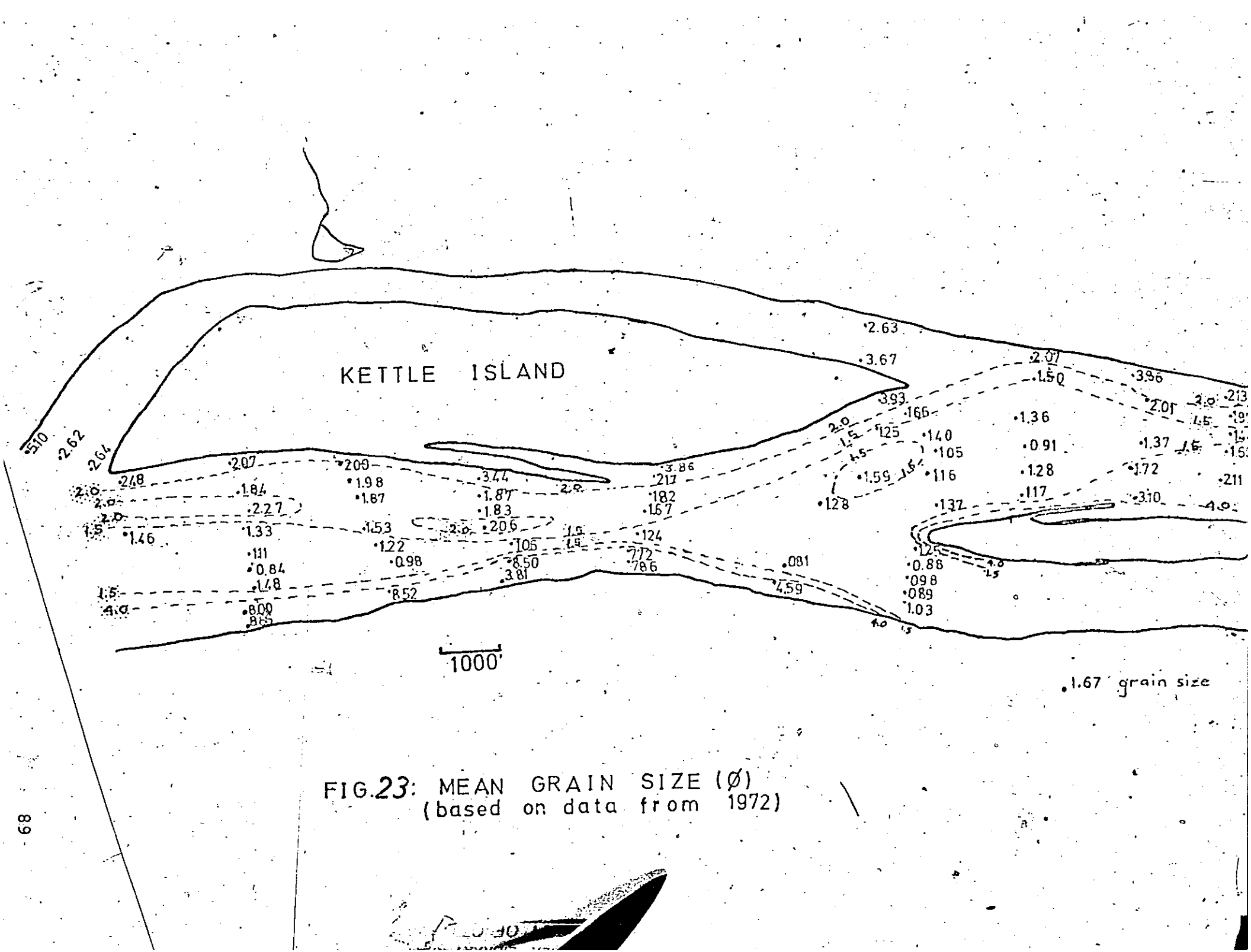

FIG.23: MEAN GRAIN SIZE (Ø)
(based on data from 1972)

analyses of samples taken one year before the samples currently under examination (the 1972 textural data is more complete at this time than the 1973 data; limited grain size data from 1973 samples show the same trends).

It is apparent that flow velocity and mean grain size are closely related, as one would expect. Coarse grained sediments occur where velocities are highest, and finer grained sediments occur where the velocities are lower. Also, the relationship between grain size and heavy metal concentration, becomes apparent again, by comparing the heavy mineral distribution patterns (Fig. 14, 15, & 16) with the mean grain size distribution pattern (Fig. 18). Heavy metal concentration appears to be directly proportional to fineness of sediment. This relationship is in accord with the literature, especially DeGroot (1973).

So as to quantify the relationship between mean Ø grain size and heavy metal concentration, graphs of the two variables were plotted (Figs. 24, 25, and 26). Logarithmic values are used due to the wide range of values.

Two linear regressions and their correlation coefficients were calculated by the Pearson method, for each heavy metal. One regression represents all sample points, the other represents all points except those

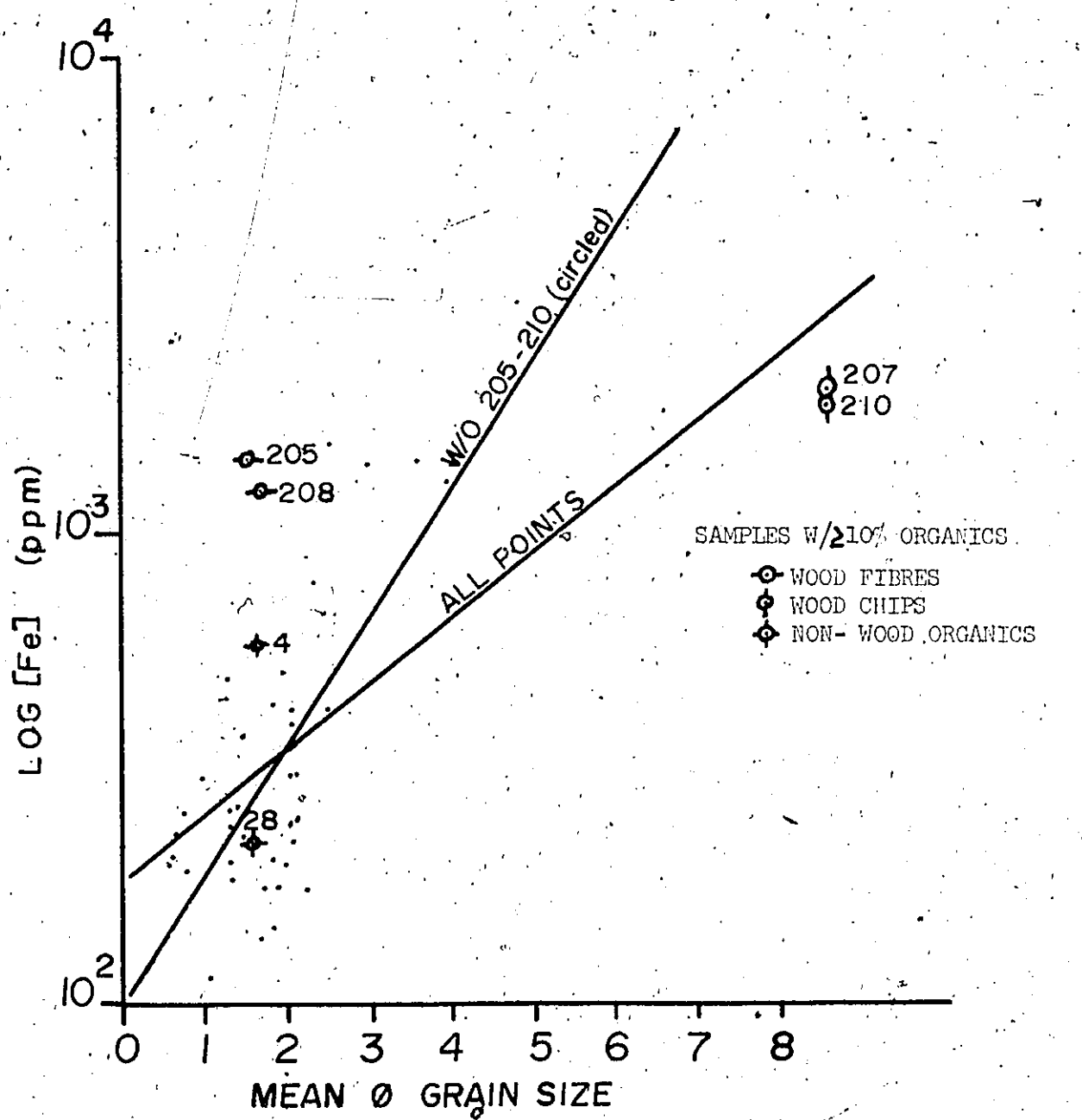

FIG. 24: Plot of LOG Fe concentration vs Mean ϕ grain size

Log Fe = 1.9999 + .2760 ϕ ; r = .7020 (all points except 205, 207, 208, & 210)

Log Fe = 2.2726 + .1374 ϕ ; r = .6464 (all points)

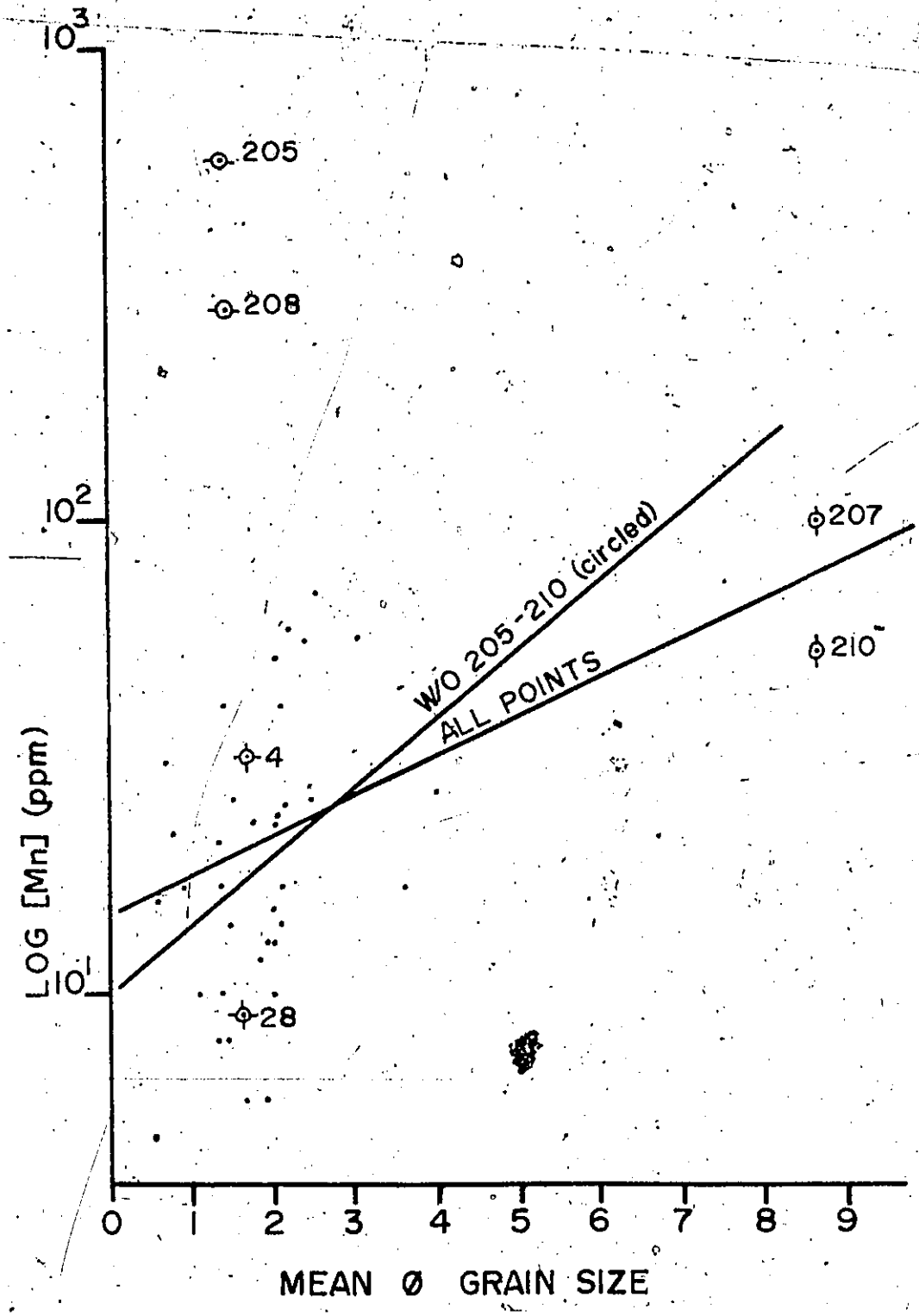

FIG. 25: Plot of LOG Mn concentration vs Mean Ø grain size
Log Mn = .9991 + .1485 Ø ; r = .3635 (all points except, 205, 207, 208, & 210)
Log Mn = 1.1837 + .0822 Ø; r = .3166 (all points)

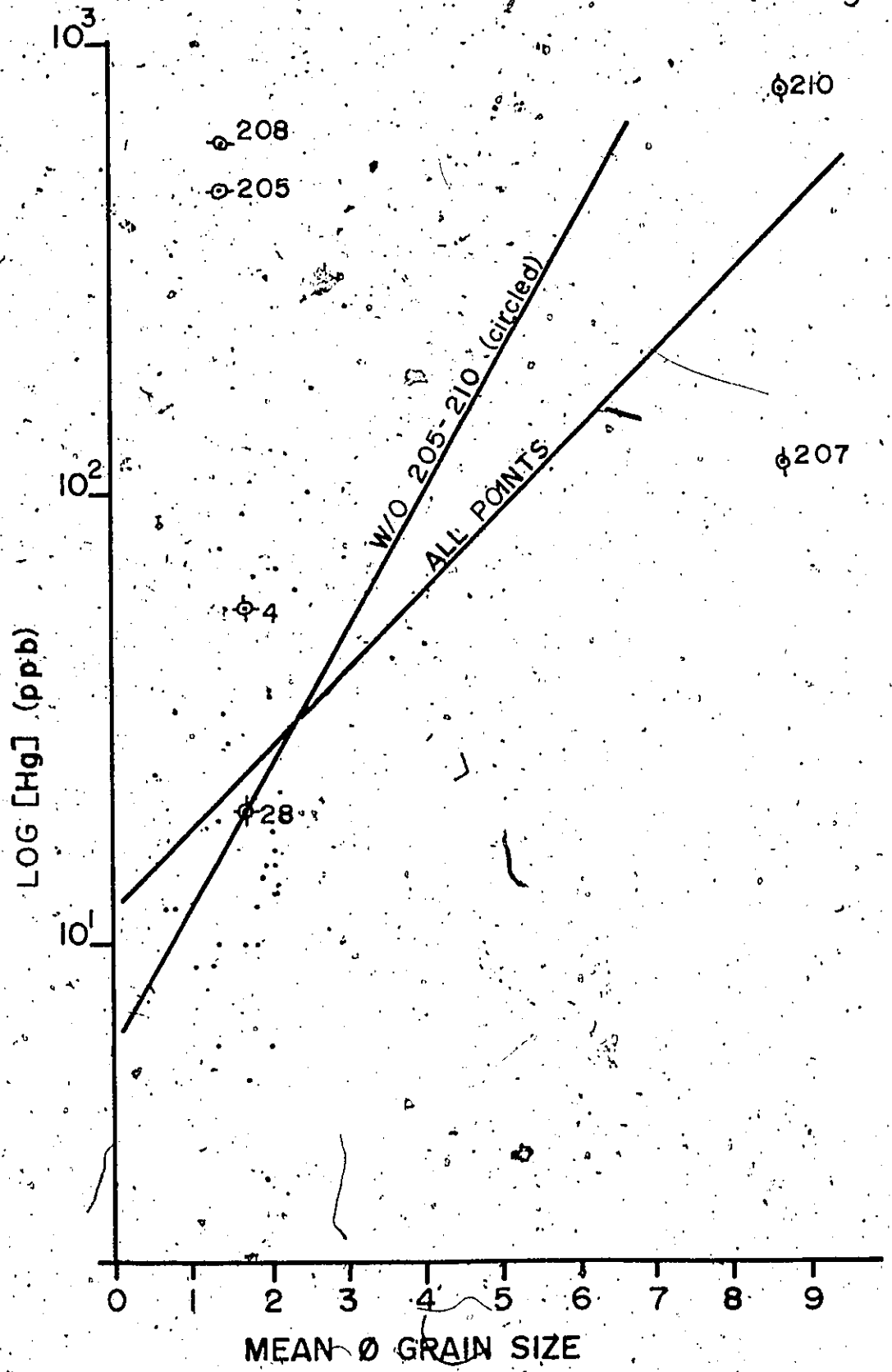

FIG. 26: Plot of LOG Hg concentration vs Mean ∅ grain size

Log Hg = .7802 + .3083 ∅; r = .4715 (all points except 205, 207, 208, & 210)

Log Hg = 1.0644 + .1779 ∅; r = .4807 (all points)

with high wood debris content (10% by weight, see Table VI). The latter regression was calculated because wood debris probably has very different surface area to 'grain' size ratios compared to sand and silt grains. Since mean Ø grain size is used only as a rough approximation of surface area, then the latter regression is probably the more useful. The correlation coefficients for each regression appears on the plots. For Fe and Hg, both regressions have better than 99 percent confidence. The positive correlations between heavy metal concentration and fineness of sediment are therefore statistically significant.

The samples with high wood debris content mentioned above appear anomalously in all three graphs. Assuming that the values of "% weight loss after ashing" reported by NRC for each sample (Table VI) represent the relative amounts of organic material present before ashing, all those samples with greater than 10 weight % organic material were highlighted in the plots of Figures 24, 25, and 26 (marked by * in Table VI).

The samples highlighted were further divided into groups on the basis of the type of organic material that they contained. Three groups were found, the types being (i) coarse wood (chips), (ii) fine wood (fibres), and (iii) other organics (not wood). Groups (i) and (ii)

TABLE VI: ORGANIC CONTENT OF SAMPLES (BY % WEIGHT LOSS AFTER ASHING

SAMPLE	% WEIGHT LOSS	SAMPLE	% WEIGHT LOSS
BS 2	.00	BS 91	8.26
4*	70.93	92	.00
6	.53	93	.52
8	2.34	94	1.04
10	1.71	95	1.04
24	1.07	96	8.27
26	.56	107	.54
28*	13.66	108	1.06
30	1.08	109	1.60
32	.00	110	4.29
45	.58	199	1.04
46	.00	200	.26
47	.56	201	.29
56	1.19	202	.30
57	.58	203	.66
58	.59	204	.52
79	.57	205*	17.56
81	.00	206	.05
83	.53	207*	11.57
85	.53	208*	11.14
87	.00	209	1.79
89	.00	210*	13.46

* indicates samples of greater than 10% organics

had anomalously high heavy metal concentrations. The non-wood organic group of samples (BS4 and BS28) do not have anomalous heavy metal concentrations. Therefore, as a previously discussed experiment also showed, the presence of wood debris is an important factor in the fixation of heavy metals in the bed sediments. The high adsorption capacity of wood debris is probably due to its porosity and high surface area.

One consideration may be that the wood debris has high Hg concentrations due to its origin in a paper products mill, where Hg concentration levels were possibly quite high. Hg was used as a slimicide agent in such industries until 1971. However, if the Hg on the wood debris was derived from the paper mill, then one would not expect a good correlation between adsorbed Hg and adsorbed Fe and Mn, since adsorbed Fe and Mn are derived largely from natural sources. As shown later in this section, Hg, Mn, and Fe concentrations of all the study reach samples are strongly correlated, therefore the high porosity and surface area of wood debris are indicated as the reasons for high adsorbed Hg concentrations.

A single grain size fraction of each of the samples comprising two cross-sections in the study area was analysed for the concentration of Fe coatings. The effect of grain size on the heavy metal concentrations is thus nullified. The normalized samples comprising the main

channel cross-section, BS79, BS81, BS83, BS85, and BS87 (see Fig. 6) still show the trend of decreasing metal concentration from the shore zones to a minimum in mid-channel (see Table VII). The normalized north channel samples, BS205, BS206, and BS207 show a similar trend. It is therefore apparent that grain size (or surface area) is not the only primary variable controlling iron concentration. It is likely that the flow speed of the water mass does have an independent affect (ie. apart from that of controlling bottom sediment grain size) on the concentration of Fe coatings. One might expect that under quiescent conditions flocculation and precipitation of iron colloids would be more favoured than under high current conditions, thus higher concentrations of Fe coatings should be found in the shore zones, with lower concentrations in mid-channel bottom sediments. An inverse relationship probably exists between the velocity of the water mass just above the bed and the Fe concentration of the bed sediments.

The relationships between the concentrations of Fe and Mn, Fe and Hg, and Mn and Hg were examined. Figures 27, 28, and 29 are graphs of the respective relations. The heavy metals have the following approximate relations:

(i) $[Mn] = .0x0\,[Fe]$

(ii) $[Hg] = x.00 \times 10^{-4}\,[Fe]$

(iii) $[Hg] = x.00 \times 10^{-3}\,[Mn]$

TABLE VII: GRAIN SIZE NORMALIZED Fe CONCENTRATIONS

SAMPLE	GRAIN SIZE FRACTION	Fe CONCENTRATION
BS79	2.0 Ø	1114.66 ppm
BS81	"	109.98
BS83	"	99.86
BS85	"	239.95
BS87	"	249.55
BS205	3.0 Ø	1636.73 ppm
BS206	"	350.00
BS207	"	2460.00

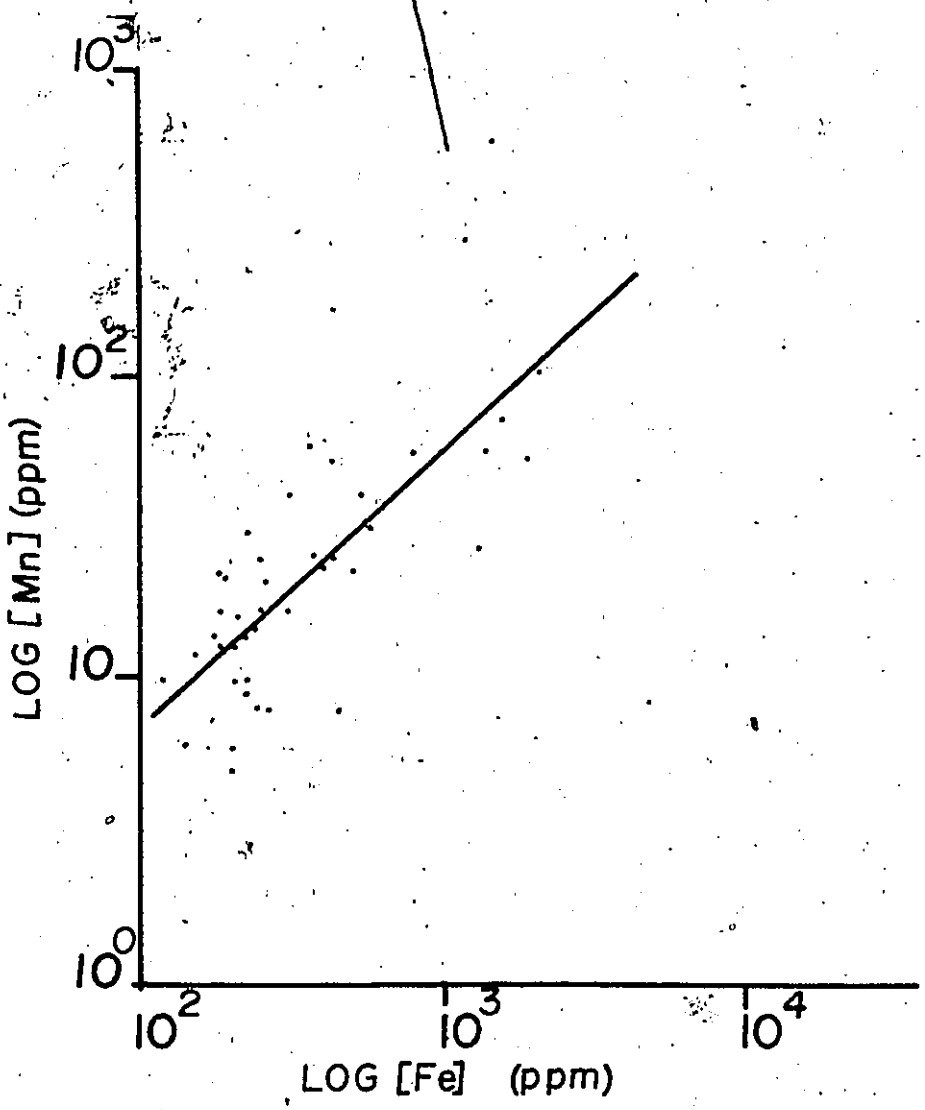

FIG. 27: LOG Mn vs LOG Fe

Log Mn = -.9723 + .9072 log Fe ; r = .7357

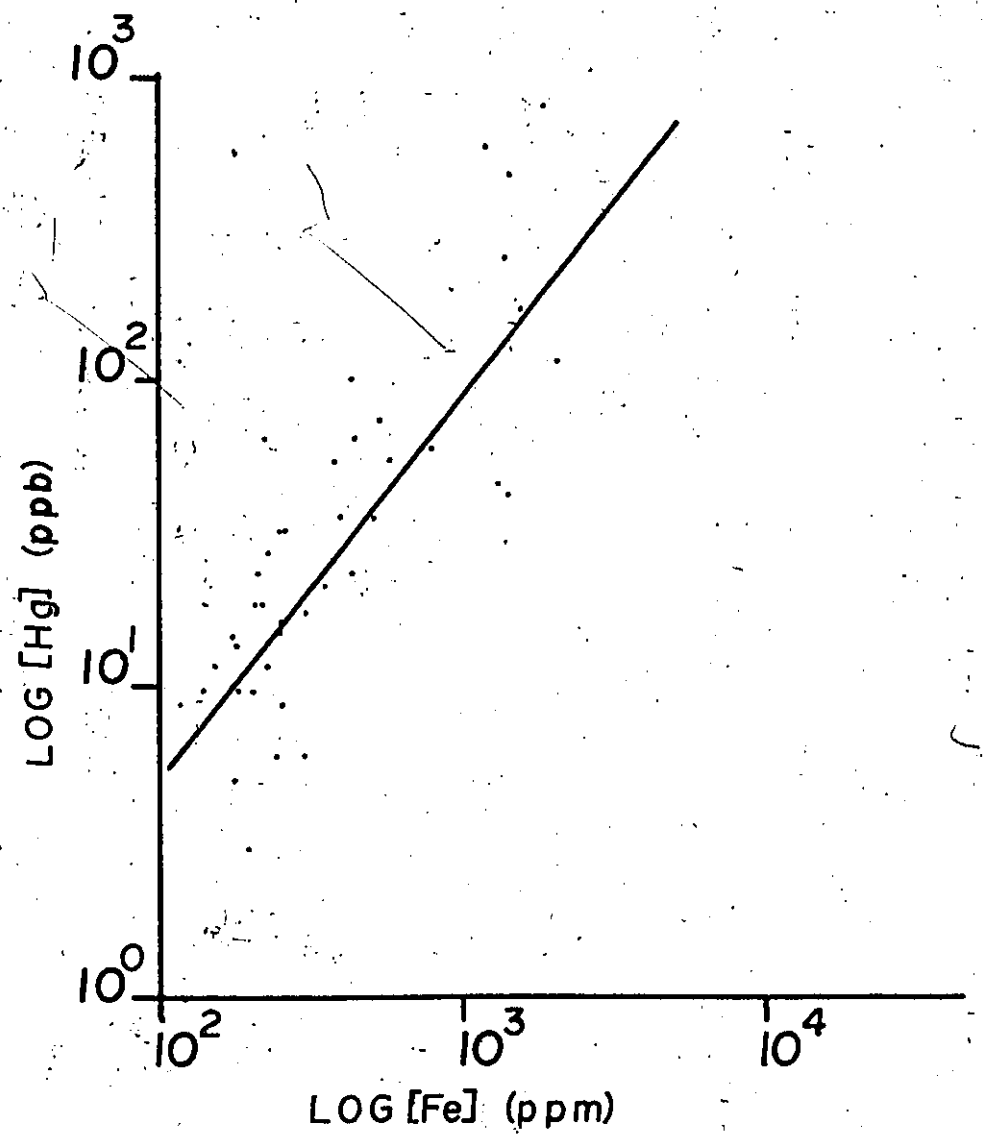

FIG. 28: LOG Hg vs LOG Fe

Log Hg = -1.7476 + 1.2382 Log Fe ; r = .7483

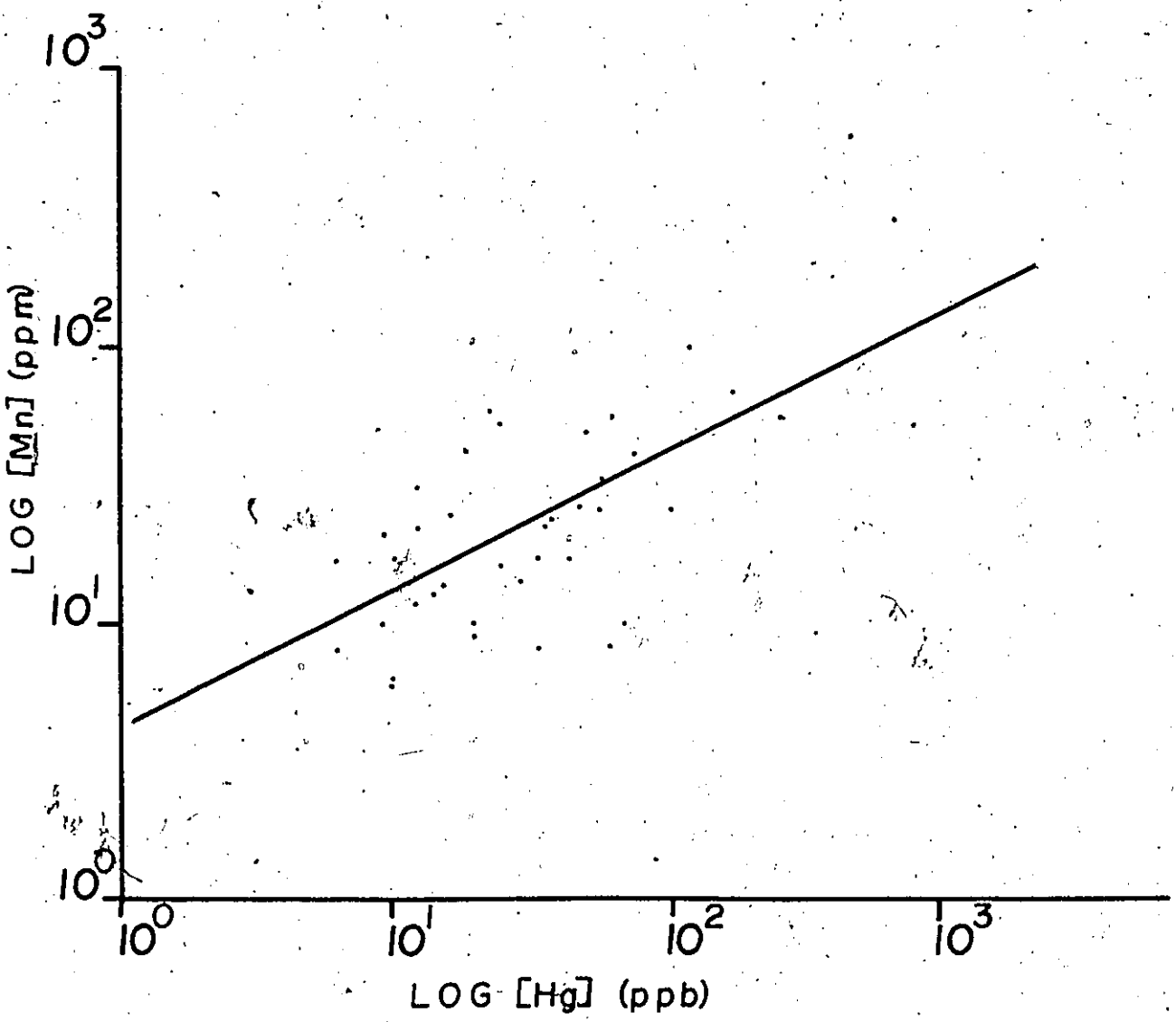

FIG. 29: Plot of LOG Mn vs LOG Hg

Log Mn = .6298 + .5002 Log Hg ; r = .7094

Logarithmic values were plotted since the points are spread over three orders of magnitude. The linear regressions and correlation coefficients were calculated in the same manner as before. For each of the relations log Mn vs log Fe, log Hg vs log Fe, and log Mn vs log Hg, the correlation is very good, with over 99 percent confidence in each case. Therefore, the three positive correlations are statistically significant.

In order to test the hypothesis that hydrous Fe and Mn oxide coatings provide adsorption sites for other trace heavy metals, and that the coatings thus control the concentration of those other heavy metals, the correlations between heavy metal concentrations vs mean Ø grain size and between the heavy metals Fe, Mn and Hg themselves (Figs. 24 to 29) were compared in matrix form (Fig. 30). It is evident from Fig. 30 that the concentration of Fe in the bed sediments is very strongly related to the grain size, and thus to the surface area of the sediments. The correlations between Mn concentration and grain size, and between Hg concentration and grain size are also good, but less so than Fe concentration vs. grain size. There are strong correlations between Mn concentration and Fe concentration, and between Hg concentration and Fe concentration, however. The interpretation is that Fe concentration is controlled mainly by sediment

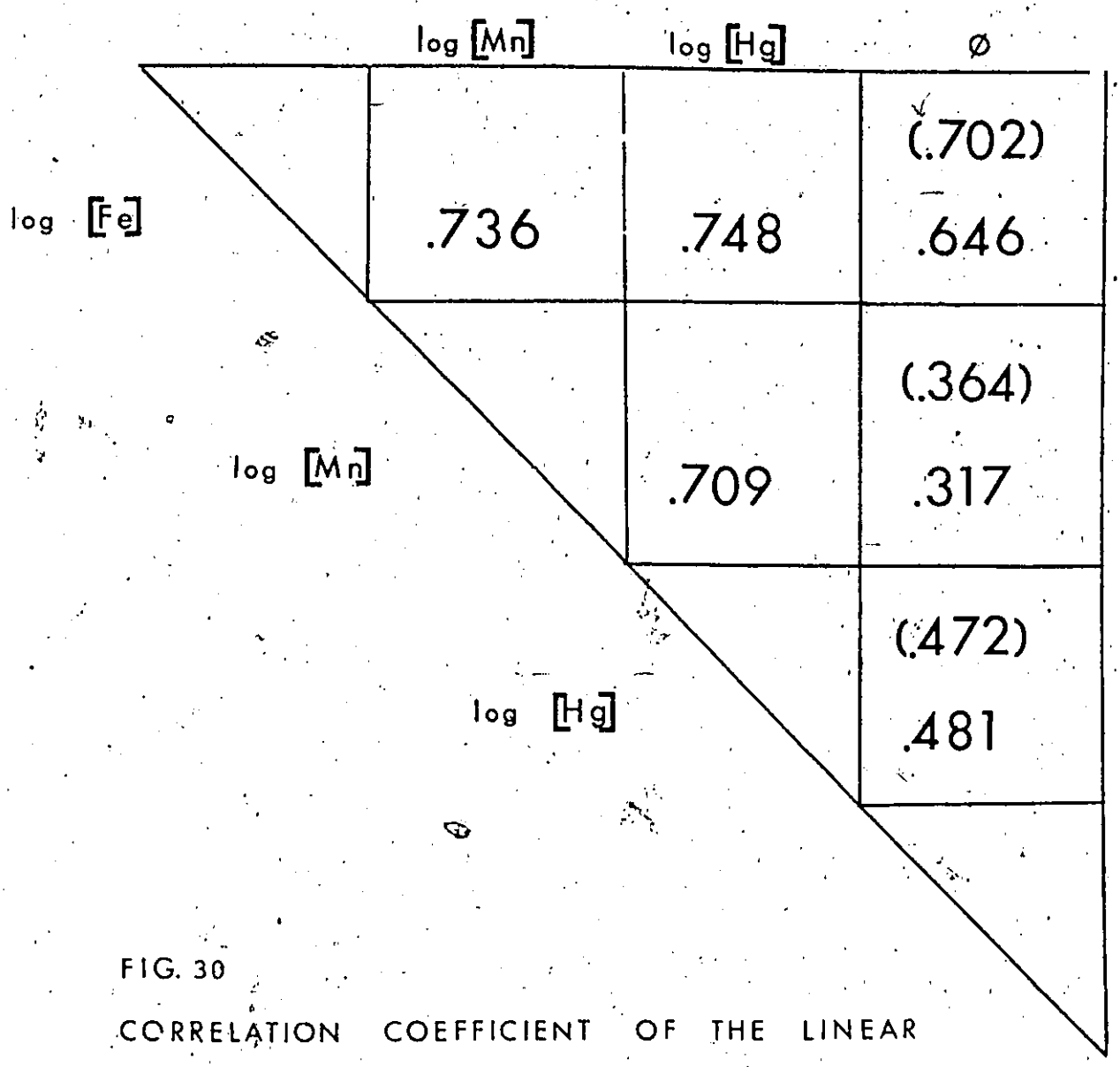

FIG. 30

CORRELATION COEFFICIENT OF THE LINEAR REGRESSIONS, r.

(Values in parentheses refer to regressions omiting samples containing large amounts of wood debris ie. BS 205, BS 207, BS 208, BS 210)

99% confidence at $r \geq .389$

95% confidence at $r \geq .301$

[99% confidence at $r \geq .428$

95% confidence at $r \geq .333$: for values in parentheses]

grain size (or more correctly, by sediment surface area), and that Mn and Hg concentrations are controlled mainly by Fe concentration. The correlation between Mn concentration and Hg concentration might be expected to be high, merely because the concentrations of both metals are so strongly correlated with a common variable, Fe concentration. Likewise, the correlations of Mn concentration and Hg concentration with grain size might be expected to be good, but not as good as Fe concentration vs grain size, because Fe concentration, to which Mn and Hg are both strongly correlated, is also strongly correlated to grain size. The hypothesis is therefore partly borne out, the only discrepency being that Fe concentration alone controls other heavy metal concentrations, Mn included. Jenne (1968, p. 341) comments that where a heavy metal is present in only minute concentrations, precipitation as the metal hydroxide is not as likely as adsorption reactions. It would appear that in the Ottawa River, Mn is not present in sufficient quantity to precipitate directly as a hydrous oxide. Another explanation would be simply that the pH is too low for the direct precipitation of Mn as an hydroxide, but that the catalysing affect of Fe coatings causes Mn to be brought down with precipitating Fe.

That the leachable iron is actually $Fe(OH)_3$ is indicated by thermodynamic considerations of the stabilities

of iron compounds occurring in natural waters (see Literature Review), and is further supported by the rapid dissolution of one phase of iron under acid attack.

Gibbs (1973), Goldberg (1954), and many others (see Literature Review) have demonstrated that several heavy metals behave similarily in the aquatic environment. Since this study has shown that Fe, Mn, and Hg occur in hydroxide grain coatings, it is likely that many other similar heavy metals are present in corresponding forms.

The high Hg concentrations observed in wood debris and in high Fe concentration samples indicates that the adsorbability of Hg can be significant, at Eh - pH levels common to rivers, as proposed by Shimomura et al (1969).

Finally, levels of Hg in the bed sediments of the study section were reported by Oliver and Kinrade (1972) for samples taken in 1971. Comparison of their values to the values obtained from 1973 at the same locations allows an estimation of the "half-life" of mercury in the bed sediments, assuming that Hg input was essentially terminated in 1970 with the government imposed controls on the industrial use of Hg. The "half-life" of Hg determined for three sample locations in the channel north of Kettle Island is on the order of twelve months.

Hg concentrations in bottom sediments were also determined by NRC for several samples taken during the

early stages of the prognamme in the summer of 1972. For the main channel sands, a 50% annual decrease in Hg is also indicated by comparison to 1973 data for the reoccupied sample sites. With samples representing only so short a time span it is unclear as to whether or not the decline in Hg concentration levels is exponential, thus the term "half-life" is merely tentative.

c. SUMMARY

The study of leachable Fe, Mn, and Hg concentrations in the Ottawa River bed sediments leads to the following conclusions:

1) Highly porous, chemically inactive wood debris has a high sorption capacity for Fe, Mn, and Hg, and plays an important role in determining the concentrations of these metals in the bed sediments.

2) The silty fraction of any sample contains 30 to 60% more heavy metals than the sandy fraction.

3) Sediment grain size in the study section is closely related to flow speeds of the water mass. Besides controlling the grain size distribution of bottom sediments, flow speed also has some control over the heavy metal concentrations coating the sediments. High flow speeds correspond to lower concentrations of heavy metals, and vice versa.

4) Mn and Hg concentrations are controlled by the concentration of Fe present as hydroxide grain coatings,

the coatings providing sites for adsorption of Mn and Hg.

5) Sediment fineness (or more correctly, surface area) controls the concentration of Fe coatings in the bed sediments, log Fe concentration vs mean Ø grain size being a positive linear relation.

6) The half-life of Hg in the study area bed sediments is on the order of twelve months.

PART IV - BEDFORMS, BEDLOAD TRANSPORT, AND THE DIVING PROGRAM

PART IV - BED FORMS, BEDLOAD TRANSPORT; AND THE DIVING PROGRAM

A. INTRODUCTION

This section of the report deals with the physical aspects (ie. transport) of the bed materials of the study area, with respect to their concentrations of heavy metals. To obtain order-of-magnitude values for the transport of persistent chemicals through the various compartments of the study area is one of the major objectives of the Ottawa River Programme; the other major objective being the determination of the distribution and occurrence of persistent chemicals in the area, which is dealt with in the preceding section of this report.

Part III showed that various heavy metals are adsorbed and/or deposited onto sediment grains. Transport of the sediment grains, therefore, must result in the transport of the heavy metals attached thereto. Since the concentrations of heavy metals in the bed materials are known, the heavy metal transport rates can be determined by considering the transport of bed material. The problem, then is to obtain order-of-magnitude values for bed load discharge in the study area, and generally investigate the sediment transport regime.

B. LITERATURE REVIEW

Bed load is defined as that material in an alluvial

channel which moves within a few particle diameters of the stream bed (Colby, 1963, p.1). Bed load particles are transported by sliding, rolling, or skipping along the bed, and are supported mainly by the bed rather than by the turbulence of the flow(Colby, 1964, p.v, and many others). The configuration of the bed of an alluvial channel is dependent upon flow conditions. Bed forms can be non-existent under some conditions (a plane-bed prevailing), or may occur as assymetric or symmetric wave forms. Since bed load transport is dependent upon bed roughness (the type of bed form prevailing), (Harms and Fahnestock, 1965, plate 1), it is necessary to investigate bed load discharge in the light of the configuration of the bed.

The terminology applied to bed forms has been confusing in the past (Middleton, 1965), but authors are now tending to use only a few different classification schemes. One of the most popular schemes, proposed by Simons and Richardson (1961) will be used in this report, and is as follows:

1) Lower Flow Regime
   - Ripples
   - Ripples on Dunes
   - Dunes
2) Transition

3) Upper Flow Regime

Plane Bed

Standing Waves

Antidunes

Increasing Stream Power

The concept of "flow regime" is used to group together similar bed forms. Flow regime is a range of flow conditions having somewhat similar resistance and sediment transport characteristics that produce similar bed forms (Simons et al, 1961, p.vi). Ripples and dunes are asymmetrical wave forms, with a gentle slope on the upstream (stoss) side; and a steeper downstream (lee) face. Dunes and ripples, although similar in shape, are not gradational (Middleton, 1965, p.250). Ripples and dunes are distinguished mainly by their sizes; ripples are small (wave length $\lambda \approx .25 - 1.5$ feet, height $\approx .1$ foot), dunes are approximately one order-of-magnitude greater in length and height. A ripple bed is usually uniform both longitudinally and laterally, but a dune bed is less so. Ripple height does not depend on water depth, although it appears that dune height does depend on depth. Ripples do not form when mean grain size is greater than .7 mm. Dunes may form and move in any grain size, as long as tractive forces are sufficient at Froude number < 1 (tranquil flow) (Simons and Richardson, 1965, p.194). Froude number is

a quantity which is based on the ratio of the mean velocity of the flow to the velocity of propagation of a surface wave. Where the effect of depth on wave length can safely be ignored, it can be approximated by $\bar{v}/\sqrt{gD}$. However, for some applications, it must be based on the wavelength of the surface wave, L, and cannot be approximated by $\bar{v}/\sqrt{gD}$ as is often done. Some authors consider that at Froude values less than 1, lower tranquil flow regime prevails, and at values approximately equal to 1, upper rapid flow regime prevails (Simons et al, 1965a, p.41), however other authors believe that 'regime of flow' determination by Froude number is not valid (Culbertson and Dawdy, 1964, p.19).

Transition bed forms are washed-out or truncated dunes of highly irregular and varied shape. Standing waves and antidunes are symmetrical wave forms which are in phase with water-surface waves. These forms together with a plane bed stage, comprise the upper flow regime and have heights and spacings of similar magnitude to dunes. Standing waves are stationary forms, whereas antidunes may migrate either upstream or downstream (Simons and Richardson, 1961).

The bed roughness in an alluvial channel is governed by many variables which are largely interdependent. Harms and Fahnestock (1965), Simons et al (1965,

a, b), and many others propose that the form of bed roughness is a function of the following variables:

form of bed roughness = f(D, S, d, σ, ρ, w),

where w = f(d, ρ_s, ρ, μ)

and in which D=depth, S=slope, d=mean grain size of the bed material, σ=measure of the size distribution (sorting) of the bed material, ρ=density of the water-suspended sediment mixture, w=fall velocity of the bed material, ρ_s=density of the sediment, and μ=apparent dynamic viscosity of the water-sediment mixture. Other parameters may be added, but they are interdependent with the above variables; ie. velocity of flow, discharge, shear stress, temperature, and concentration of suspended sediment.

Depth and slope are factors in the bed roughness function mainly because of their effect on shear stress τ, ($\tau=\gamma DS$, where γ=specific weight of the fliud), which is the force responsible for particle motion at the bed (Pettijohn et al, 1972, p.348). With increasing shear stress or stream power, τV (where V=velocity of flow), the bed roughness changes from ripples to dunes, through upper regime wave forms. The effect of depth on ripple and dune dimensions has been investigated by various authors. Ripple length and height are independent of depth, but dune length and height are dependent on depth (Yalin, 1964, p.113; Pettijohn et al, 1972, p.353).

Yalin (1964, p. 113) has empirically derived the equation $\lambda = 5D$ for dunes, and Nordin (1964, p. 12) found $\lambda = 4.2D$ for standing waves.

The factor d (physical size of sediment particles) is primarily important for its influence on the fall velocity of the sediment, but the effect of grain size on resistance to flow can be important for plane beds, antidunes, and to a lesser extent, for dunes. The factor σ, which represents the uniformity of bed material, also affects bed roughness due to its influence on the resistance to flow. For two sands with the same median fall velocity but with different degrees of sorting, the resistance to flow of uniform sand is greater than graded sand for ripples, dunes, and antidunes, but the opposite is true for upper regime plane bed. The affect of increased resistance to flow causes the ripples and antidunes of uniform sand to be larger than those of graded sand. The dunes of uniform sand develop superposed ripples, and are smaller than dunes of graded sand (Simons and Richardson, 1965, fig. 5).

The interaction between the bed material and the fluid is determined primarily by the fall velocity of the bed material, w. For any given depth and slope, w governs the form of bed roughness that prevails, the dimensions of the bed form, and the resistance to

flow (neglecting the effect of grain roughness) (Simons et al, 1965a, p.48). Dune length increases and angularity decreases with low fall velocity. The critical shear stress where incipient particle motion occurs, or the magnitude of the shear stress at the upper-lower flow regime boundary, increases with high fall velocity. Changes in bed form occur regardless of whether the fall velocity is varied, as a result of viscosity or bed material density changes. Viscosity is dependent upon the concentration of suspended sediments and temperature of the fluid-sediment mixture.

Ripple length and height depend on the fall velocity or fall diameter of bed material; both ripple dimensions increasing with higher fall velocities (coarseness of particles) (Pettijohn et al, 1972, p.353; Simons et al, 1965a, p.38). Yalin (1964, p.113) has determined that ripple length $\lambda \approx 1000$ mean grain size. Dune height and length, on the other hand, are independent of physical grain size (Yalin, 1964, p.115), but dune length increases as the fall velocity decreases, hence parameters such as fluid density, temperature, viscosity, and concentration of suspended sediment also affect dune morphology (Simons and Richardson, 1965, p.195).

High concentrations of suspended sediment occur in

most natural channels, usually during periods of peak discharge, thus the role of suspended material is important in considerations of bed roughness. Fall velocities in a sediment-water mixture are considerably less, due to higher viscosity and density of the fluid, as compared to a cleaner water medium (Nordin, 1963, p.12). The increased specific weight, γ, of a water-sediment mixture affects the shear stress and stream power, which have direct control on the form of bed roughness (Simons et al, 1965a, p.50).

A few general observations have been made on the dependence of shape on some of the above variables. Although ripple size is independent of depth, Allen (1968, fig. 4-61) has noted that as depth increases relatively straight and continuous ripple patterns change to curved and discontinuous patterns. Although grain size is a determinant of ripple size, ripple shape is independent of grain size (Simons et al, 1965a, p.38).

For dunes, shape is governed primarily by fall velocity and shear stress. Fine sediments (which usually have small fall velocities) produce a less angular dune than coarse sediments, since much of the fine bed load is carried beyond the front of the lower slopes (Simons et al, 1965, a, p.39). Pettijohn et al (1972, p.351) describe the effect of tractive force (shear stress)

on the angularity of a dune; flow separation occurs at the crest of a dune, regressive ripples on the foreset may form as a result of turbulent eddies. If tractive force is small, most grains roll or slide down the foreset, the largest ones commonly travelling farthest, and angular crossbedding results. As tractive force increases, more and more bed load is catapulted into the turbulent eddy, and is deposited in front of the lower slopes, such that angular foresets become tangential or concave upward.

Every factor that is a variable in the bed roughness function is also a factor in the bed-material transport function, since bed-material discharge depends on bed form. Harms and Fahnestock (1965, plate 1) sum up particle motion for different bed configurations in the light of continuity and shear velocity. Lower-flow regime bed forms are characterized by intermittant particle motion, while upper-flow regime is characterized by continuous particle motion. Accordingly, shear velocity and sediment transport gradually increase from a minimum for a ripple bed to a maximum for antidunes.

Colby (1964, p.7) states that bed-load discharge (q_B) is necessarily a function, [f(shear velocity, fall velocity)] , and therefore many other dependent variables (discussed previously) will affect bed load discharge.

He finds that the most satisfactory correlation between bed load discharge and any of the controlling variables is with shear velocity (the velocity of the flowing water adjacent to and in contact with the bed) or alternatively, mean velocity. Fall velocity, (or alternatively grain size), may have a large effect on the discharge of sands at low velocities in any depth of flow, or at high velocities in deep flows. Colby has produced a set of graphs, based on empirical data, which show the discharge of sands knowing mean velocity and depth. About three-fourths of the data used to produce the graphs fall within limits that are 100 per cent larger and 50 per cent smaller than the computed values, and data not used to produce the graphs also fall within similar limits. In his discussion of the applicability of the graphs in predicting discharges for other streams, Colby proposes that much inaccuracy could be avoided if shear velocity could be measured satisfactorily. In fact, if an accurate measurement of shear velocity was made, the only other important parameter would be the size (or fall diameter) fall velocity) of the bed material. However, Reynolds (1964, p.114) points out that without resorting to empiricism we cannot do more than merely predict the order of magnitude of the sediment moved downstream since bed forms depend on local changes in flow para-

meters. Nordin (1964, p.29, 33) on the other hand, maintains that unless a channel is actively aggrading or degrading, the bed load discharges at any two cross sections must be equal. Nordin finds that field data do not confirm that bed load is an imposed variable, therefore a stream can adjust its flow characteristics in order to transport all bed material available, in the same manner as a stream carries all the available suspended material.

There are two basic methods of obtaining values of bed load discharge in natural channels; theoretical mathematical computations, and direct measurement by various apparatus. Colby (1964, p.4) reviews the generally known procedures for computing bedload discharge, the Meyer-Peter and Müller equation [1], the Einstein equations [2], and the Bagnold equation [3]. For all

---

(1) Meyer-Peter, R., & Müller, R. (1948); Formulas for Bed Load Transport; International Assoc. Hydraul. Structures Research, 2d mtg., Stockholm, Sweden, p.39-64.

(2) Einstein, H.A. (1950); The Bed Load Function for Sediment Transportation in Open Channel Flows; U.S. Dept. of Agriculture Tech. Bull. 1026, 70p.

(3) Bagnold, R.A. (1956); The Flow of Cohesionless Grains in Fluids; Royal Soc. (London) Philos. Trans., v. 249, p.235 - 297.

their comprehensiveness, each of these procedures suffers considerably from the number of simplifying assumptions that are necessary to reduce the extremely complex problem of sediment transport to manageable proportions. The procedures are all subject to gross errors for every application except a very simple situation. Natural systems as a whole are far from simple.

Colby elects to express the relationships between discharge of sands and characteristics of flow and sediment in graphs, based on laboratory and field information, and on the general concepts of sediment transportation. Culbertson and Dawdy (1964, p.50-54), Beckman and Furness (1962, p.31), and Nordin (1964, p.38) have applied transport equations to natural systems, and in each case found them to be unsatisfactory. The theories are not without some significance, however, as they do provide some insight into some qualitative aspect of sediment transport and deposition (Colby, 1963, p.18).

Direct measurement of bed load discharge with some type of apparatus is the other common procedure in the study of sediment transport. Hubbell (1964) has conducted a thorough investigation of available and proposed measuring apparatus and procedures. The simplest and most practical method for measuring the weight of bedload passing a section in a given time is to collect the

sediment in some type of sampler. However, several problems are encountered with this method. Since the sampler must rest on the bed, the flow pattern and bed load discharge in the vicinity of the sampler are altered to some extent. If the sampling is to be accurate, the sampler must be designed so that the bed load discharge is not affected by the instrument, so that it retains the bed load particles, and so that it can be oriented in such a way that all particles have an equal opportunity for entrance. According to Hubbell, these criteria cannot be completely satisfied, and therefore the efficiency of a sampler must be determined. He also notes that since the factors governing the efficiency of a sampler, for example velocity, depth, grain size, and bed configuration, are highly variable in a natural stream, efficiencies are themselves highly variable and uncertain.

Another problem that must be overcome in the sampling of bed load discharge is the oscillatory variation. Ehrenberger and Muhlhofer[1], studying the Danube and Inn rivers, respectively, found periods of

---

(1) Ehrenberger, R. (1931); Direct Bed Load Measurements on the Danube at Vienna and their Results to Date; Vienna, Die Wasserwirtschaft, Issur 34, p.1-9 (Trans. No. 39-20, U.S. Waterways Expt. Sta., Vicksburg, Miss.)

oscillation to be nearly constant, at 20 and 15 minutes, also respectively (values taken from Hubbell, p.5).[3] Still another problem which besets sampling is inadvertent scooping-up of bed material as the sampler swings to the bed. Since samplers are lowered from the surface, guiding the sampler in a current is very difficult, and the operators have no control over the final resting place of the sampler.

To overcome the inherent difficulties in bed load sampling, various elaborate apparatus have been designed. In order to provide better control in strong currents, samplers have been deliberately weighted, commonly to several hundreds of pounds, and stabilizing fins have been attached. This procedure, however, makes the sampler outsized, and hence variations of flow occur near the sampler. Box or screen samplers collect bed material that is deposited due to a reduction in flow or that is screened from the flow. However, these types of apparatus are wholly dependent on the grain sizes of the bed material, and their efficiencies vary widely. Pan or tray samplers direct bed material up a ramp, where the particles drop into a series of slots or baffles. The drawback of these samplers is that they cause changes in the flow, and in local sediment discharge, thus they do not measure a representative discharge.

Pressure-difference samplers are an attempt to remedy the problems of the pan or tray samplers. Stream velocity and entrance velocity are equalized by means of a pressure drop at the sampler exit, created by diverging sampler walls. Samplers of this type provide nearly 100% hydraulic efficiencies, but sampling efficiencies are much lower. Slot or pit samplers are placed into the stream bed, and therfore are not subject to the problems of the previously described apparatus. Sediment is deposited in the pit as the grains move along the bed, simply because flow separation occurs at the leading edge of the pit. Sampler efficiency of these types is essentially 100%, where openings of 100 to 200 grain diameters are used. The disadvantage of slot or pit samplers is that they must be placed into the bed by an operator.

Several new indirect methods for measuring bed load have been developed. Among these are photographic techniques, generally unsatisfactory due to poor visibility in natural streams, acoustic instruments that measure relative sediment movement only, a tiltmeter which measures the changing configuration of the bed with time, (a questionable method), and most promising, tracking of dune or ripple movement by ultrasonic sounding.

Richardson et al (1961) describe a method of measuring the velocity of bed waves using an accurate sonic depth sounder. Once velocity and shape of the bed waves are known, it is a simple matter to calculate bed load discharge (with some correction for porosity of the bed). Hubbell (1964, p.43-49) and Richardson et al (1961) propose similar equations to derive bed load discharge from velocity and shape of sand waves, a slightly modified form of which is as follows:

$$q_B = [(K-\lambda)/2]\, vh\, dw$$

where

q_B = bedload discharge by volume or weight

K = a constant, the ratio of particles deposited on the stoss slope of the sandwave downstream to the particles deposited on the lee slope of the same wave from which they were eroded, ie. a correction for those particles which are nearly always in suspension. For a dune bed this constant would be close to unity.

λ = porosity of the sand bed

v = velocity of the wave crest

h = average height of the wave

dw = incremental width over which the particular measurements are valid

Simons, et al (1965b) applied the above method to 101 observations of bedload transport in a flume, and calculated and observed bedload discharge were in excellent agreement. They found, however, that for natural systems the equation is more suited for a dune-bed configuration than for ripples. Also, coarse bed material gives better values than fines, due to the angularity of coarse sand bed forms.

a. Summary of the Literature Review

The form of bed roughness, and hence the magnitude of bed load discharge, are governed by several flow and sediment parameters, the effects of which, in natural systems, can only be described qualitatively.

Empirically based graphs have been developed that will predict order-of-magnitude values of bed load discharge for a narrow range of natural systems, however more accurate methods of measuring shear velocity are required to make the method satisfactory.

Natural systems are too complex to allow precise mathematical relationships to be developed for the prediction of bed load discharge.

Direct measuring techniques for bed load discharge have been generally unsatisfactory because the operator at the surface has little or no control over the sampler on the bed. Pit or slot type bed load samplers are

nearly 100% efficient, but must be manually placed in the stream bed.

Indirect methods of measuring transport of bed load are becoming highly sophisticated, but have not, as yet, been proven effective. A relatively simple method, based on tracking wave crest movement by sonic depth sounding, however, has been shown to have great merit.

As noted by Stichling and Smith (1968, p.15), bed load measurement has been, and still is a most challenging problem.

C. BEDFORMS IN THE OTTAWA RIVER STUDY SECTION

Of all the factors on which the form of bed roughness depends, the depth of water over the bed is the most easily measured. While bed load measurements were being made, dune sizes and corresponding water depths were recorded along several cross-traverses (Fig. 31). The types of bedforms prevailing in various areas of the study reach were established by inspection of sonar profiles (which indicate the presence of dune forms), and by diver observations. The particular instruments used for sonic depth sounding were a Kelvin-Hughes recording echo sounder, and a Raytheon echo sounder. Dunes occur at depths greater than about 4 meters in all areas of cohesionless sandy sediments in the main channel of the study area. The dune train is bounded on the north side of the main channel by 5 meters depth, and bounded to the south by outcropping Pleistocene clay (Fig. 32).

Graphs of dune length vs. water depth and dune height vs. water depth were plotted, in order to determine the relationship between size parameters and depth (Figs. 33 and 34). Linear regressions were calculated for the distributions, along with their correlation coefficients and levels of significance. For dune length vs. depth, the regression yields an equation:

$$\text{dune length} = 4.3782\ \text{Depth} - .9857$$

and for dune height, the equation is:

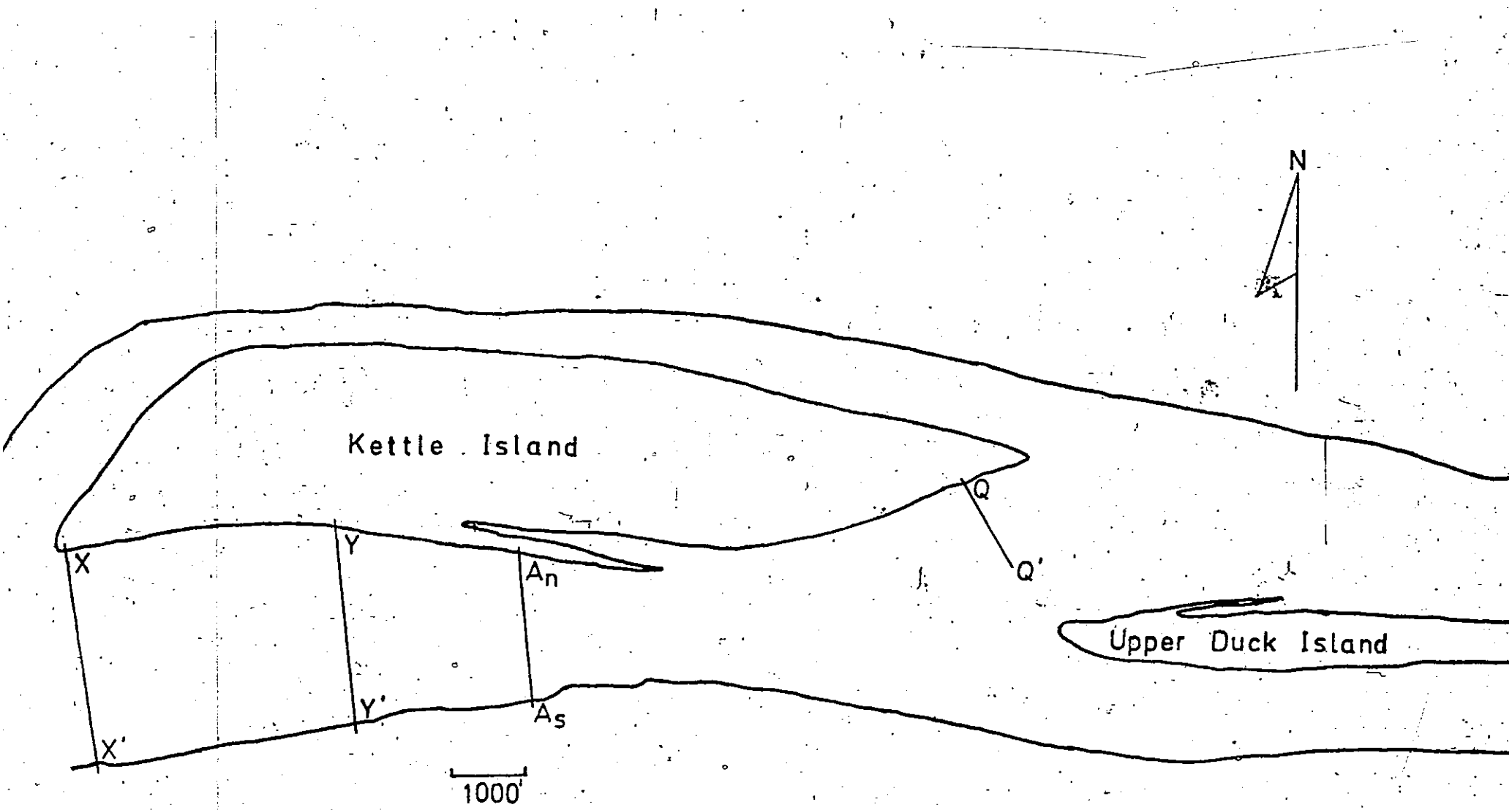

FIG. 31: DUNE PARAMETER TRAVERSES

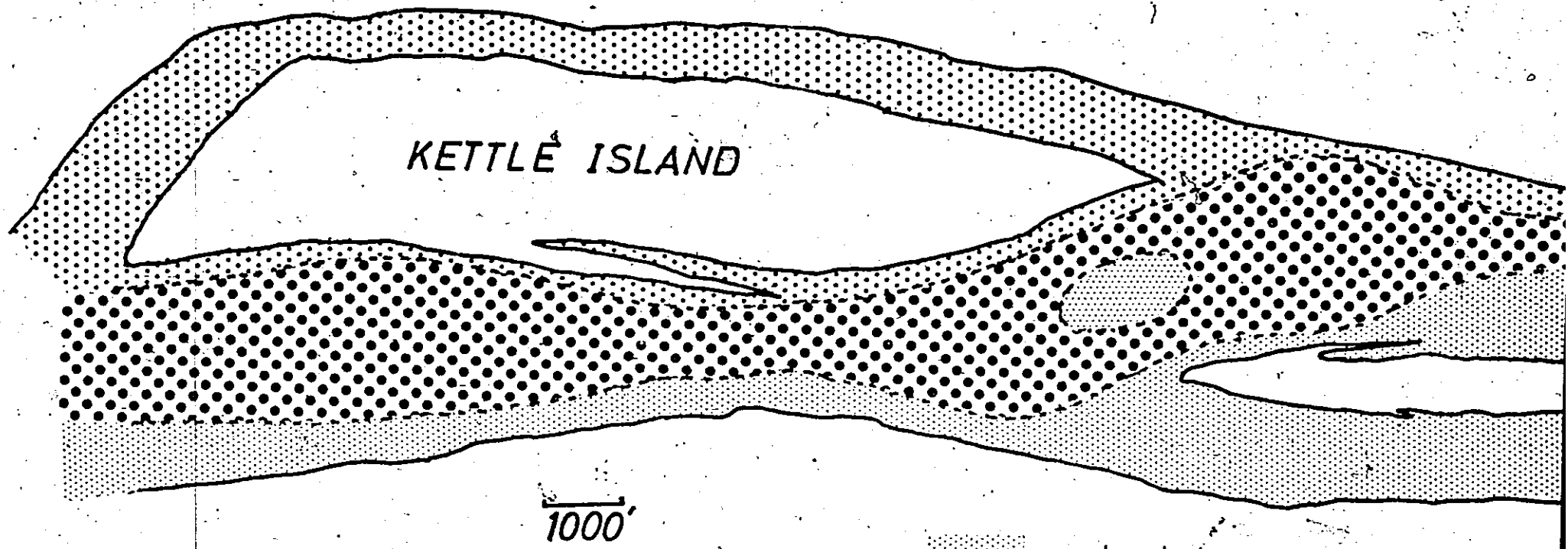

FIG. 32 FORMS OF BED ROUGHNESS

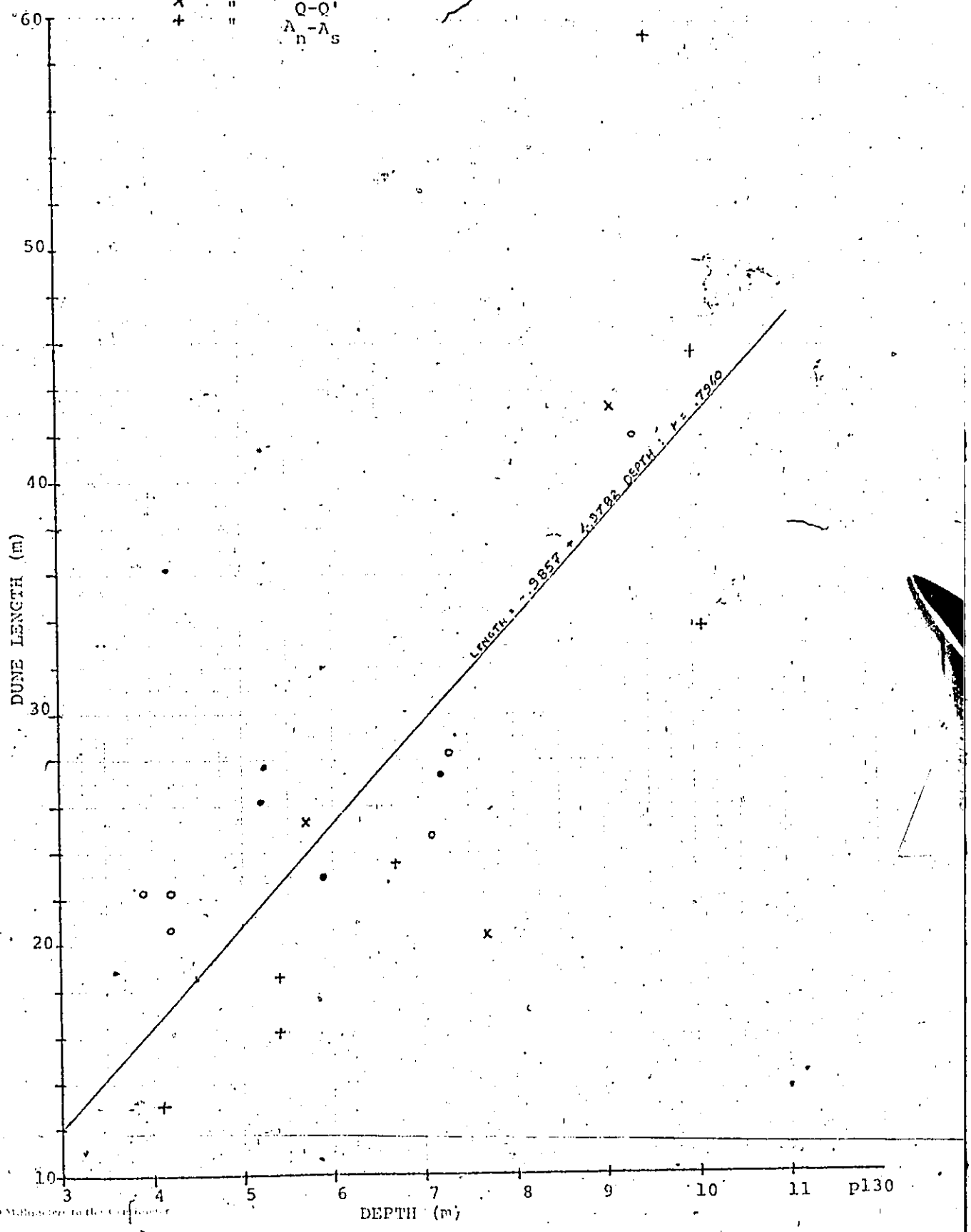

FIG. 33 DUNE LENGTH vs WATER DEPTH

p130

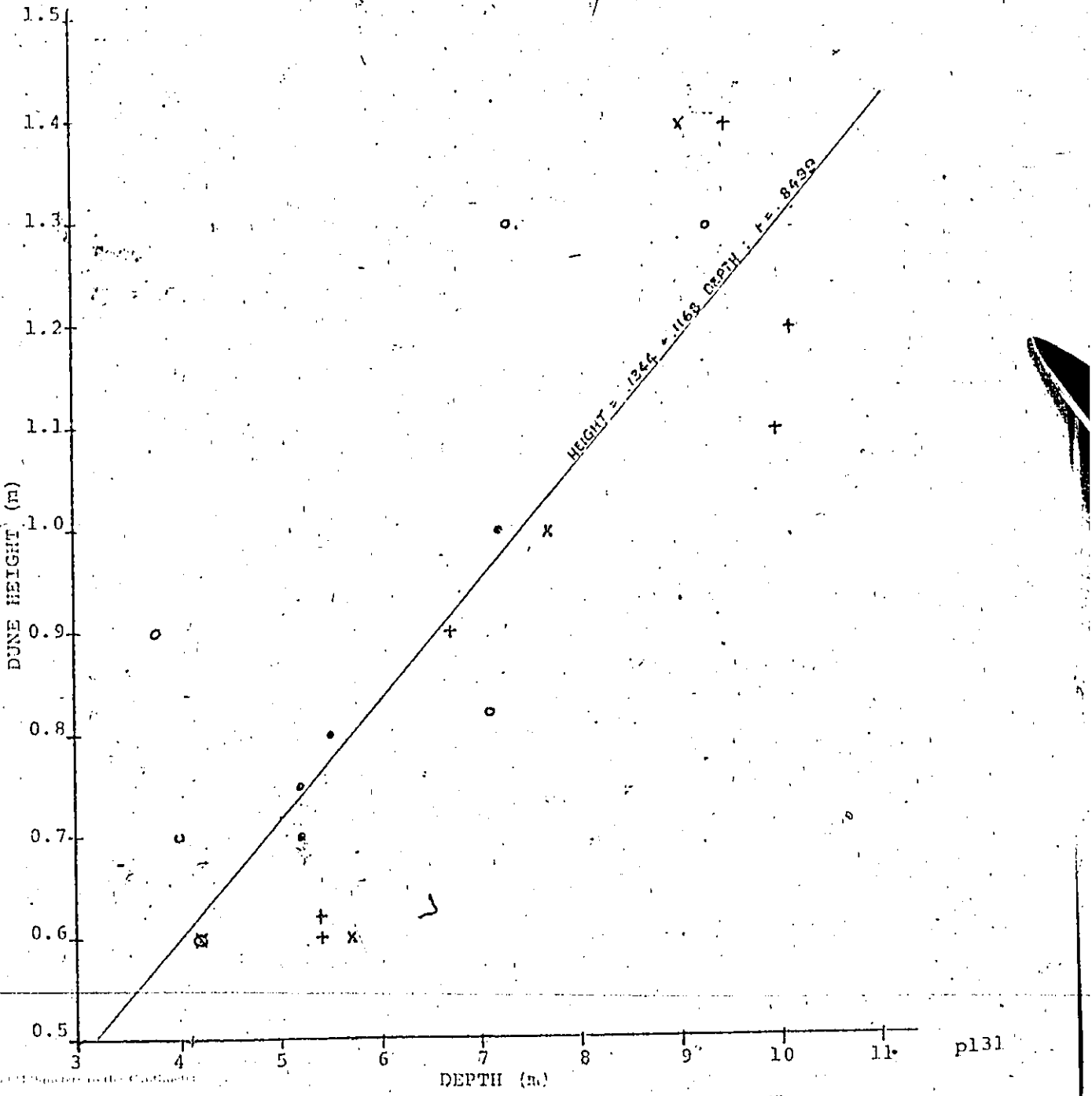

FIG. 34: DUNE HEIGHT vs WATER DEPTH

dune height = .1168 Depth + .1344.

Both relations show good correlations, with r = .7960 for the length/depth relation, and r = .8499 for the height/depth relation, and both regressions are over 99% significant. The dune length vs. depth relationship was studied by Yalin (1964, p.113) as discussed in a previous section of this report. He proposed an empirically derived equation relating dune length and depth, namely (Dune length = 5 X Depth). Yalin's equation is in quite good agreement with the prevailing conditions in the Ottawa River study section.

The form of bed roughness prevailing in the north channel is a rippled bed. Depth is generally less than 5 meters, and current speeds are low. The ripples are straight crested, and are continuous perpendicular to flow. This is in contrast to the shape of the ripples which are found superposed on the main channel dunes. The deeper water ripples have discontinuous, cuspate shapes. The different nature displayed by the relatively shallow- and deep-water ripples is in accord with Allen's (1968, Fig.4-61) observations on ripple shapes (see Literature Review).

An additional observation made concerning the ripples associated with the dune bed may have significance for those studying ripple orientations in ancient rocks.

A current was observed in the trough of dunes, moving in a direction normal to the flow of the major stream current. This current seems to be confined to that part of the dune trough which is below the plane of flow separation, and everywhere its direction is towards deeper water. The presence of the current is revealed by the occurrence of the assymetrical, straight-crested ripples which it produces. The trough-ripples are oriented with their crests parallel to the major river flow, and with lee slopes towards deeper water. The current is evidently a result of back-eddy turbulence in the lee of dunes. The direction of the current may be due to the different flow speeds of the water mass just above the bed in shallow water and just above the bed in deeper water. The higher deep-water flow speeds might create a low pressure zone in the trough area, with the current from shallower depths supplying the water mass to equalize the differential.

That part of the bed which lies between the eastern tip of Kettle Island and the western tip of Upper Duck Island has an anomalous nature with respect to bed roughness, as well as having anomalously high heavy metal concentrations and anomalously fine grained sediments (see Part III, Occurrence and Distribution of Heavy Metals...). The anomalous area is a plane bed, consisting

of cohesive, bedded fine sediments. The area is evidently a relict of some past sedimentation conditions, as the hard floor is now being slowly eroded. The area is one of eddying currents, however, and flow speeds are low even now.

D. A DIVER OPERATED BEDLOAD SAMPLER

Realizing the limitations of the various apparatus and procedures available to measure or otherwise determine the rate of bedload transport, the author undertook to design a bedload sampler that would be nearly 100% efficient.

It seems that all of the instruments designed to capture sediment grains as they are transported along the bed suffer because they must necessarily be operated remotely, from the surface. Unfortunately, the operators actually have very little control over the positioning and operation of the devices. The requirement which must be met before truly accurate bedload measurements can be made, therefore, is that of complete control over the operation of the bedload sampler.

An effective method by which direct control over bedload sampling can be obtained involves the use of SCUBA-equipped divers. A diver can position and moniter a bedload sampler so that it does not adversely affect the flow conditions in the neighborhood of the sampler, so that the sampler is stable, and so that it accepts

all the material being transported along the bed.

According to Hubbell (1964), a pit-type bedload sampler is the only type that can nearly achieve 100% sampling efficiency, but he comments that the use of such a sampler is impractical, since it must be placed within the bed, and cannot be emptied except by pumping. However, if a diver is used then neither placing a pit-type sampler within the bed nor removing it and the captured sediment are problems.

The ideal opening in a pit-type sampler is 100 to 200 grain diameters (Hubbell, 1964). A versatile sampler should therefore have an opening which can be adjusted to suit the sediment size. This feature, among others, was incorporated into the design of the author's bedload sampler.

Plate 6 shows the sampler and its components. The sampler consists of a pan, sized 6" X 12" X 2" deep, with the two long sides extending up an additional 2". A lid is fitted so that it will slide over the 2" ends, and close the pan. The lid itself has a large opening, which is covered by a sieve screen with a convenient mesh size. Mesh #180 was used in this study.

The sampler is easily placed in the bed without disturbing the bed upstream of the sampler. The top of the 2" ends are made level with the bed surface. The sampler is oriented with the long sides exactly

parallel to flow, so that the flow does not 'feel' the thin raised sides. The lid is opened wide enough to allow the collection of all material being transported along the bed, and the sampling period is timed. The lid is then closed, the sampler is removed from the bed and taken to the surface, where the trapped sediment is emptied, dried, and weighed.

The principle by which the sampler operates is as follows. The flow of water just above the bed separates from the bed and drops into the pan after passing over the leading edge of the sampler. Back eddies occur beneath the flow separation, where bedload material is deposited as a delta which progrades into the pan (Fig. 35).

The raised sides ensure that no bed material enters the pan from the sides. The partially opened lid allows bed material to enter the pan, while the sieve mesh retains any small grains that were not deposited at the front of the pan, as the flow exits from the sampler.

A diving procedure was developed which allows divers to descend and work in even powerful flows. The surface vessel is anchored by the bow, and two weights (approx. 80 lbs. each), connected with a 2' length of rope, are lowered by two long ropes off the stern. The lines from the weights to the surface are made fast at the surface

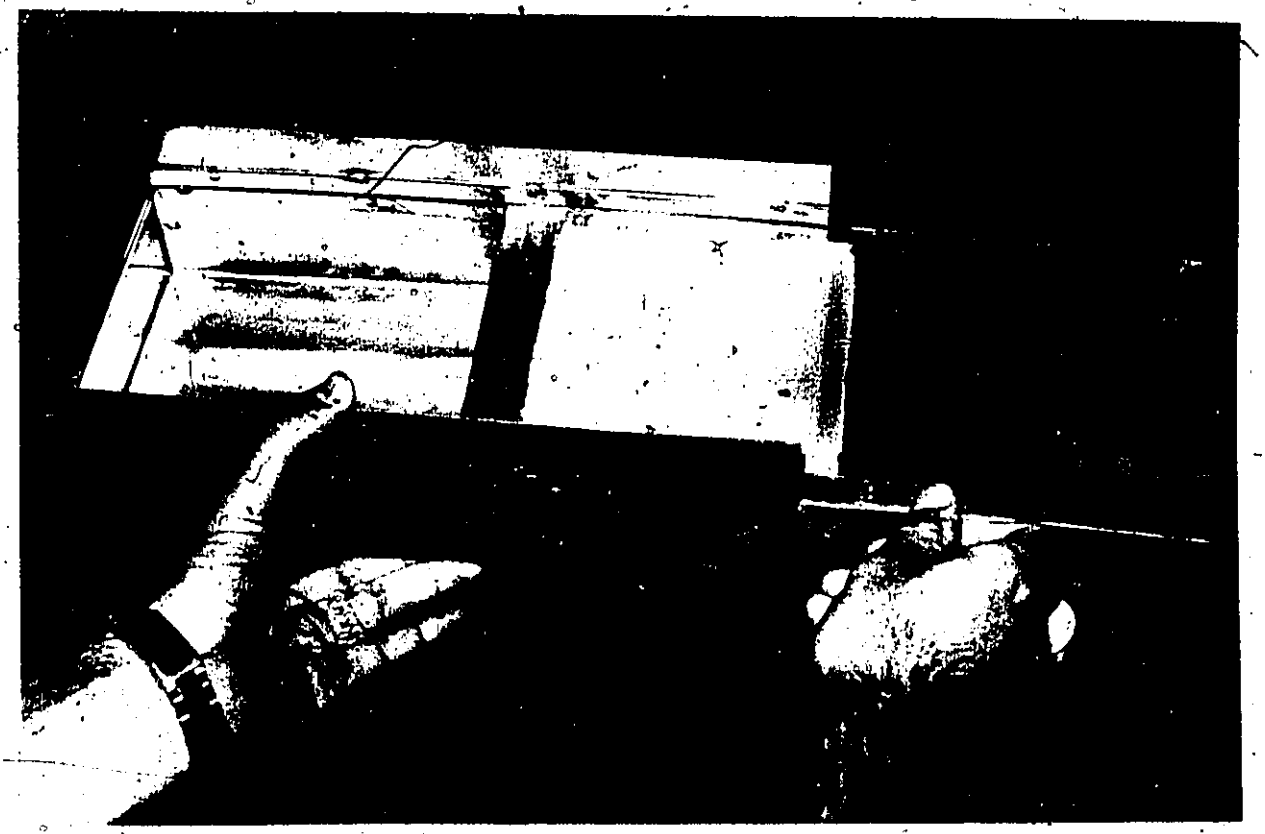

PLATE 6:

Bed sediment sampler

after the weights have come to rest on the bed. The divers can descend along the lines, and can therefore maintain close proximity to each other, an important requisite of scuba diving. Two other ropes, one attached to each of the weights, lie along the bed downstream from the weights. These provide support for the divers working on the bottom.

a. Bedload Sampling

The transport of bedload in the study section was measured with the sampler described in the preceeding section. Four stations were established along one cross section in the main channel south of Kettle Island, and one station was established in the channel north of Kettle Island (Fig. 36).

The south channel at the particular cross section studied has the profile shown in Fig. 37. The entire width of the channel is not covered by sediments being actively transported. The sand and silt introduced to the Ottawa River by the Gatineau River occur as a belt which meanders on a stiff glacial clay floor through the south channel (for provenance of the study section sediment, see Part II of this report). The boundary between the actively transported sand bed and the clay floor of the channel is marked on both Figs. 36 and 37. It is evident, then, that bedload is not an imposed variable

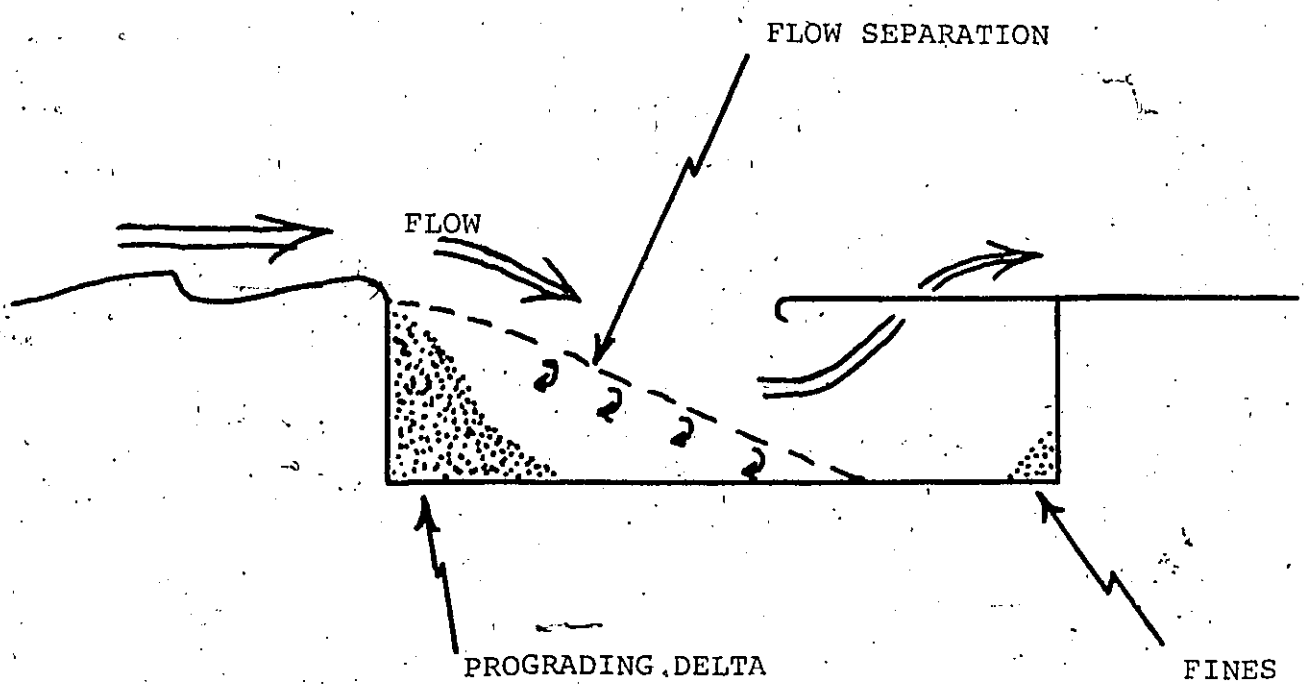

FIG. 35: BED LOAD SAMPLER

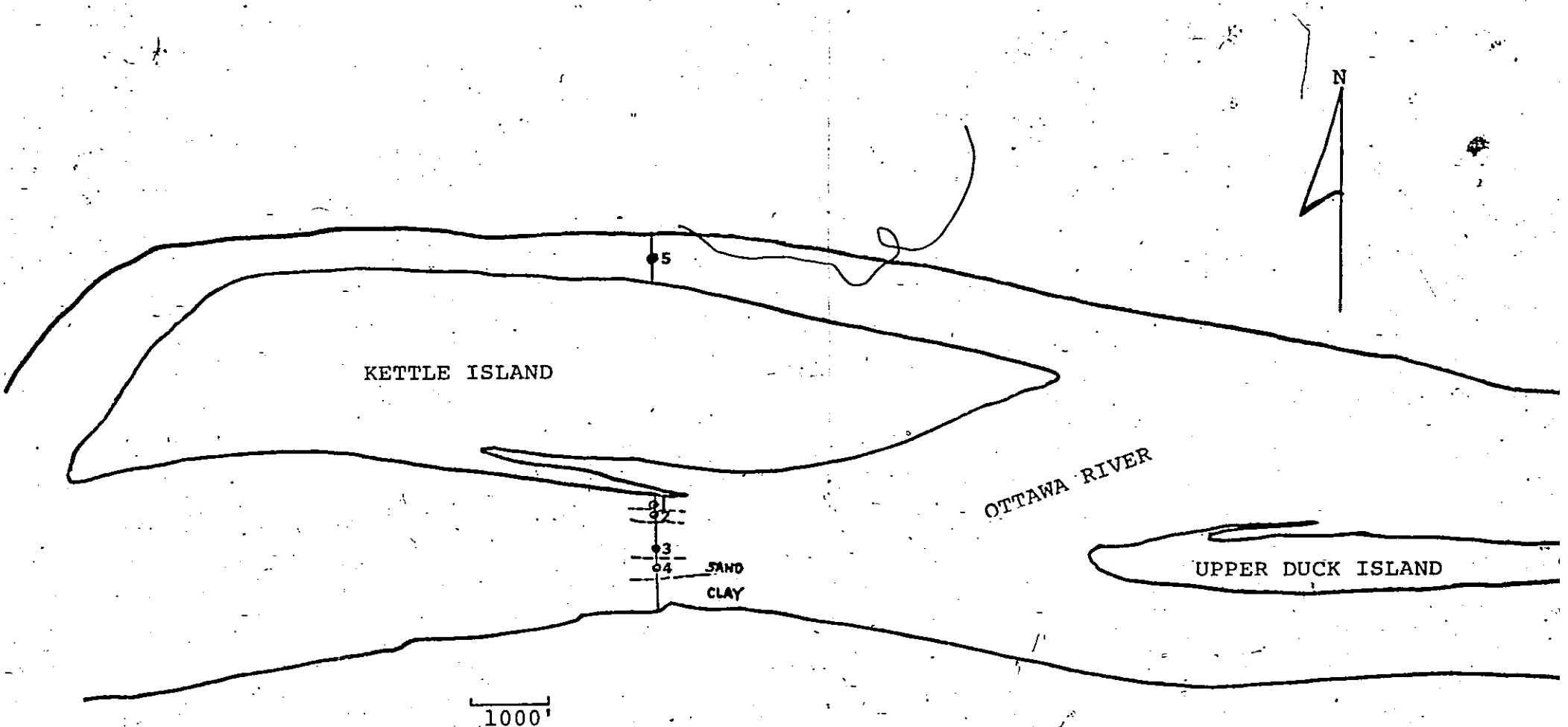

FIG. 36 : DIVING AND DUNE TRACKING STATIONS

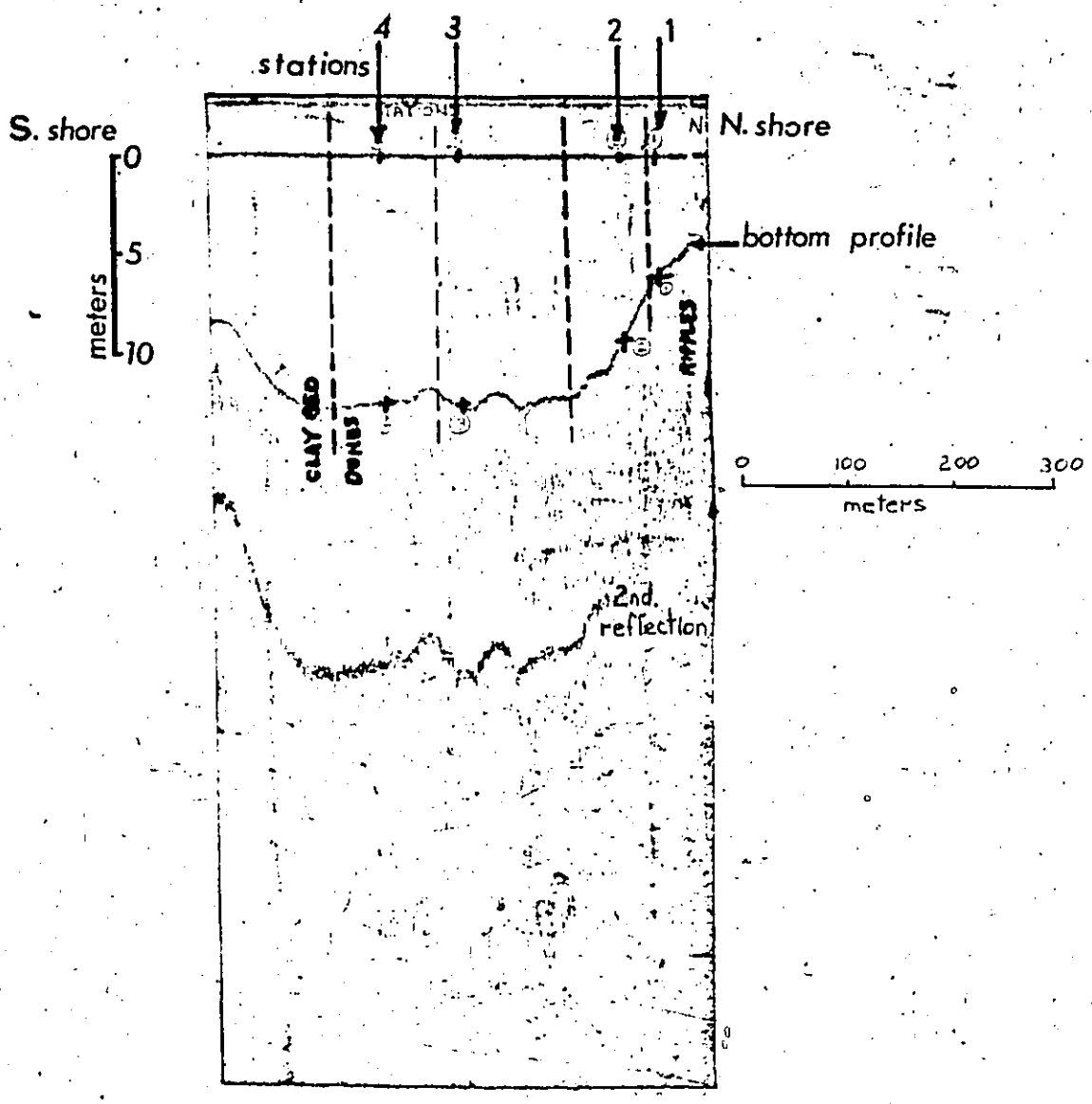

FIG. 37: Bedload measuring stations – Main channel cross-section

in this river, but rather as Nordin (1964, p.29) points out, a river will adjust its flow characteristics to transport all the material available. Measuring sediment discharge at one cross-section only is therefore sufficient, for unless the channel is aggrading or degrading, sediment discharge must be the same at all cross sections. Aerial photos covering the study section were consulted, and in the last 50 years the channel configuration has remained constant. The discharge measured at the cross section in Fig. 36 is therefore valid for the study section as a whole.

The clay floor which outcrops south of the boundary shown in Figs. 36 and 37 is covered in places by a thin veneer of silt, held to the clay by cohesive forces. It was this silty material that was collected by grab sampling, and that was subjected to the textural and chemical analyses discussed in Part III. The author considers transport of this material to be negligible, and so total discharge figures reported represent the sand bed north of the boundary.

The north channel has the profile shown in Fig. 38 at the cross section indicated on Fig. 36. The extreme flatness of the channel probably results in nearly constant sediment transport over the width of the channel, thus only one station was monitored.

The measurements conducted at station 1 were considered

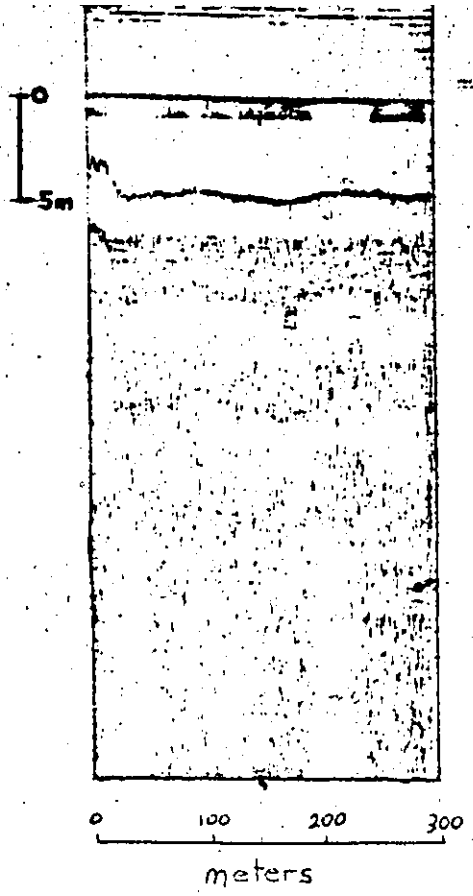

— at Kettle Island's downstream tip

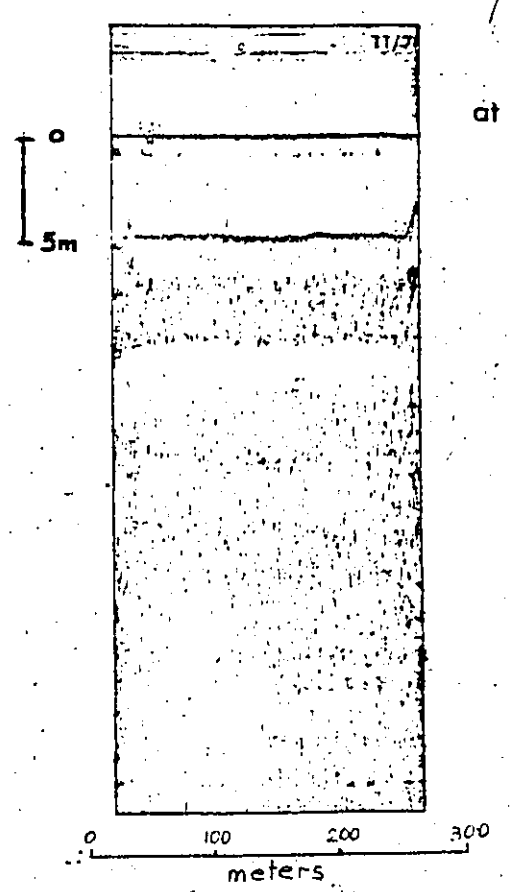

at the cross—section shown in fig. 36

FIG. 38: NORTH CHANNEL BOTTOM PROFILES

valid over the width indicated on Figs. 36 and 37, on the basis of bed form type. A ripple bed prevails in that width, the point of incipient dune formation providing the southern boundary. Water depth varies between 0 and 6.5 m., averaging 5m. in this compartment. Station 2 is considered valid over the channel width shown in Fig. 36 and 37. The bed is in dune regime (dunes approx. 2' in height), and water depth increases along a nearly constant drop-off from 6.5m to 12.5m. Station 2 itself is at 9m depth. Stations 3 and 4 are located on the relatively flat floor of the channel, station 3 is valid over depths from 12.5m to 13.5m and station 4 is valid over the channel width from the 13.5m boundary with station 3 to the clay floor outctop. The contact between the sand bed and the clay floor is abrupt. Table VIII records the weight of sediment collected at each station at various times over a 6 day period. During the 6 day period gauge height of the river was practically constant, although the river was in falling stage when the measurements were taken, after an abnormally high peak flow.

The sample weights were averaged for each station, and a discharge calculated over the width for which the measurements were considered valid. It is obvious that transport rates vary widely, probably due to the oscillatory nature of bedload transport. In addition, current gusts

TABLE VIII: BEDLOAD MEASUREMENTS - JUNE 7 TO JUNE 13, 1974

STATION	VALID WIDTH	COLLECTING TIME	SEDIMENT WEIGHT
1	185' (57.4m)	300 secs.	353.3 grams
		200	370.6
		200	51.8
2	148 (45.9m)	200	354.1
		200	667.4
		200	121.7
		200	35.5
3	482 (149.4m)	200	212.8
		100	412.1
		200	145.2
		200	596.5
4	296 (91.8m)	200	479.3
		100	378.0
		200	643.6
		200	438.3
		200	216.0
5	750 (232.5m)	5 mins.	18.7

were noted by the divers to occur as often as three times per minute. The gusts caused notable increases in sediment transport rates. The accuracy of this method would therfore increase with the collecting time and with the number of measurements taken at a given station. Further, the narrower the widths over which the measurements are applied, the greater the accuracy.

For the south channel, sediment discharge is calculated to be 3.87 X 10^5kg/day. The total discharge, including the north channel figure of .08 X 10^5kg/day, is on the order of 3.95 X 10^5kg/day (see Appendix III).

E. BEDLOAD DISCHARGE BY DUNE TRACKING

An indirect method of measuring bedload discharge, tracking of dune crest movement by sonic depth sounding, has been proven effective in flume studies, and may have merit in natural systems as well (see Part IV, Literature Review). This method was applied to the same cross-section of the study section that was subjected to bedload measurements, so that discharge figures obtained by two entirely different approaches could be compared. The stations previously discribed were used for the dune tracking method as well, and the discharge was measured over the same 6 day period. Dune crest positions in relation to station buoys were monitored by depth sounding, and the downstream migration was measured at the end of the

6 day period. Station 1 could not be used since there is only a rippled bed at that compartment. Measurements at station 2 were therefore considered to be valid over the width of stations 1 and 2. The total discharge value, then should be erroneously high.

Dune velocity at station 2 was approximately 3.4 ft/day, at station 3, 3.2 ft/day, and at station 4, 3.6 ft/day. Average dune height at station 2 was 2 feet, at station 3, 5.2 feet, and at station 4, 6.5 feet. Bedload discharge was calculated using the equations developed by Richardson et al (1961) and Hubbell (1964, p.43-49),

$$q_B = [(K-\lambda)/2]\ vh\ dw,$$

where q_B is volume discharge, K is unity (see Literature Review), λ is porosity (taken as 30%), v is the velocity of the dune crests, and h is the average dune height. The volume discharge obtained was 6.0×10^3 cu.ft./day, which is equivalent to 4.5×10^5 kg/day using a specific gravity conversion factor of 2.65 grams/cc.

The discharge values obtained by the two methods, sampling and dune tracking, are in close agreement, 3.87×10^5 kg/day by the sampling method, and 4.5×10^5 kg/day by the dune tracking method. The dune tracking result is probably erroneously high, due to the ripple bed ignored at station 1, so the two method do support each other quite well.

The accuracy of the total sediment discharge figure

obtained by the sampling method, then, is probably much better than order-of-magnitude, since the results obtained by an entirely different method are within 16%.

F. Hg DISCHARGE IN BOTTOM SEDIMENTS

The approximate weight of Hg adsorbed to bottom sediment particles that passes a given cross-sectional line of the study reach can be calculated since average Hg concentrations and average bedload discharges are known.

Figure 39 is a representation, from bottom to top, of bedload discharge per unit width, bedload discharge per compartment, average Hg concentration within a compartment, and finally the Hg discharge per compartment. The compartment number and its width appear along the bottom of the histogram, and for the main channel cross-section, North and South are indicated at the top of the figure. The values for average bedload discharge per foot are those determined by the diver-operated sampler method. The total bedload discharge per compartment values take in to account the compartment width (see figures 36 and 37 for location of compartments) and the discharge/foot values in the bottom histogram. Average Hg concentrations of the bottom sediments lying along the cross-sectional traverse line shown on figure 36 were estimated using the Hg distribution pattern of Figure 21. These values

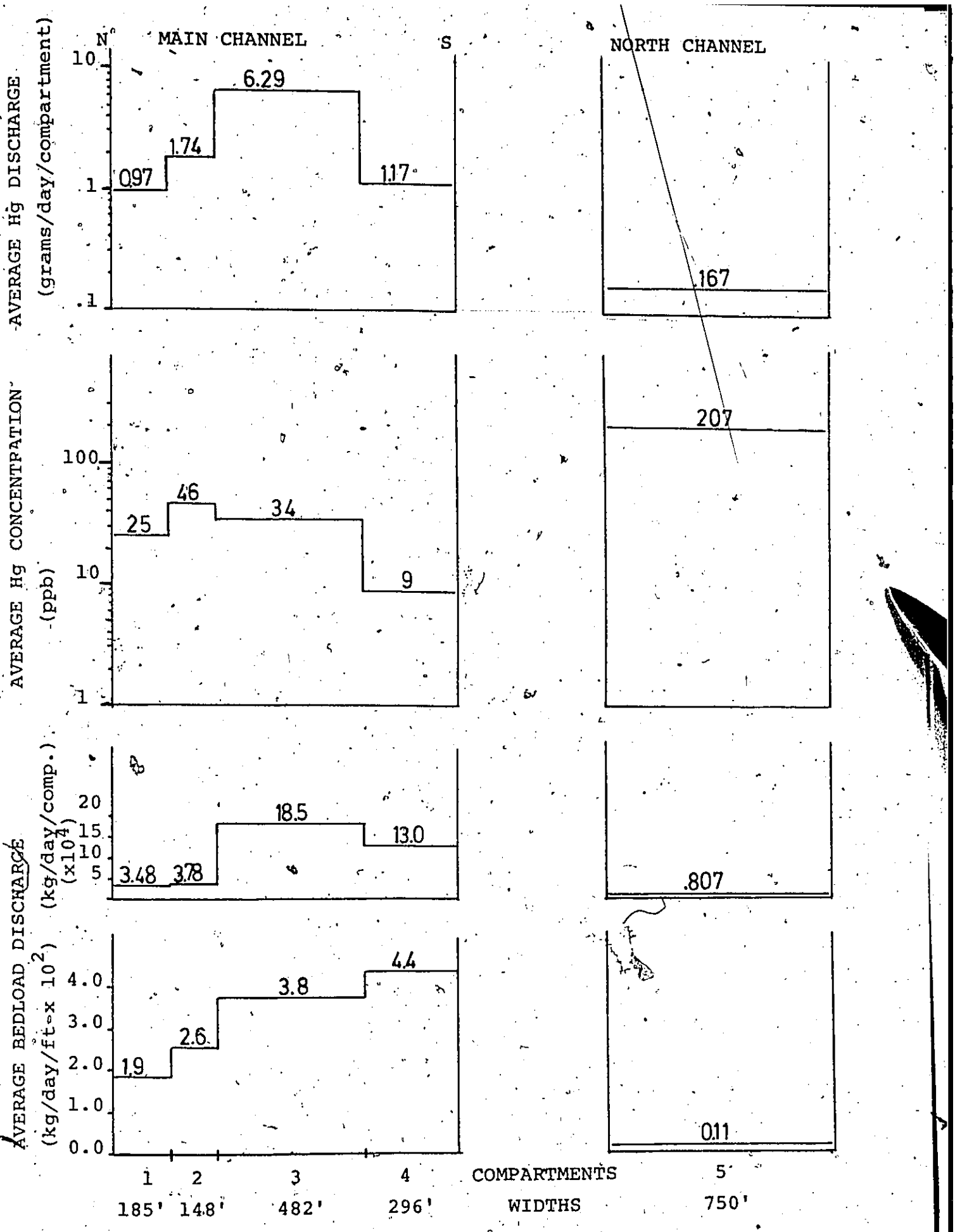

FIGURE 39: Hg DISCHARGE

appear in the third histogram of figure 39. The value for Hg discharged by each compartment is the product of the average Hg concentration and the average bedload discharge per compartment. The values calculated are shown in the top histogram of figure 39.

Compartment 5, the north channel compartment, discharges only .167 g Hg/day, despite the very high average Hg concentrations, due to the low bedload discharge rates. Of the main channel compartments, number three discharges the greatest total amount of Hg; although it is intermediate in bedload discharge and Hg concentration, this high discharge is due to the (arbitrarily) large width of the compartment. Hg discharge of station 1 is 0.97 g/day, of station 2, 1.74 g/day, of station 3, 6.29 g/day, and of station 4, 1.17 g/day. The total daily Hg discharge of the Ottawa River at the study reach is therfore 10.49 g/day. This figure is valid only for the 6 day period commencing June 7, 1974, during which time the river stage was at about 3/4 normal peak flow. Hg discharge would be less for many months after, and greater for a short while (one month) before this period. However the figure is useful since it indicates the order-of-magnitude of Hg discharge in the study reach bed sediments.

It was determined in Part III (p.105-106) that the concentration of Hg in bed sediments of the study reach

is decreasing with a half-life on the order of 12 months. This rate of decrease was valid for both the north and main channels. It is clear that bedload discharge/foot in the north channel is less than 1/10 that of the main channel (Fig. 39), and yet Hg decrease is the same for both channels. It is apparent, then, that flushing of the bed sediments out of the study reach is not the sole factor causing the Hg decrease. Chemical desorption is probably the important factor in the north channel and in marginal areas; whereas the effects of both chemical desorption and transport out of the section combine to reduce main channel Hg levels.

G. SUMMARY

1) Sand dunes, .5 to 3.0m in height and 30 to 250 feet in length underlie much of the study reach. The occurrence of dunes is limited to water depths greater than 16 ft. (approx. 5m) and to beds of non-cohesive sandy sediment. In areas shallower than 16 feet a ripple bed prevails, and in areas of cohesive sediment, a plane bed prevails. The relation ship between dune length and water depth (λ=4.4 Depth) is statistically significant and is in accord with the literature. Dune height is also well correlated with water depth (height = .12 Depth).

2) The channel floor is only partially occupied by a sand tract which meanders through the study reach on a bed of outcropping Pleistocene clay.

3) Lateral mixing of marginal and mid-channel sands may be partially achieved by currents occupying the troughs of dunes. The currents flow perpendicular to the main flow from the channel margins to deeper water, and have sufficient competency to transport the bottom material present. Assymetric ripples, produced by the flow-normal currents, are oriented with lee slopes facing deeper water.

4) A diver-operated bedload sampler yields a bedload discharge figure that agrees closely with the bedload discharge figure determined by tracking dune crest movement. For the main channel, where dunes prevail, the two methods indicate bedload discharge on the order of 4×10^5 kg/day for the 6 day sample period. The rippled bed of the north channel did not allow dune tracking; therefore the sampler alone was used, indicating a low discharge rate of 8×10^2 kg/day.

5) The discharge of Hg associated with the bottom sediments is on the order of 10,5 g/day, the highest discharge rates occurring in mid-channel dune areas of intermediate Hg concentration.

6) Chemical desorption as well as sediment flushing appear to be responsible for declining Hg levels in the bed sediments.

PART V - THESIS SUMMARY

PART V - THESIS SUMMARY

The sandy sediments of the Ottawa River study reach are derived from the metamorphic Precambrian Shield rocks to the north. The tributary Gatineau River supplies the largest part of the bed sediments. The tributary Rideau River introduces detritally unstable sedimentary rock fragments to the Ottawa but these do not persist into the study reach. The upper Ottawa River sediments are ponded in several places, and hence contribute little to the study reach. The sand tract introduced by the Gatineau meanders through the study reach covering only 75% to 85% of a channel floor consisting of outcropping Pleistocene clay.

The high surface area components of the bed sediments (fine grains and wood debris) adsorb greater amounts of heavy metals than the coarser sand grains. Sediment fineness (or more correctly, sediment surface area) controls in part the concentration of Fe hydroxide coatings on bed material particles, such that high Fe values are found in high surface area sediments. Mn and Hg, which occur in concentrations 1/10 and 1/10,000 (respectively) that of Fe, are controlled by the concentation of Fe coatings. Quiescent conditions apparently favour higher concentrations of Fe coatings.

Hg concentration levels have decreased with an

approximate half-life of 12 months since government imposed controls on the industrial use of Hg were brought into effect in 1971. The half-life appears to be independent of sediment discharge, suggesting that both chemical desorption and sediment flushing are operating to reduce Hg levels

Two methods used to determine bedload discharge, a diver-operated bedload sampler and dune crest tracking by sonic depth-sounding, yielded similar results. Bedload discharge for the sampling period was on the order of 4×10^5 kg/day. The discharge of Hg associated with the bottom sediments is on the order of 10.5g/day, the highest discharge rates occurring in mid-channel dune sediments with intermediate Hg concentrations.

Transport is acheived by dune migration in water depths greater than 5 meters ($\sim$ 16.5 feet) and by ripples in shallower water. Dune height and length are strongly correlated with water depth.

A current was observed that flows perpendicular to the main flow direction. It occupies the troughs of the dune train, and flows from shallow marginal areas towards deeper mid-channel water. The power of the current is sufficient to transport bed material in the ripple regime, and thus causes lateral mixing of bed sediments.

REFERENCES

1) Adamson, A.W. (1960); Physical Chemistry of Surfaces; INTERSCIENCE PUB., N.Y. 629p.

2) Allen, J.R.L. (1968); Current Ripples; North-Holland Publishing Co., Amsterdam; 433p.

3) Baird, D.M. (ed.) (1972); Geology of the National Capital Area; International Geological Congress Guidebook, Excursions B-23 to B-27, 1972.

4) Bear, F.E. (1964); Chemistry of the Soil; A.C.S. Monograph Series, No. 160; REINHOLD, N.Y. 515p.

5) Beckman, E.W., and Furness, L.W. (1962); Flow Characteristics of Elkhorn River Near Waterloo, Nebraska; U.S.G.S. Water-Supply Paper 1498-B; 34p.

6) Brunauer, S., Emmett, P.H., and Teller, E. (1938); Adsorption of Gases in Multimolecular Layers; J. AMER. CHEM. SOC., v. 60, p309.

7) Buser and Graf (1955); Differentiation Between Manganous (II) manganite and -MnO_2 by means of B.E.T. Surface Measurements; HELV. CHIM. ACTA. 38, p830.

8) Colby, B.R. (1961); Effect of Depth of Flow on Discharge of Bed Material; U.S.G.S. Water-Supply Paper 1498-D; pp. 1-12.

9) Colby, B.R. (1963); Fluvial Sediments - a Summary of Source, Transportation, Deposition, and Measurement of Sediment Discharge; U.S.G.S. Bull. 1181-A.

10) Colby, B.R. (1964); Discharge of Sands and Mean-Velocity Relationships in Sand-bed Streams; U.S.G.S. Prof. Paper 462-A; 47p.

11) Culbertson, J.K. and Dawdy, D.R. (1964); A Study of Fluvial Characteristics and Hydraulic Variables, Middle Rio Grande, New Mexico; U.S.G.S. Water-Supply Paper 1498-F; 74p.

12) de Groot, A.J. (1973); Field Observations on the Transport of Heavy Metals in Sediments; in Proceedings of the Conference on Heavy Metals in the Aquatic Environment, Nashville (Tennessee).

13) Fairbridge, ed. (1973); Encyclopedia of Geochem. and Environ. Sci., van NOSTRAND (pub.), N.Y. 1321p.

14) Fyfe, W.S., Turner, F.J., and Verhoogen, J. (1962); Metamorphic Reactions and Metamorphic Facies; GSA Memoir 73, 259p.

15) Garrels, R.M. and Christ, C.L. (1965); Solutions, Minerals, and Equilibria; Harper and Row, N.Y.; 450p.

16) Gibbs (1973); Mechanisms of Trace Metal Transport in Rivers; SCIENCE, v.180, No. 4081 p71-73.

17) Goldberg, E.D. (1954); Chemical Scavengers of the Sea; JOUR. GEOL., v.63, p249.

18) Goldberg, E.D. (1963); The Oceans as a Chemical System, in THE SEA, v.2, Composition of Seawater, Comparative and Descriptive Oceanography; Hill, editor.

19) Harms, J.C. and Fahnestock, R.K. (1965); Stratification, Bed Forms, and Flow Phenomens; in Primary Sedimentary Structures and their Hydrodynamic Interpretation; S.E.P.M. sp. pub. no. 12.

20) Hem and Cropper (1959); Survey of Ferrous-Ferric Chemical Equilibria and Redox Potentials; U.S.G.S. Water-Supply Paper 1459A, p.1-30.

21) Hem, J.D. (1960); Chemical Relationships among Sulfur Species and Ferrous Iron; U.S.G.S. Water-Supply Paper 1459-C, p.57-73.

22) Hem, J.D. (1960); Complexes of Ferrous Iron with Tannic Acid; U.S.G.S. Water-Supply Paper 1459-D, p.75-94.

23) Hem and Skougstad (1960); Coprecipitation of Ferrous, Ferric, and Cupric Ions; U.S.G.S. Water-Supply Paper 1459-E, p.95-110.

24) Hem, J.D. (1967); Chemical Equilibria and Rates of Manganese Oxidation; U.S.G.S. Water-Supply Paper 1667A, p.A1-A64.

25) Hem, J.D. (1964); Deposition and Solution of Manganese Oxides; U.S.G.S. Water-Supply Paper 1667B, p.B1-B42.

26) Hem, J.D. (1972); Chemical Factors that Influence the Availability of Iron and Manganese in Aqueous Systems; GSA BULL. 83; p.443-450.

27) Hogarth, D. (1962); A Guide to the Geology of the Gatineau-Lievre District; The Canadian Field Naturalist, v. 76, no. 1, pp.1-55.

28) Hubbell, D.W. (1964); Apparatus and Techniques for Measuring Bedload; U.S.G.S. Water-Supply Paper 1748, 74p.

29) Jenne, E.A. (1968); Controls on Mn, Fe, Co, Ni, Cu, and Zn Concentrations in Soils and Water: The Significant Role of Hydrous Mn and Fe Oxides; Advances in Chemistry Series, No. 73, Trace Inorganics in Water, 337-387.

30) Johnston, W.A. (1917); Pleistocene and Recent Deposits in the Vicinity of Ottawa, with a Description of the Soils; G.S.C. Memoir 101, Ottawa.

31) Krausdopf, K.B. (1956); Factors Controlling the Concentrations of Thirteen Rare Metals in Seawater; Geochemica et Cosmochimica Acta 9, p.1-32.

32) Krausdopf, K.B. (1967); Introduction to Geochemistry; McGraw-Hill, N.Y.; 721p.

33) Langmuir and Whittmore (1971); Stability of Ferric Oxyhydroxides; Non-Equilibrium Systems in Natural Waters; Advances in Chemistry Series 106, p.209-234.

34) Lee, G.F. (1964); (in reply to Morgan and Stumm, (ref. 27); Proceedings of the Second International Conference, p.124.

35) Lee, G.F. (1973); Role of Hydrous Metal Oxides in the Transport of Heavy Metals in the Environment; Proceedings of Conference on Heavy Metals in the Aquatic Environment.

36) Linke, W.F. (1965); Solubilities; Amer. Chem. Soc.

37) Maloney, J.M. (1969); Petrology and Structural History of the Hogsback, Ottawa; unpub. B.Sc. Thesis, University of Ottawa.

38) Medema, J. and Houtman, J.P.W. (1969); B.E.T. Specific Measurement of Solids Using Krypton; Anal. Chem., v.41(1), p.209-211.

39) Middleton, G.V. (ed.) (1965); Primary Sedimentary Structures and Their Hydrodynamic Interpretation; S.E.P.M. sp. pub. no. 12; Introduction, pp.1-4.

40) Miller, D.R. (1974); Ottawa River Project Annual Report; N.R.C., Ottawa.

41) Milner, H.B. (1962); Sedimentary Petrography; Allen & Unwin, London; 2v.

42) Moorhouse, W.W. (1959); The Study of Rocks in Thin Section; Harper, N.Y.; 514p.

43) Morgan and Stumm (1964); Colloid-chemical Properties of Manganese Dioxide; Journal of Colloid Science, v. 19, no. 4, p.347-359.

44) Morgan and Stumm (1964); The Role of Multivalent Metal Oxides in Limnological Transformations; in Advances in Water Pollution Research, Proceedings of the 2nd International Conference; Pergamon Press p.103-117.

45) Nordin, C.F. (1963); Study of Channel Erosion and Sediment Transport; Journ. of the Hydraulics Division, Proceedings of the Amer. Soc. Civil Eng., v. 90, no. HY4; pp.173-192.

46) Nordin, C.F. (1964); Aspects of Flow Resistance and Sediment Transport, Rio Grande Near Bernalillo, New Mexico; U.S.G.S. Water-Supply Paper 1498-H; 41p.

47) Oliver and Kinrade (1972); Heavy Metal Concentrations in the Rideau and Ottawa Rivers; Inland Waters Branch, Dept. of the Environ.

48) Ontario Water Resources Commission and Quevec Water Board (1971); Ottawa River Basin, Water Quality and its control in the Ottawa River; v.1, 125p.

49) Parks, G.A. (1967); Aqueous Surface Chemistry of Oxides and Complex Oxides Minerals; in Equilibrium Concepts in Natural Water Systems; Advances in Chem. Series, v.67, p.121-160.

50) Pettijohn, Potter, and Siever (1972); Sand and Sandstone; Berlin, N1Y., Springer-Verlag; 618p.

51) Posselt, H.S., Anderson, F.J., and Weber, W.S. (1968); Cation Sorption on Colloidal Hydrous Manganese Dioxide; Environ. Sci. and Tech. v.2, p.1087-1093.

52) Reimers, R.S. and Khrenkel, P.A. (1973); Sorption Phenomenon in the Organics of Bottom Sediments; in Proceedings of Conference on Heavy Metals in the Environment, Nashville, Tennessee.

53) Reynolds, A.J. (1964); Waves on the Erodible Bed of an Open Channel; J. Fluid Mechanics, V.22, Part 1, pp.113-133.

54) Richardson, E.V., Simons, D.B., and Posakony, G.J., (1961); Sonic Depth Sounder for Laboratory and Field Use; U.S.G.S. Circular 450; 7p.

55) Shimomura, S., Nishihara, Y., Fukumoto, Y., and Tanase, Y. (1969); Adsorption of Mercuric Ion on Ferric Hydroxide; Journal of Hygienic Chemistry, v.15, p.84-89.

56) Simons, D.B. and Richardson, E.V. (1961); Forms of Bed Roughness in Alluvial Channels; A.S.C.E. Proceedings, Journ. Hydraulics Div. 87, HY3; p.87-105.

57) Simons, D.B. and Richardson, E.V. (1965); A Study of Variables Affecting Flow Characteristics and Sediment Transport in Alluvial Channels; in Proceedings of the Federal Interagency Sedimentation Conference, Agriculture Research Service, Misc. Pub. no. 970, U.S. Dept. of Agriculture; p.193-207.

58) Simons, D.B., Richardson, E.V., and Nordin, C.F. Sr. (1965a); Sedimentary Structures Generated by Flow in Alluvial Channels; in Primary Sedimentary Structures and their Hydrodynamic Significance; S.E.P.M. sp. pub. no 12, p.34-52.

59) Simons, D.B., Richardson, E.V., and Nordin, C.F. Sr. (1965b); Bedload Equation for Ripples and Dunes; U.S.G.S. Professional Paper 462-H, 9p.

60) Stichling, W. and Smith, T.F. (1968); Sediment Surveys in Canada; Inland Waters Branch, Tech. Bull. no. 12; Dept. of Energy, Miners and Resources, Ottawa; 17p.

61) Tanaka, M. (1964); in reply to Morgan and Stumm, Proceedings of the 2nd International Conference (ref.27 above), p.118.

62) Taylor, H.S., and Glasstone, S. (1951); A Treatise on Physical Chemistry, v.2, States of Matter, p.607, Nostrand Co., Toronto.

63) Truesdell, A.H. (1972); Ion Exchange; in the Encyclopedia of Geochem. and Environ. Sci., R.W. Fairbridge (ed); Reinhold, N.Y., p.591-594.

64) Weast, R.C. (1974); Handbook of Chemistry and Physics; 54th ed., Chemical Rubber Co., Ohio.

65) Wilson, A.E. (1946); Geology of the Ottawa-St. Lawrence Lowland, Ontario and Quebec; G.S.C. Memoir No. 241, Ottawa.

66) Winkler, H.G.F. (1965); Petrogenesis of Metamorphic Rocks; Springer-Verlag New York Inc.; 220p.

67) Yalin, M.S. (1964); Geometrical Properties of Sand Waves; Journal of the Hydraulics Division, Proceedings of the Amer. Soc. of Civil Eng., vol. 90, no. HY5, pp.105-119.

APPENDIX I - HEAVY MINERAL EXAMINATION

IDENTIFICATION OF OPTICAL MINERALS

1. TRANSPARENT √ TRANSLUCENT OPAQUE	2. COLOUR RED	3. HABIT FACETED EUHEDRA & ROUNDED GRAINS	4. SHAPE ANGULAR SUBANGULAR ROUNDED √	5. FRACTURE SUB-CONCH.
6. CLEAVAGE NONE DIRECTION	7. SURFACE FEATURES	8. R.I.(oil) R.I.(min) R.I. = ≡ 1.765	9. INCLUSIONS ABUNDANT	
10. PLEOCHROISM NIL	11. ISOTROPIC √ ANISOTROPIC	12. BIREFRINGENCE	13. EXTINCTION STRAIGHT OBLIQUE (ANGLE)	
14. UNIAXIAL BIAXIAL	15. OPTIC SIGN +'ve -'ve	16. 2V °	17. DISPERSION	
BS 24	18. IDENTITY ALMANDITE			

EXAMINATION OF DETRITAL MINERALS

1. TRANSPARENT ✓ TRANSLUCENT to ✓ OPAQUE	2. COLOUR YELLOW, BROWN, GREEN	3. HABIT PLATES, SOME TABULAR	4. SHAPE ANGULAR SUBANGULAR ROUNDED	5. FRACTURE IRREGULAR
6. CLEAVAGE BASAL & 1 OTHER EXTINCTION ⊥	7. SURFACE FEATURES —	8. R.I.(oil) R.I.(min) 1.645 >
1.700 < R.I. = VARIABLE	INCLUSIONS ABUNDANT	
10. PLEOCHROISM YELLOW → DARK GREEN max absorption // elongation	11. ISOTROPIC ANISOTROPIC ✓	12. BIREFRINGENCE MOD → HIGH	13. EXTINCTION STRAIGHT OBLIQUE ✓ (ANGLE)	
14. UNIAXIAL BIAXIAL ✓	15. OPTIC SIGN +ve -ve ✓	16. 2V SMALL < 10°	17. DISPERSION	
BS.24	18. IDENTITY INTERMEDIATE BIOTITE → CHLORITE?			

IDENTIFICATION OF DETRITAL MINERALS

1. TRANSPARENT ✓ TRANSLUCENT OPAQUE	2. COLOUR GREEN	3. HABIT PRISMATIC	4. SHAPE ANGULAR ✓ SUBANGULAR ROUNDED	5. FRACTURE IRREG. → SUB-CONCH
6. CLEAVAGE 2 DIRECTION ~ 90°	7. SURFACE FEATURES STRIATION ∥ ELONGATION	8. R.I.(oil) R.I.(min) 1.660 >
1.700 <
1.676 >
R.I.	9. INCLUSIONS TRANSPARENTS BROWN PRISMS SOME ⊥ ELONGATION	
10. PLEOCHROISM STRONG PINK - GRAY OR COLOURLESS MAX. ABSORB ⊥ POLAR	11. ISOTROPIC ANISOTROPIC ✓	12. BIREFRINGENCE MOD. → HIGH ALTERATION HALOES GIVE ANOMALOUS BIREFRINGENCE	13. EXTINCTION STRAIGHT ✓ OBLIQUE (ANGLE)	
14. UNIAXIAL BIAXIAL ✓	15. OPTIC SIGN +'ve -'ve ✓	16. 2V 20°	17. DISPERSION STRONG	

B.S. 24

18. IDENTITY CHLORITE (?) - AMPHIBOLE
ALTERED PYROXENE

EVALUATION OF DETRITAL MINERALS

1. TRANSPARENT ✓ TRANSLUCENT OPAQUE	2. COLOUR COLOURLESS	3. HABIT PRISMATIC W/ VARIETY OF TERMINATIONS	4. SHAPE ANGULAR ✓ SUBANGULAR ROUNDED	5. FRACTURE CONCHOIDAL
6. CLEAVAGE # ? DIRECTION	7. SURFACE FEATURES ⊥	8. R.I.(oil) R.I.(min) 1.700 < 1.648 < 1.596 < > R.I.=	9. INCLUSIONS PRESENT, OPAQUE & TRANSPARENT	
10. PLEOCHROISM SLIGHT YELLOW→BRWN. ORANGE	11. ISOTROPIC ANISOTROPIC ✓	12. BIREFRINGENCE MODERATE	13. EXTINCTION INCOMPLETE STRAIGHT ✓ OBLIQUE (ANGLE)	
14. UNIAXIAL BIAXIAL ✓	15. OPTIC SIGN +'ve -'ve ✓	16. 2V LARGE	17. DISPERSION —	
← POOR FIGURES →				
BS.24	18. IDENTITY CORDIERITE			

IDENTIFICATION OF DETRITAL MINERALS

1. TRANSPARENT √ TRANSLUCENT OPAQUE	2. COLOUR -LESS	3. HABIT NO XSTAL FACES	4. SHAPE ANGULAR SUBANGULAR ROUNDED √	5. FRACTURE ?
6. CLEAVAGE ≥ 1 DIRECTIONS ?	7. SURFACE FEATURES	8. R.I.(oil) R.I.(min) 1.735 < 1.596 > 1.700 < 1.640 > 1.676 ≡ R.I. = 1.676	9. INCLUSIONS COLOURLESS	
10. PLEOCHROISM	11. ISOTROPIC ANISOTROPIC √	12. BIREFRINGENCE MOD→HIGH	13. EXTINCTION STRAIGHT OBLIQUE √ (ANGLE ?)	
14. UNIAXIAL BIAXIAL √	15. OPTIC SIGN +'ve √ -'ve	16. 2V - 60°	17. DISPERSION	

B.S. 24

18. IDENTITY DIOPSIDE

EXAMINATION OF PETRICAL MATERIAL

1. TRANSPARENT √ TRANSLUCENT OPAQUE	2. COLOUR PALE GREEN	3. HABIT LATH-SHAPED	4. SHAPE ANGULAR √ SUBANGULAR ROUNDED	5. FRACTURE UNEVEN
6. CLEAVAGE 2 DIRECTION ~ 90°	7. SURFACE FEATURES	8. R.I.(oil) R.I.(min 1.596 >
1.676 <
1.636 >
1.660 >
R.I. = 1.660<R.I<1.676	9. INCLUSIONS VARIED	
10. PLEOCHROISM COLOURLESS →PALE GREEN	11. ISOTROPIC ANISOTROPIC √	12. BIREFRINGENCE MOD.→HIGH	13. EXTINCTION STRAIGHT OBLIQUE √ (ANGLE ~20°)	
14. UNIAXIAL BIAXIAL √	15. OPTIC SIGN +'ve √ -'ve	16. 2V INTERMEDIATE	17. DISPERSION	
BS 24	18. IDENTITY DIOPSIDE			

EXAMINATION OF DETRITAL MINERALS

1. TRANSPARENT √ TRANSLUCENT OPAQUE	2. COLOUR YELLOWISH – GREEN	3. HABIT VARIABLE	4. SHAPE ANGULAR √ SUBANGULAR ROUNDED	5. FRACTURE UNEVEN
6. CLEAVAGE 1 DIRECTION ?	7. SURFACE FEATURES *	8. R.I.(oil) R.I.(min) R.I. = > 1.700	9. INCLUSIONS ALIGNED PRISMS ⬭ ZIRCON ?	
10. PLEOCHROISM WEAK GREEN → GR.–YELLOW	11. ISOTROPIC ANISOTROPIC √	12. BIREFRINGENCE MOD → STRONG	13. EXTINCTION STRAIGHT √ OBLIQUE (ANGLE)	
14. UNIAXIAL BIAXIAL √	15. OPTIC SIGN +ve –ve √	16. 2V HIGH 760°	17. DISPERSION	
P.S. 24	18. IDENTITY EPIDOTE			

EXAMINATION OF MINERAL GRAINS

1. TRANSPARENT ✓ TRANSLUCENT OPAQUE	2. COLOUR COLOURLESS	3. HABIT POOR HEX. FACES	SHAPE ANGULAR SUBANGULAR ✓ ROUNDED ✓	5. FRACTURE CONCHOIDAL
6. CLEAVAGE 0 DIRECTION	SURFACE FEATURES IRON STAINED	8. R.I.(oil) R.I.(min) 1.596 >
1.700 >
1.735 ≥ R.I. - slightly ≥ 1.735	9. INCLUSIONS OPAQUES & PRISM. PURPLISH	
10. PLEOCHROISM	11. ISOTROPIC ✓ ANISOTROPIC	12. BIREFRINGENCE	13. EXTINCTION STRAIGHT OBLIQUE (ANGLE)	
14. UNIAXIAL BIAXIAL	15. OPTIC SIGN +'ve -'ve	16. 2V	17. DISPERSION	
BS. 24	18. IDENTITY GROSSULARITE			

EXAMINATION OF THIN SECTION MINERALS

1. TRANSPARENT ✓ TRANSLUCENT OPAQUE	2. COLOUR GREEN	3. HABIT PRISMATIC	4. SHAPE ANGULAR ✓ SUBANGULAR ROUNDED	5. FRACTURE UNEVEN
6. CLEAVAGE // 2 DIRECTION ? PRISMATIC	7. SURFACE FEATURES STRIATIONS // PRISM	8. R.I.(oil) R.I.(min) R.I.= < 1.700	9. INCLUSIONS OPAQUES	
10. PLEOCHROISM PALE GREEN -DARK GREEN	11. ISOTROPIC ANISOTROPIC ✓	12. BIREFRINGENCE MODERATE	13. EXTINCTION STRAIGHT OBLIQUE ✓ (ANGLE 25°)	
14. UNIAXIAL BIAXIAL ✓	15. OPTIC SIGN +'ve -'ve ✓	16. 2V >60°	17. DISPERSION	
BS.24	18. IDENTITY HORNBLENDE			

EXAMINATION OF DETRITAL MINERALS

1. TRANSPARENT √ TRANSLUCENT OPAQUE	2. COLOUR YELLOW	3. HABIT ABSENCE OF XSTAL FACES	4. SHAPE ANGULAR SUBANGULAR ROUNDED √	5. FRACTURE UNEVEN
6. CLEAVAGE 1 DIRECTION (?)	7. SURFACE FEATURES	8. R.I.(oil) R.I.(min R.I. = HIGH	9. INCLUSIONS	
10. PLEOCHROISM LIGHT YELLOW →DARK YELLOW	11. ISOTROPIC ANISOTROPIC √	12. BIREFRINGENCE MOD→HIGH	13. EXTINCTION STRAIGHT OBLIQUE (ANGLE)	
14. UNIAXIAL BIAXIAL √	15. OPTIC SIGN +'ve √ -'ve	16. 2V SMALL (~10°)	17. DISPERSION	
PS 2	18. IDENTITY - MONAZITE			

EXAMINATION OF MINERAL GRAINS

1. TRANSPARENT ✓ TRANSLUCENT ✓ OPAQUE —	2. COLOUR AMBER	3. HABIT PLATES	4. SHAPE ANGULAR — SUBANGULAR ✓ ROUNDED —	5. FRACTURE UNEVEN
6. CLEAVAGE 1 DIRECTION BASAL	7. SURFACE FEATURES —	8. R.I.(oil) R.I.(min.) R.I. = slightly < 1600	9. INCLUSIONS —	
10. COLOUR BROWN — BROWNISH YELLOW	11. ISOTROPIC — ANISOTROPIC ✓	12. BIREFRINGENCE —	13. EXTINCTION STRAIGHT — OBLIQUE ✓ (ANGLE —)	
14. UNIAXIAL — BIAXIAL ✓	15. OPTIC SIGN +'ve — −'ve ✓	16. 2V 5°	17. DISPERSION —	
BS 24	18. IDENTITY PHLOGOPITE			

EXAMINATION OF PETRIAL MINERALS

1. TRANSPARENT ✓ TRANSLUCENT ____ OPAQUE ____	2. COLOUR COLOURLESS	3. HABIT PRISMATIC	4. SHAPE ANGULAR ✓ SUB-ANGULAR ✓ ROUNDED ____	5. FRACTURE UNEVEN
6. CLEAVAGE 1 DIRECTION ____	7. SURFACE FEATURES STRIATED // EXT REGULAR	8. R.I.(oil) R.I.(min) 1.604 >. 1.660 slightly > R.I. = ____	9. INCLUSIONS —	
10. PLEOCHROISM COLOURLESS → PINKISH	11. ISOTROPIC ____ ANISOTROPIC ✓	12. BIREFRINGENCE MODERATE	13. EXTINCTION STRAIGHT ✓ OBLIQUE ____ (ANGLE ____)	
14. UNIAXIAL ____ BIAXIAL ✓ centered O.A. figure	15. OPTIC SIGN +'ve ✓ -'ve ____	16. 2V. ~30°	17. DISPERSION —	
BS. 24	18. IDENTITY SILLIMANITE		N.B. REGULARLY STRIATED SILLIMANITE COMPARATIVELY RARE	

EXAMINATION OF [illegible]

1. TRANSPARENT √ TRANSLUCENT OPAQUE	2. COLOUR AMBER	3. HABIT POSSIBLE XSTAL FACES, DIAMOND SHAPED	4. SHAPE ANGULAR SUBANGULAR √ ROUNDED √	5. FRACTURE UNEVEN
6. CLEAVAGE 1 (?) DIRECTION (?)	7. SURFACE FEATURES —	8. R.I.(oil) R.I.(min. R.I. = HIGH (<1930)	9. INCLUSIONS OPAQUES	
10. PLEOCHROISM YELLOW → DARK RED STRONG	11. ISOTROPIC ANISOTROPIC √	12. BIREFRINGENCE (?)	13. EXTINCTION INCOMPLETE STRAIGHT OBLIQUE (ANGLE)	
14. UNIAXIAL BIAXIAL √	15. OPTIC SIGN +'ve √ -'ve	16. 2V ~ 30°	17. DISPERSION STRONG $\rho > v$	
E.S. 24	18. IDENTITY SPHENE			

EXAMINATION OF [illegible] MATERIALS

1. TRANSPARENT √ TRANSLUCENT OPAQUE	2. COLOUR BLUISH WHEN THICK	3. HABIT HEXAGONAL	4. SHAPE ANGULAR SUBANGULAR √ ROUNDED	5. FRACTURE CONCH
6. CLEAVAGE 1 DIRECTION ?	7. SURFACE FEATURES IRON STAINED	8. R.I.(oil) R.I.(min) 1.596 >
1.700 >
1.735 = R.I. = 1.735	9. INCLUSIONS (ALIGNED) ⟺ PURPLISH & OPAQUES	
10. PLEOCHROISM	11. ISOTROPIC √ ANISOTROPIC	12. BIREFRINGENCE	13. EXTINCTION STRAIGHT OBLIQUE (ANGLE)	
14. UNIAXIAL BIAXIAL	15. OPTIC SIGN +'ve -'ve	16. 2V	17. DISPERSION	
B.S. 24	18. IDENTITY SPINEL			

175

V

DETERMINATION OF CRYSTAL MINERALS

1. TRANSPARENT ✓ TRANSLUCENT OPAQUE	2. COLOUR COLOURLESS	3. HABIT PRISMATIC	4. SHAPE ANGULAR ✓ SUBANGULAR ROUNDED	5. FRACTURE CONCHOIDAL
6. CLEAVAGE POOR DIRECTION	7. SURFACE FEATURES —	8. R.I.(oil) R.I.(min) R.I. = high (>1690)	9. INCLUSIONS ABOUND OPAQUE & TRANSPARENT	
10. PLEOCHROISM	11. ISOTROPIC ANISOTROPIC ✓	12. BIREFRINGENCE HIGH	13. EXTINCTION STRAIGHT ✓ OBLIQUE (ANGLE)	
14. UNIAXIAL ✓ BIAXIAL	15. OPTIC SIGN +ve −ve ✓ (length fast)	16. 2V —	17. DISPERSION	
BS 24	18. IDENTITY TOURMALINE		N.B. COLOURLESS TOURMALINE IS RARE.	

176

EXAMINATION OF DETRITAL MINERALS

1. TRANSPARENT ✓ TRANSLUCENT OPAQUE	2. COLOUR -LESS	3. HABIT PRISMATIC	4. SHAPE ANGULAR ✓ SUBANGULAR ROUNDED	5. FRACTURE IRREG.—UNEVEN
6. CLEAVAGE 1 GOOD DIRECTION || PRISM	7. SURFACE FEATURES ALTERATION FLAKES, POWDER	8. R.I.(oil) R.I.(min) R.I.= ≤1.700	9. INCLUSIONS OPAQUES	
10. PLEOCHROISM NONE	11. ISOTROPIC ANISOTROPIC ✓	12. BIREFRINGENCE STRONG	13. EXTINCTION STRAIGHT OBLIQUE ✓ (ANGLE 25°)	
14. UNIAXIAL BIAXIAL ✓	15. OPTIC SIGN +'ve -'ve ✓	16. 2V > 60°	17. DISPERSION	
B.S. 81	18. IDENTITY TREMOLITE			

DESCRIPTION OF OPAQUE MINERALS

1. TRANSPARENT ✓ TRANSLUCENT OPAQUE	2. COLOUR BROWNISH	3. HABIT NO CRYSTAL FACES	4. SHAPE ANGULAR SUBANGULAR ROUNDED ✓	5. FRACTURE ?
6. CLEAVAGE ? DIRECTION	7. SURFACE FEATURES —	8. R.I.(oil) R.I.(min) 1.700 > R.I. = HIGH	9. INCLUSIONS —	
10. PLEOCHROISM SLIGHT BROWN → RED	11. ISOTROPIC ANISOTROPIC ✓	12. BIREFRINGENCE HIGH	13. EXTINCTION UNDETERMINED STRAIGHT (rounded grains) OBLIQUE (ANGLE)	
14. UNIAXIAL BIAXIAL	15. OPTIC SIGN +'ve ✓ -'ve	16. 2V —	17. DISPERSION —	
BS. 24	18. IDENTITY ZIRCON			

APPENDIX II - A.A.S. WORKING CURVES

WORKING CURVE : ABSORBANCE VS. Fe CONC. [IN 12% HCl]

N.B. RANGE SHOWN REPRESENTS MEAN AND VARIATION FOR DUPLICATE [AND TRIPLICATE, IN SOME CASES] READINGS.

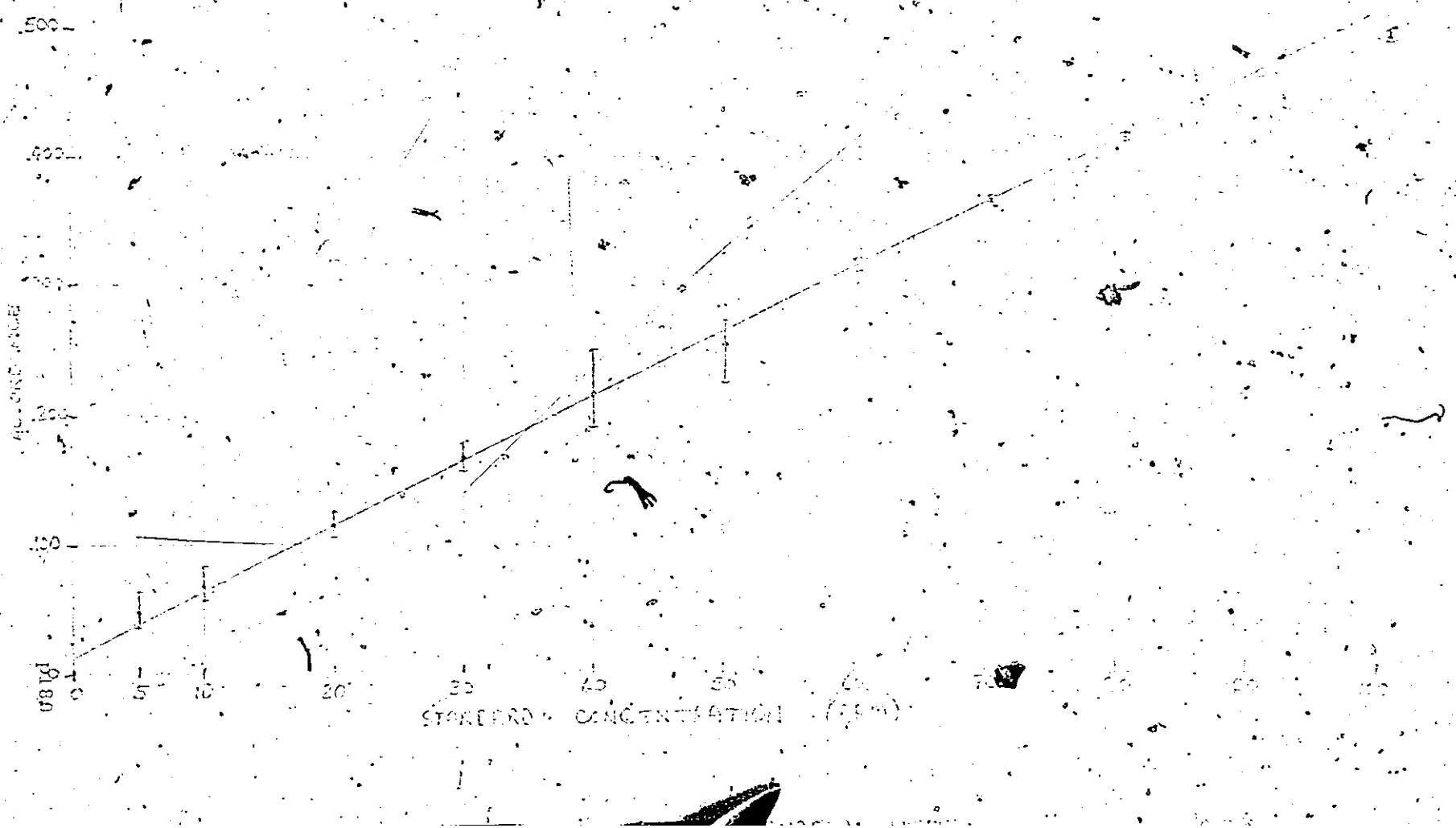

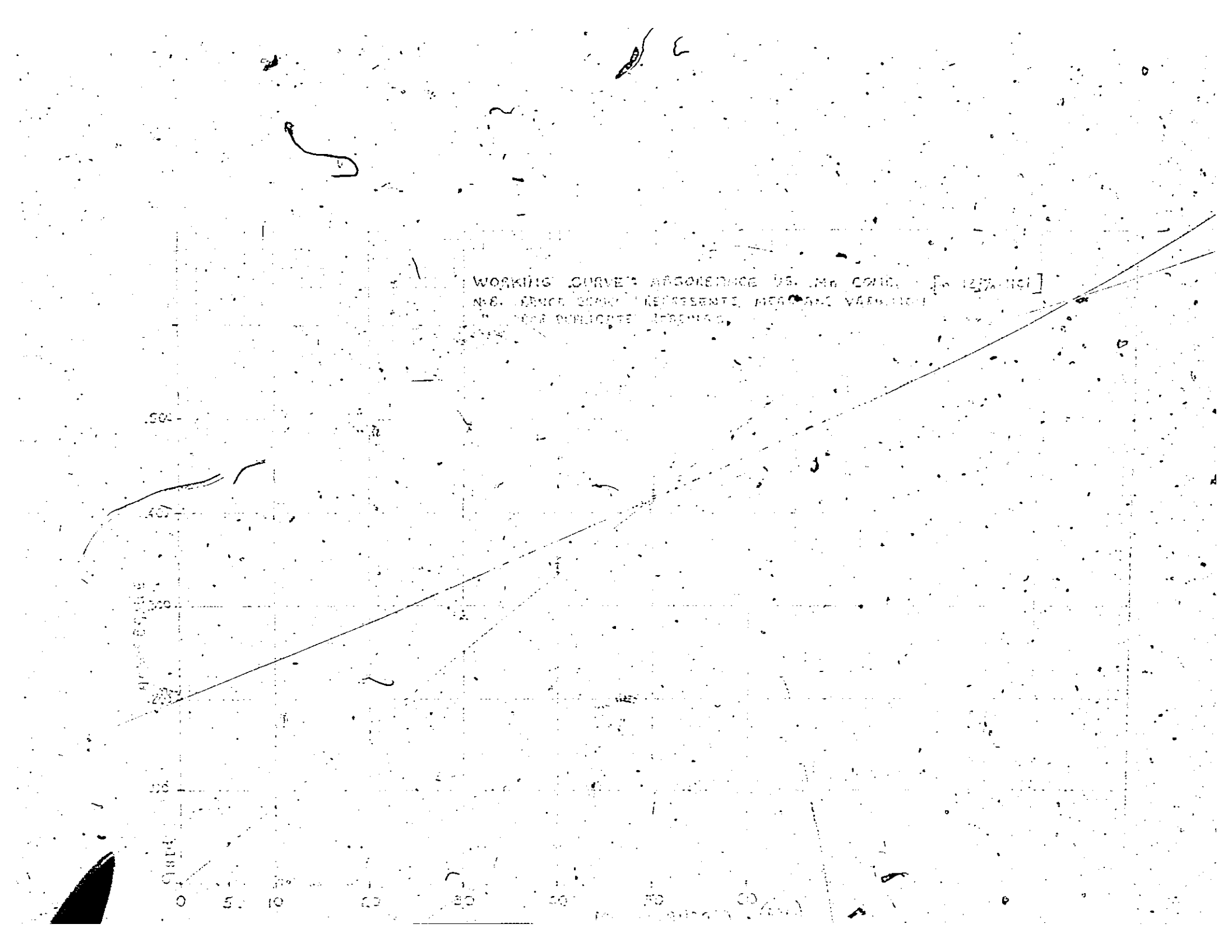
WORKING CURVES ABSORBENCE VS. Mn CONC. [in 12% HCl]
N.B. SINCE SOME REPRESENTS MEASURING VARIATION
0
5
10
20
30
50

APPENDIX III - BEDLOAD DISCHARGE CALCULATIONS

BEDLOAD DISCHARGE BY DUNE TRACKING METHOD

$$q_B = ((K - \lambda)/2) \; \bar{v} \; h \; dw$$ (see page 146)

compartment 1 (assuming same conditions as compartment 2):

$$q_B = ((1-.3)/2)\ (3.4 \text{ ft/day})\ (2 \text{ ft})\ (185 \text{ ft})$$
$$= 440 \text{ ft}^3/\text{day}$$

compartment 2 :

$$q_B = ((1-.3)/2)\ (3.4 \text{ ft/day})\ (2 \text{ ft})\ (148 \text{ ft})$$
$$= 352 \text{ ft}^3/\text{day}$$

compartment 3 :

$$q_B = ((1-.3)/2)\ (3.2 \text{ ft/day})\ (5.2 \text{ ft})\ (482 \text{ ft})$$
$$= 2805 \text{ ft}^3/\text{day}$$

compartment 4 :

$$q_B = ((1-.3)/2)\ (3.6 \text{ ft/day})\ (6.5 \text{ ft})\ (296 \text{ ft})$$
$$= 2424 \text{ ft}^3/\text{day}$$

THEREFORE... Main Channel discharge $= \sum_{1}^{4} x\ (q_{Bx}) = 6.0 \times 10^3 \text{ ft}^3/\text{day}$

$1 \text{ ft}^3/\text{day} = 2.83 \times 10^4 \text{ cm}^3/\text{day}$

$6.0 \times 10^3 \text{ ft}^3/\text{day} = 1.7 \times 10^8 \text{ cm}^3/\text{day}$

and using a density conversion for study area sands @ 2.65 g/cm^3...

$$\Sigma q_B = (1.7)(10^8)(2.65)(10^{-3}) \text{ kg/day}$$
$$= 4.5 \times 10^5 \text{ kg/day}$$

BEDLOAD DISCHARGE BY SAMPLER METHOD

(see page 148 for average bedload discharge by unit width and by compartment)

Values of discharge/ft obtained by the following :

q_B/ft = (Average sample weight (page 144)) / (Sample time) / (sampler width)

Values of discharge/compartment obtained by :

q_B/comp. = q_B/ft X compartment width (page 148)